Spectrum sensing techniques in cognitive wireless sensor networks

Shaoyang Men

UNIVERSITE BRETAGNE LOIRE

UNIVERSITÉ DE NANTES

Thèse de Doctorat

Shaoyang MEN

Mémoire présenté en vue de l'obtention du
grade de Docteur de l'Université de Nantes
sous le sceau de l'Université Bretagne Loire

École doctorale : Sciences et technologies de l'information et mathématiques (STIM)

Discipline : Electronique
Spécialité : Communications numériques
Unité de recherche : IETR UMR 6164

Soutenue le 27 Octobre 2016

Spectrum sensing techniques in cognitive wireless sensor networks

JURY

Président :	**M. Tanguy RISSET**, Professeur, Insa-Lyon
Rapporteurs :	**M. Emanuel RADOI**, Professeur, Université de Bretagne Occidentale
	M. Mohammad-Ali KHALIGHI, Maitre de conférences HDR, École Centrale de Marseille
Directeurs de thèse :	**M. Sébastien PILLEMENT**, Professeur, École Polytechnique de l'Université de Nantes
	M. Pascal CHARGÉ, Professeur, École Polytechnique de l'Université de Nantes

Acknowledgments

First of all, I would like to express my sincere gratitude to my supervisors Prof. Sébastien Pillement and Prof. Pascal Chargé for their patient guidance, constant encouragement and professional advice throughout the entire three years of my PhD study. I have been extremely lucky to work with so great supervisors who cared so much about my research work, who responded to my questions so promptly, and who spent countless hours correcting the manuscripts.

I would also like to thank Prof. Yide Wang, for his helpful suggestions and encouragement.

Of course, I have to thank the jury, for their patient review and for taking them too much time.

In addition, I am sincerely grateful for all the help of Marc Brunet, Sandrine Charlier and all the other members of staff in IETR laboratory of Polytechnique de L'Université de Nantes.

I also want to thank my friends, we really had a wonderful time for my PhD life in France.

Finally, I must express my gratitude to my parents and my wife, for their continued support and encouragement.

Résumé de la thèse en français

Aujourd'hui, avec le développement rapide des technologies de communication sans fil, des services de plus en plus nombreux apparaissent dans tous les aspects de notre vie tels que les soins de santé, les bâtiments intelligents, la surveillance du trafic, l'observation de champs de bataille, des applications multimédias. Le spectre étant considéré comme une ressource limitée, il en résulte une compétition croissante entre les applications sans fil. En outre, en raison de la stratégie d'allocation du spectre fixée par l'autorité de régulation, la plupart des bandes de fréquences sont a priori réservées pour certains utilisateurs agréés. Par exemple, la gamme de fréquences comprise entre 512 MHz et 608 MHz est attribuée aux canaux de télévision 21-36. Il n'existe que très peu de bandes libres dans le spectre électromagnétique exploitable par les applications sans fil. De plus, les bandes réservées semblent ne pas être pleinement exploitées; de manière inattendue le taux d'utilisation du spectre semble être de moins de 30% [1].

Afin de faire face à la rareté et à la sous-exploitation des ressources spectrales, des stratégies de partage du spectre ont été proposées. L'idée de base est de permettre à chacun d'utiliser le spectre sous licence lorsqu'il n'est pas occupé par son propriétaire officiel (utilisateur primaire). L'utilisateur secondaire n'est donc pas prioritaire et ne doit causer aucune interférence à l'utilisateur primaire [2, 3, 4, 5]. Les technologies de radio cognitive [6], se sont imposées dans cette stratégie, en utilisant un mécanisme de cognition pour détecter le spectre, déterminer des groupes vacants et utiliser ces bandes disponibles de manière opportuniste [7, 8]. La première étape du cycle de la cognition est la détection du spectre, elle joue un rôle essentiel et central dans la radio cognitive. L'utilisateur cognitif (utilisateur secondaire) doit détecter rapidement et de manière certaine que l'utilisateur autorisé est présent ou non dans une bande de fréquence considérée. Il existe diverses méthodes de détection de spectre pour la radio cognitive dans la littérature [9, 10], mais très peu d'entre elles semblent être vraiment appropriées au contexte des réseaux cognitifs de capteurs sans fil.

Les réseaux cognitifs de capteurs sans fil sont définis comme des réseaux distribués de nœuds cognitifs de capteurs sans fil. Généralement conçus pour relever des mesures

ou détecter des événements, les nœuds capteurs du réseau collaborent entre eux et communiquent dynamiquement sur les bandes de fréquences disponibles. Un réseau cognitif de capteurs sans fil possède donc des capacités cognitives pour l'exploitation du spectre [11]; ce qui n'est pas le cas des réseaux sans fil traditionnels. Par conséquent, les nœuds de capteurs sans fil sont équipés de la capacité cognitive. Les avantages attendus sont multiples: (1) Utilisation plus efficace du spectre: Les nœuds des réseaux de capteurs sans fil existants utilisent généralement une bande fixe sans licence pour communiquer. Ces bandes libres sont donc en général très fréquentées par d'autres appareils. Par conséquent, l'accès au spectre de manière opportuniste est en mesure d'améliorer la cohabitation efficace des plusieurs utilisateurs/services. (2) Plusieurs canaux de communication potentiels: Dans les réseaux de capteurs sans fil à forte densité de déploiement, un grand nombre de nœuds de capteurs tentent d'accéder au même canal en même temps. Cela augmente la probabilité de collisions et de pertes de paquets, ce qui diminue la fiabilité globale de communication avec une consommation d'énergie excessive. Les réseaux cognitifs de capteurs sans fil ont en revanche la capacité d'exploiter plusieurs canaux selon leur disponibilité de façon opportuniste pour atténuer ces problèmes potentiels. (3) Efficacité énergétique: Les réseaux cognitifs de capteurs sans fil sont en mesure de modifier leurs paramètres de fonctionnement selon les conditions du canal afin d'optimiser leur consommation d'énergie liée aux transmission. (4) Opérabilité mondiale: La réglementation d'exploitation du spectre peut être différente d'une région à une autre, certaines bandes sont libres dans une région tandis qu'elles ne sont pas exploitables dans un autre pays. Les réseaux de capteurs cognitifs peuvent s'adapter à n'importe quelle réglementation grâce à l'agilité spectrale des nœuds cognitifs.

Cependant, la réalisation de réseaux cognitifs de capteurs sans fil et les avantages potentiels ci-dessus nécessitent de répondre à certains défis. En général, un nœud cognitif de capteurs sans fil se compose de cinq éléments de base: une unité de détection-capteur, une unité de traitement et de stockage, une unité dite de traitement-décision dédiée aux fonctions radio-cognitives, un module radio émetteur-récepteur et une alimentation. Souvent imposé par le contexte d'application, le nœud doit généralement répondre à de nombreuses contraintes (limitation de la consommation, capacité de calcul, durée de vie, la durée de détection, fiabilité des mesures ...). Notamment, les nœuds sont parfois situés dans des endroits inaccessibles, ce qui exclut le remplacement des piles et entraine dans ce cas que l'une des principales préoccupations pour l'exploitation du réseau cognitif est la consommation d'énergie. Parmi les composants des nœuds de capteurs, l'unité radio émetteur-récepteur consomme beaucoup d'énergie

afin de fournir une connectivité aux autres nœuds. En outre, le traitement et la mémoire sont également limités. En raison des contraintes de coût et de taille, les capacités de traitement des nœuds peuvent s'avérer relativement limitées par rapport à d'autres systèmes embarqués [12]. Cependant, les différentes méthodes existantes de détection du spectre pour la radio cognitive dans la littérature ne considèrent pas ces limites de ressources des nœuds de capteurs. Par conséquent, concevoir une technologie spécifique de radio cognitive pour les réseaux cognitifs de capteurs sans fil est un sujet non résolu.

Dans le chapitre 2, nous présentons les techniques de détection de spectre développée dans la littérature. Ce chapitre reprend aussi les indicateurs de performance qualifiant ces techniques. La détection du spectre peut se faire uniquement localement au niveau de chaque nœud (détection locale), ou de manière coopérative entre plusieurs nœuds du réseau (détection coopérative). Dans le cas de la détection locale du spectre, nous présentons plusieurs méthodes basées sur les principes suivants: détection de l'énergie, la détection à base de valeurs propres de la matrice de covariance des observations, test du Goodness-of-Fit etc.. Concernant la détection coopérative du spectre, nous discutons de la détection du spectre de coopération centralisée et la détection du spectre coopératif distribuée. Ensuite, nous nous concentrons sur la présentation des méthodes de fusion. Il s'agit de générer une décision en combinant les données issues des nœuds, à partir de règles (hard decision, soft decision, théorie des croyances de Dempster-Shafer, etc.). Cependant, comme indiqué dans le chapitre 2, la plupart de ces méthodes ont leurs limitations. Par exemple, la détection d'énergie permet d'atteindre une bonne performance de détection uniquement lorsque la taille de l'échantillon est suffisamment grande [13]. De même, de nombreuses méthodes de détection basées sur l'analyse des valeurs propres de la matrice de covariance ont été proposées [14, 15, 16, 17, 18], mais la plupart d'entre elles ont des exigences intenables en termes de durée d'observation (ce qui génère une grande taille de l'échantillon) et de complexité de calcul.

Considérant les contraintes et les limitations précédentes des méthodes de détection du spectre de la littérature, nous proposons d'étudier de nouvelles techniques permettant de détecter le spectre à partir d'un faible nombre d'échantillons. Cette caractéristique est en effet un moyen de limiter la consommation des circuits et la complexité des traitements. Un petit nombre d'échantillons permet de réduire considérablement la durée d'observation du spectre, ce qui se traduit aussi par une économie d'énergie et une prolongation de la durée de vie de l'ensemble du réseau.

Dans le chapitre 3, une méthode locale de détection du spectre est proposée. Cette

méthode repose sur un modèle statistique des signaux reçus ainsi que sur l'utilisation de la théorie des croyances de Dempster-Shafer. Les échantillons du canal sont tout d'abord séparés en plusieurs groupes pour former une variable aléatoire pour chaque groupe. Le nombre d'échantillons étant faible, il apparaît que cette variable suit une loi t de Student. Les paramètres de cette loi sont différents selon que le canal ne comporte que du bruit ou qu'il soit utilisé par un utilisateur primaire. Cette différence va être exploitée pour distinguer les deux hypothèses ($\mathcal{H}_0$ absence d'utilisateur primaire / $\mathcal{H}_1$ présence d'un utilisateur primaire) en s'appuyant sur la théorie des croyances de Dempster-Shafer. Ainsi pour chaque groupe d'échantillons, des BPA (Basic Probability of Assignement) sont calculées pour les deux hypothèses: $m_i(\mathcal{H}_0)$ et $m_i(\mathcal{H}_1)$. Le processus de fusion de Dempster-Shafer est ensuite utilisé pour produire une décision finale à partir des BPA de tous les groupes d'échantillons. Les résultats de simulation montrent que la probabilité de détection de la méthode proposée est supérieure aux autres méthodes locales de la littérature lorsque le nombre d'échantillons est faible.

Dans le chapitre 4, une méthode coopérative de détection du spectre est proposée. La technique repose aussi sur la théorie des croyances de Dempster-Shafer, mais le processus de fusion permettant d'obtenir la décision globale exploite les BPA fournies par chacun des nœuds du réseau. Cette fusion est faite au niveau d'un nœud particulier appelé centre de fusion. Au niveau de chaque nœud (utilisateur secondaire) il s'agit donc de calculer les BPA relatives aux deux hypothèses à partir d'un faible nombre d'échantillons. Pour cela, la technique s'appuie à nouveau sur un modèle statistique des observations. En effet, chaque utilisateur secondaire forme une matrice de covariance de ses observations. Ici encore, le nombre d'échantillons pour calculer cette matrice de covariance est faible et de plus le taux d'échantillonnage est choisi relativement faible de telle manière que les échantillons sont considérés indépendants. Il s'avère dans cette situation que la plus forte valeur propre de la matrice de covariance est régie par une loi statistique de Tracy-Widom. Comme précédemment, les paramètres de la loi sont différents selon que l'on soit en présence ou non d'un utilisateur primaire. Cette différence est exploitée au niveau de chaque utilisateur secondaire pour calculer les BPA pour les deux hypothèses. Les résultats de simulation permettent de vérifier l'efficacité de la méthode proposée pour les faibles nombres d'échantillons.

Dans le chapitre 5, une autre technique coopérative de détection du spectre est proposée. L'approche est différent du chapitre précédent car les critères privilégiés sont ici la consommation et la fiabilité de la décision. Dans un premier temps l'organisation du réseau en cluster est étudiée. Les nœuds (utilisateurs secondaires) sont donc regroupés en clusters de manière à réduire la consommation globale liée aux communications

pour effectuer la détection coopérative à l'échelle du cluster. Basé sur l'algorithme K-mean, la technique de formation du cluster permet aussi de désigner le meilleur nœud centre de fusion pour la détection de spectre dans le cluster. Ensuite la méthode de détection de spectre consiste à mettre en œuvre un double critère de fiabilité des utilisateurs. La théorie des croyances de Dempster-Shafer est une nouvelle fois utilisée pour qualifier les deux hypothèses des utilisateurs secondaires et combiner ces informations au niveau du centre de fusion du cluster. La technique repose d'une part sur une estimation du niveau de bruit reçu par chaque utilisateur et d'autre part sur le soutien mutuel que s'accordent les utilisateurs entre eux. De cette manière un utilisateur évoluant dans un milieu trop bruité verra sa crédibilité diminuer, et de même un utilisateur fournissant des BPA trop différentes des autres verra aussi baisser sa crédibilité (soutien mutuel). Enfin, les utilisateurs dont la crédibilité est trop basse sont rejetés du processus de fusion pour la décision globale dans le cluster. Ce principe permet d'améliorer la fiabilité de la décision car les utilisateurs secondaires les moins crédibles ne participent pas à la décision. Un utilisateur peut être considéré non crédible par exemple lorsque sa perception du canal est trop mauvaise ou simplement lorsqu'il est défectueux. Des résultats de simulation sont fournis pour illustrer les performances du système proposé.

La thèse se termine par une conclusion reprenant les différentes contributions et indiquant quelques perspectives.

Contents

List of Figures

List of Symbols

χ^2 ..... Chi square distribution

γ ..... Signal to noise ratio

λ_{max} ..... Maximum eigenvalue

λ_{min} ..... Minimum eigenvalue

σ_w^2 ..... Variance of noise

ζ ..... Threshold

m ..... Basic probability assignment function

N_s ..... Number of samples

N_{su} ..... Number of secondary users

P_d ..... Probability of detection

P_{fa} ..... Probability of false alarm

P_m ..... Probability of miss

$\mathcal{H}_0$ ..... Hypothesis of only noise

$\mathcal{H}_1$ ..... Hypothesis of signal plus noise

$\mathcal{N}$ ..... Gaussian distribution

$\mathcal{T}$ ..... Test statistic

List of Abbreviations

AWGN ..... Additive White Gaussian Noise
BPA ..... Basic Probability Assignment
CDF ..... Cumulative Distribution Function
CFD ..... Cyclostationary Feature Detection
CR ..... Cognitive Radio
CSS ..... Cooperative Spectrum Sensing
CWSNs ..... Cognitive Wireless Sensor Networks
D-S ..... Dempster-Shafer
EBS ..... Eigenvalue Based Sensing
ED ..... Energy Detection
FC ..... Fusion Center
GoF ..... Goodness of Fit
LSS ..... Local Spectrum Sensing
MFD ..... Matched Filter Detection
MME ..... Maximum Minimum Eigenvalue
PDF ..... Probability Density Function
PU ..... Primary User
ROC ..... Receiver Operating Characteristic
SNR ..... Signal to Noise Ratio
SS ..... Spectrum Sensing
SU ..... Secondary User
TW ..... Tracy Widom
WBS ..... Waveform Based Sensing
WSNs ..... Wireless Sensor Networks

1

Introduction

1.1 Background

Nowadays, with the rapid development of wireless communication technology, more and more wireless services are used in all aspects of life such as health care, intelligent buildings, vehicle traffic monitoring, battlefield surveillance, multimedia applications and so on. The limited spectrum resource can not meet the growing demand of wireless application. In addition, due to the existing fixed spectrum allocation strategy, most frequency bands are specified for the licensed user (LU) where the other communication device is not allowed to utilize it in spite of the unoccupied band. For example, the frequency range between 512 MHz and 608 MHz is assigned as TV channel 21-36, which means that only TV user can use it, but the others can not occupy it at any time. A mass of allocated frequency bands cause that the available spectrum is so little. Even more unfortunately, the spectrum utilization rate of LU are unexpectedly under 30% [1], as shown in Figure 1.1. The fixed mobile frequency band 1850-1990 MHz and the air traffic control frequency band 108-138 MHz are even used at 5%.

In order to solve the scarcity of spectrum resource and the low spectrum utilization, dynamic spectrum allocation (DSA) which is a flexible and intelligent spectrum management mode has been proposed [2]. In DSA, according to the actual requirements of wireless communication system, spectrum resource is dynamically allocated to those wireless systems. When this process is finished, the spectrum is taken back by

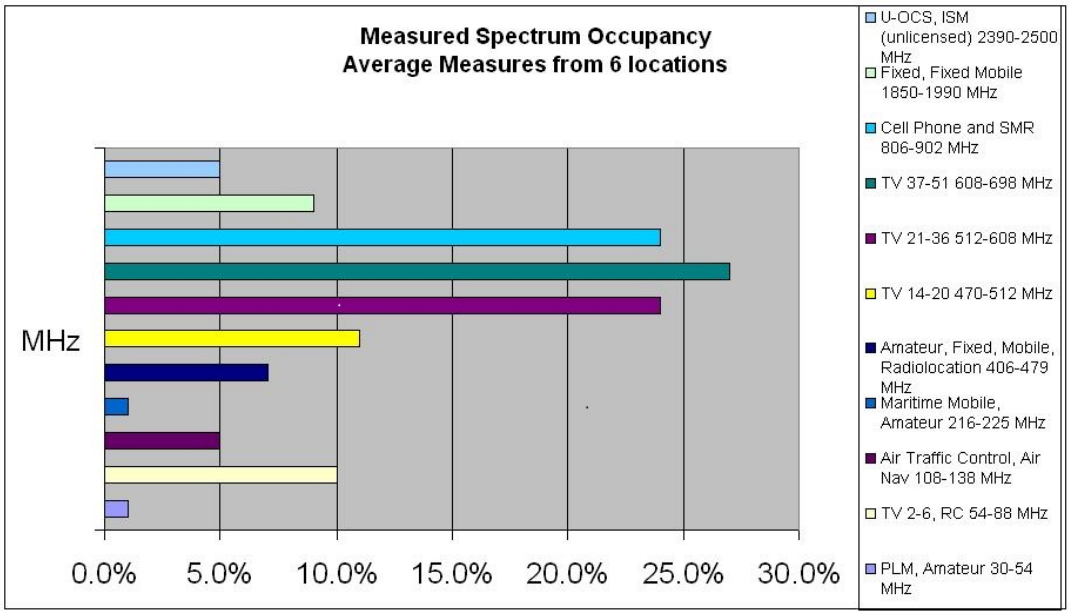

Figure 1.1 – A snapshot of spectrum utilization where each band averaged over 6 locations [1].

the assignment system. Although this management mode is efficient for the spectrum utilization, it changed the current static frequency allocation schemes. Therefore, spectrum sharing strategy without altering the current frequency allocation schemes which is considered as the popular spectrum sharing technique has been proposed. The basic idea is to open licensed spectrum to unlicensed users while limiting the interference perceived by licensed user. It mainly includes two approaches to spectrum sharing: spectrum underlay and spectrum overlay [3].

The spectrum underlay approach allows that the unlicensed user accesses the licensed spectrum with a extremely low power, which results in multiple communication system using the same frequency band simultaneously [4]. Due to the very low power of the unlicensed user, like a background noise for the licensed user, there is no serious interference with the licensed user when the licensed and unlicensed users execute their own operations at the same time under the same frequency band. According to this, the unlicensed ultra-wideband (UWB) working in the frequency range from 3.1 GHz to 10.6 GHz, whose power spectrum density emission is limited -41.3 dBm/MHz, can coexist with the worldwide interoperability for microwave access (WiMAX) at 3.5 GHz band [5]. On the other hand, the spectrum overlay approach does not necessarily impose severe restrictions on the transmission power of unlicensed users, but rather on when and where they may transmit. In other words, when the licensed frequency band

is unoccupied at spatial and temporal scales, the unlicensed user is allowed to operate in the frequency band. In this spectrum overlay, two approaches including opportunity spectrum sharing and cooperation spectrum sharing are considered.

In cooperation spectrum sharing, the licensed user needs to know whether the unlicensed user is present or not. And when the licensed user prepares working, if the unlicensed user is using the licensed frequency band, the licensed user chooses the other unoccupied sub-channels for operating and does not interrupt the communication of the unlicensed user. In opportunity spectrum sharing, it does not know the situation of the unlicensed user and has no cooperation between the licensed and unlicensed user. When the unlicensed user needs to access the licensed frequency band, it needs to detect whether the licensed user is present or absent. If the licensed frequency is occupied by the licensed user, the unlicensed user can not access the spectrum; otherwise, it can use the licensed spectrum. When the licensed user reoccupies the frequency band, the unlicensed user needs to quit immediately and look for a new unoccupied frequency band. Therefore, this approach is sufficient for Cognitive Radio (CR) which is first proposed by Mitola [6] and is defined by Federal Communications Commission (FCC) as : "*A radio or system that senses its operational electromagnetic environment and can dynamically and autonomously adjust its radio operating parameters to modify system operation, such as maximize throughput, mitigate interference, facilitate interoperability, access secondary markets.*" [7].

CR utilizes a mechanism called cognition cycle as shown in Figure 1.2 [8] for sensing the spectrum (spectrum sensing, SS), determining the vacant bands (spectrum decision) and making use of these available bands in an opportunistic manner (spectrum mobility and spectrum sharing). As the first step of cognition cycle, spectrum sensing plays an essential and central role in CR. The key of SS is that the cognitive user (as the secondary user, SU) needs to detect quickly and reliably that the licensed user (as the primary user, PU) is present or not in a considered frequency band. There are various method of spectrum sensing for CR in the literature [9, 10], but a very few of them seem to be really suitable in the context of cognitive wireless sensor networks (CWSNs).

CWSNs is defined as distributed networks of wireless cognitive radio sensor nodes, which sense event signals and collaboratively communicate their readings dynamically over available spectrum bands in a multihop manner to ultimately satisfy the application-specific requirements [11], which can be constructed by incorporating CR technology into the traditional wireless sensor networks (WSNs). Therefore, the sensor nodes in WSNs are equipped with cognitive ability, which may benefit the WSNs.

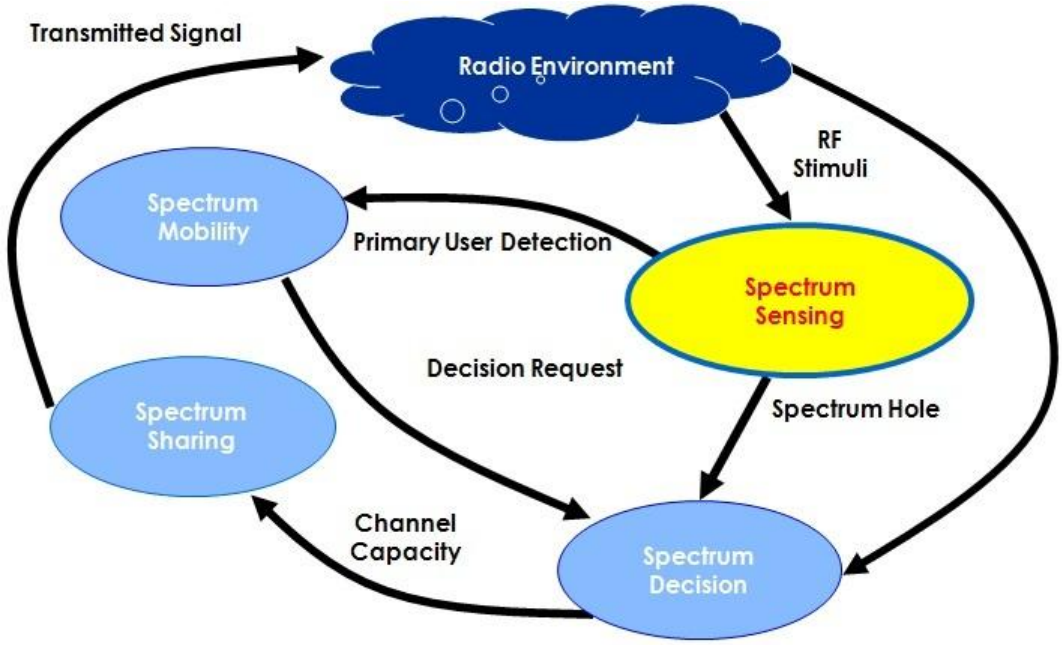

Figure 1.2 – Cognition cycle.

The advantages of using CR in WSNs are discussed in the following:

- **Efficient spectrum utilization:** Current WSNs are deployed over unlicensed frequency band, such as industrial, scientific and medical (ISM) radio bands, which faces an increased level of interference from various wireless system. ISM bands are overcrowded which limits the development of new technologies. Dynamic spectrum access in CR is able to make SU cooperate efficiently with other types of users.
- **Multiple channels utilization:** In traditional WSNs referring to the detection of an event, several sensor nodes generate bursty traffic. Especially, when in densely deployed WSNs, a large number of sensor nodes attempt to access the same channel at the same time. It increases the probability of collisions and packet losses, which decreases the communication reliability with excessive power consumption. CWSNs access multiple channels opportunistically to alleviate these potential challenges.
- **Energy efficiency:** CWSNs may be able to change their operating parameters according to the surrounding channel conditions in order to avoid the power waste for packet retransmission due to packet losses in traditional WSNs.
- **Global operability:** Due to different spectrum regulations, a certain band in one

specific region or country may be available, while it is not available in another places. However, the sensor nodes with cognitive capability in CWSNs may overcome this potential problem.

However, the realization of CWSNs and the potential advantages above depends on addressing some challenges that are introduced by the wireless sensor node equipped with cognitive capability in CWSNs. Generally, a cognitive wireless sensor node consists of five basic units: a sensing unit, a processing and storage unit, a CR unit, a transceiver unit and a power unit. Just like a traditional wireless sensor node, it has hardware constrains in terms of computational power, storage and energy. Therefore, considering the limitation of processing, memory and energy, it is still a serious challenge to design specific CR technology in CWSNs.

1.2 Motivation

It is provided that the cognitive wireless sensor node in CWSNs is resource constrained that refers to power limitation, hardware limitations, sensing duration and reliability. Because most WSNs are inaccessible or it is not feasible to replace the batteries of the node when the limited battery power is exhausted, the main concern for the operation of CWSNs is the energy consumption. Among the components of sensor nodes, the transceiver unit consumes the most energy in order to provide connectivity to the other nodes. In addition, the processing and memory are also constrained. Due to the cost and size constraints, the processing power of current nodes is seriously lower than the other embedded systems [12]. However, the existing various methods of spectrum sensing for CR in the literature do not consider these limits of resource of sensor nodes. For example, energy detection is able to achieve a good detection performance only when the sample size is sufficiently large [13]. Numerous covariance matrix or eigenvalue based detection methods have been proposed in [14, 15, 16, 17, 18], most of them have the requirements of the long sensing time (large sample size) and the high computational complexity.

Motivated by the constrained resource described and the limitation of the existing spectrum sensing methods above, as a way of solving this problem, small sample size is proposed to design new efficient CR techniques, especially in spectrum sensing algorithms, which is able to preferably adapt in CWSNs. A small number of samples can greatly reduce the data burden of the transceiver unit, which results in an exciting energy saving. Due to the most energy consumed by the transceiver unit as shown

above, small samples size plays a role to prolong the usage of sensor nodes and even extend the lifetime of the whole network. Besides, it also alleviates the limits of the processing power and memory. Therefore, small sample size is an efficient method to adopt in CWSNs where sensor nodes are resource constrained and additional CR actions is required.

In order to cope with the small sample size, we firstly propose to reformulate the spectrum sensing into a student's t-distribution test problem. It is demonstrated that the student's t-distribution test under small sample size can also provide a low error rates close to the 5% nominal value [23]. Thus, according to this characteristic of student's t-distribution and taking into account several goodness of fit (GoF) tests [24], an efficient local spectrum sensing method is proposed on basis of both hypotheses of presence and absence of PU signal, which is able to get a high reliability of detection. However, in order to focus on dealing with the small sample size, we do not consider the channel condition in the system model of the proposed method. Hence, considering the SU practically experiencing path loss, multipath and shadowing, we propose to adopt a cooperative spectrum sensing strategy based on multiple sensor nodes in order to improve the reliability of detection, which is based on an adjusted Tracy-Widom distribution that is suitable for small sample size. In summary, two solutions to small sample size including the student's t-distribution and the adjusted Tracy-Widom distribution are proposed at the beginning.

However, small sample size really increases the uncertainty of the observation samples and reduces the reliability of final decision. Therefore, our efforts begin with the Dempster-Shafer (D-S) theory of evidence that can deal with the uncertainty from the small observation samples and improve the reliability by fusing different data groups. According to the D-S theory of evidence, after coping with the small number of samples, some basic probability assignment (BPA) are estimated with the characteristic of the student's t-distribution or the adjusted Tracy-Widom distribution. Finally, relying on the fusion of different probability assignment estimations, we make a reliable final decision whether a PU signal is present or not. These refer to the proposed local spectrum sensing (LSS) based on the GoF principle and cooperative spectrum sensing (CSS) based on D-S theory of evidence.

In addition, the energy efficiency of the whole network and the reliability of the decision are also great challenges. On the one hand, an unreasonable allocation of sensor nodes in the network can result in a great waste of the transmission power among sensor nodes. On the other hand, it is necessary to consider the security issues of sensor nodes in the whole networks. For example, sometimes some nodes inevitably

fail in sending the information data due to battery depletion, electronic device under harsh environment or even being attacked by malicious users. Considering the situation mentioned above, a robust and energy efficient cooperative spectrum sensing scheme is proposed, which is based on a clustering algorithm and utilizes a double reliability evaluation.

1.3 Contributions

The main contributions of this thesis are summarized as follows.

- An efficient local spectrum sensing with small sample size is proposed. In the proposed method, we reformulate spectrum sensing into a student's t-distribution test problem and propose some new basic probability assignment evaluations. Then, the D-S theory of evidence is used to make a decision relying on both hypotheses of presence or absence of PU. Simulation results show that the proposed method can achieve a higher probability of detection than other compared methods with small sample size.
- An efficient cooperative spectrum sensing with small sample size is proposed. In the proposed method, considering the channel condition at each SU, a more reasonable Tracy-Widom approximation is utilized to form a thin observation matrix. Then, we also propose some new BPA functions based on the largest eigenvalue of the received sample covariance matrix, which considers the credibility of local spectrum sensing. Finally, a more reliable final decision is made. Simulation results verify the effectiveness of the proposed method for small sample size scenarios.
- A robust and energy efficient cooperative spectrum sensing scheme in CWSNs is proposed. In the proposed method, firstly, considering the energy consumption of sensor nodes, we propose a cluster-based cooperative spectrum sensing scheme where the energy consumption of the communications unit for the SU is reduced extremely and the spectrum utilization of the spectrum hole for the whole network is remarkably improved. Secondly, taking the reliability problem into account, we propose a method that allows to consider simultaneously the reliability of each SU in the cluster and the mutually supportive degree among the whole set of SUs in the cluster, namely double reliability evaluation. Finally, after removing the nodes of low credibility, the energy efficiency and reliability of each cluster is improved. Simulation results show that the proposed CSS

scheme clearly allows to save energy and provides a more robust decision under faulty nodes situation.

1.4 Outline of the thesis

The remainder of this thesis is organized into five chapters as listed below.

- Chapter 2 overviews the developed spectrum sensing techniques in the literature. At first, the performance indicators of spectrum sensing techniques are given. Then, we discuss the local spectrum sensing techniques, where several local spectrum sensing methods such as energy detection, eigenvalue based sensing, GoF test based sensing, etc. are presented. After that, we introduce the cooperative spectrum sensing, which includes the centralized cooperative spectrum sensing and the distributed cooperative spectrum sensing. We focus on presenting fusion methods such as hard-decision, soft-decision combining data fusion schemes, bayesian fusion rule, D-S theory of evidence, etc..
- Chapter 3 presents the proposed local spectrum sensing with small sample size. First of all, we take advantage of the student's t-distribution to cope with the small number of samples. Then some new basic probability assignment functions are proposed in order to evaluate the reliability of observation samples. At last, the D-S theory of evidence is used to make a decision. The simulation results referring to the performance comparisons are also given.
- Chapter 4 presents the proposed cooperative spectrum sensing with small sample size. At the beginning, the system model considering channel conditions is given. We then consider an adjusted Tracy-Widom distribution and use the eigenvalue based method at each SU. After that, we estimate the reliability of each SU and combine these results to make a final decision using D-S theory of evidence. Some simulation results and analyses are given at the end.
- Chapter 5 introduces the proposed robust and energy efficient cooperative spectrum sensing scheme in CWSNs where some faulty nodes are existing. On one hand, we make use of the clustering algorithm in the whole network. On the other hand, a double reliability evaluation is presented in each cluster to remove the nodes of low credibility. We also show the simulation results of each method and give the performance comparisons with other methods.
- Chapter 6 gives the conclusions of this thesis and the possible directions in the future work.

2

Overview of spectrum sensing techniques

In order to improve spectrum efficiency and alleviate the problem of spectrum resources constraints, the concept of cognitive radio is proposed which is a smart wireless communication system. A cognitive radio is able to be aware of its environment and learn from the surrounding, then change the corresponding operating parameters, such as transmission power, carrier frequency, its modulation mode, etc., finally in real time adjust the internal state of cognitive radio user to accommodate the impending change in radio frequency excitation [25].

In cognitive radio, a major challenge is that the SU needs to sense the presence of PU in a licensed frequency band, and to leave it as quickly as possible when the PU emerges in order to avoid interference to the PU. This technique is called spectrum sensing. As a critical part of CR, spectrum sensing has attracted a large amount of interest and several spectrum sensing techniques have been widely studied in the literature [9, 10, 20, 21]. According to whether the sensing needs collaboration or not, we can classify all spectrum sensing algorithms into two main types: local and cooperative spectrum sensing, (as shown in Figure 2.1). In local spectrum sensing, the detector makes a decision only on basis of its own sensing, whereas cooperative spectrum sensing is able to use multiple devices and combine their measurements to make a decision. Those techniques are briefly explained in Section 2.2 and Section 2.4, respectively.

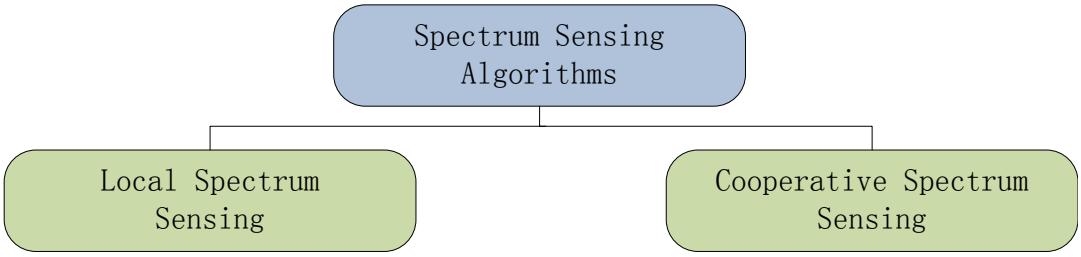

Figure 2.1 – The classification of spectrum sensing techniques.

Before exploring local spectrum sensing and cooperative spectrum sensing, we describe performance indicators of spectrum sensing techniques in Section 2.1.

2.1 Performance indicators of spectrum sensing techniques

Before showing the performance indicators of spectrum sensing techniques, the general signal detection model and decision criterion are described. The spectrum sensing, in a simple form can be formulated as a binary hypothesis testing problem [9, 19],

$$\begin{aligned} &\mathcal{H}_0 : y[n] = w[n] && n = 1, 2, \cdots, N_s \\ &\mathcal{H}_1 : y[n] = \overbrace{h[n] \otimes s[n]}^{x[n]} + w[n], && n = 1, 2, \cdots, N_s \end{aligned} \tag{2.1}$$

where $\mathcal{H}_0$ is the hypothesis of the absence (vacant channel) whereas the hypothesis $\mathcal{H}_1$ denotes the presence (occupied channel) of the PU's signal, $y[n]$ represents the received data at the SU with $s[n]$ and $w[n]$ denoting the signal transmitted from the PU and the additive white Gaussian noise (AWGN) with variance σ_w^2, respectively. Moreover, $h[n]$ denotes the channel impulse response from the PU to the SU, and $x[n]$ is the received PU signal with channel effects. N_s is the number of samples. Note that, for purpose of guaranteeing that the received data $\mathbf{y}$ ($\mathbf{y} = \left[y[1]y[2]\cdots y[N_s]\right]^T$) does not include SU's own signal, we assume that the SU executes alternatively spectrum sensing and data transmission.

In order to decide whether the observation $\mathbf{y}$ is generated under hypothesis $\mathcal{H}_0$ or hypothesis $\mathcal{H}_1$, it is typically accomplished by firstly forming a test statistic $\mathcal{T}(\mathbf{y})$ with the received data $\mathbf{y}$ according to different spectrum sensing algorithms, and then

comparing $\mathcal{T}(\mathbf{y})$ with a predetermined threshold ζ [9, 10]. In this way, we can decide that the hypothesis $\mathcal{H}_1$ is true if $\mathcal{T}(\mathbf{y}) > \zeta$ whereas the hypothesis $\mathcal{H}_0$ is true if $\mathcal{T}(\mathbf{y}) < \zeta$, as shown in Equation (2.2).

$$\mathcal{T}(\mathbf{y}) \underset{\mathcal{H}_0}{\overset{\mathcal{H}_1}{\gtrless}} \zeta \tag{2.2}$$

In general, spectrum sensing needs to be able to reliably detect the presence of PU and leave PU's frequency band as quickly as possible in order to avoid interference to PU. On the other hand, it needs to provide spectrum access opportunities as many as possible to SU. In order to specifically show the performance of spectrum sensing, some indicators are defined as follows [26]:

- **Probability of detection** (P_d)
  It denotes the probability that we decide $\mathcal{H}_1$ when $\mathcal{H}_1$ is true.

$$P_d = P(\mathcal{T}(\mathbf{y}) > \zeta | \mathcal{H}_1) \tag{2.3}$$

- **Probability of miss** (P_m)
  It denotes the probability that we decide $\mathcal{H}_0$ but $\mathcal{H}_1$ is true.

$$P_m = 1 - P_d = P(\mathcal{T}(\mathbf{y}) < \zeta | \mathcal{H}_1) \tag{2.4}$$

- **Probability of false alarm** (P_{fa})
  It denotes the probability that we decide $\mathcal{H}_1$ but $\mathcal{H}_0$ is true.

$$P_{fa} = P(\mathcal{T}(\mathbf{y}) > \zeta | \mathcal{H}_0) \tag{2.5}$$

As shown in Equation (2.3) and Equation (2.5), the high probability of detection indicates that the SU provides reliable protection for PU and the high probability of false alarm indicates that the SU loses spectrum access opportunities. Then, for an outstanding spectrum sensing algorithm, both high probability of detection and low probability of false alarm need to be accomplished as fully as possible. In order to preferably show the performance of spectrum sensing, the receiver operating characteristic (ROC) curve is presented in Figure 2.2, which gives the probability of detection as a function of the probability of false alarm [19]. As shown in Figure 2.2, the ROC curve is a concave function. The better spectrum sensing algorithm is, the deeper the concave of the ROC is. In that case, both a low probability of false alarm and a high probability of detection are obtained. Therefore, the ROC curve is a key indicator to evaluate the performance of spectrum sensing techniques.

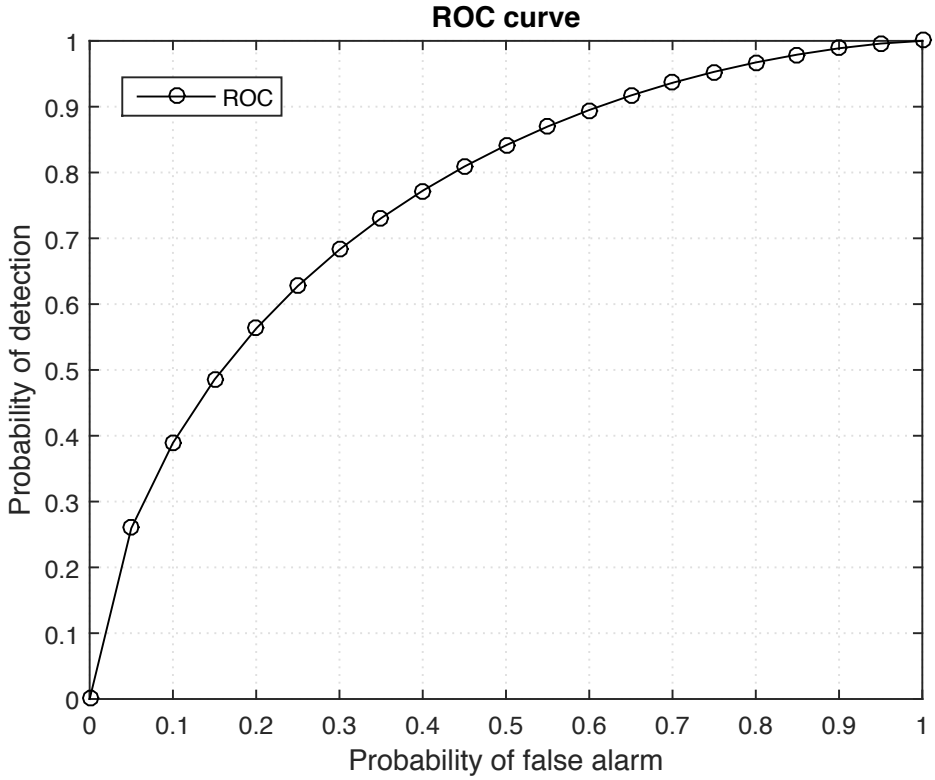

Figure 2.2 – Illustration of the ROC curve in [19].

In addition, other indicators, such as detection sensitivity and sample complexity, can be used to evaluate the performance of spectrum sensing algorithms. Detection sensitivity presents the smallest signal to noise ratio (SNR) of received signal at SU when the probability of detection of SU satisfies some conditions. For example, the detection sensitivities of the digital television (DTV) signal and the wireless microphone signal are respectively determined to -117 dBm (SNR = -22 dB) and -107 dBm (SNR = -12 dB) by IEEE 802.22 working group [27]. Thus, an excellent spectrum sensing method should meet the requirement of the detection sensitivity at least in order to apply it in practical systems. Sample complexity refers to the number of samples N_s, on which spectrum sensing algorithms can achieve some level of performances under certain SNR conditions. It is generally denoted as a function of the SNR, P_{fa} and P_m, and defined as $N_s = \xi(\text{SNR}, P_{fa}, P_m)$ [28]. For reasonable spectrum sensing algorithms, $\xi(\text{SNR}, P_{fa}, P_m)$ is a monotonically decreasing function. For example, the sample complexity of a classic energy detection scales as $N_s = O(1/\text{SNR}^2)$ [29]. These metrics are used together to evaluate the performance of different spectrum sensing algorithms in the rest of this thesis.

2.2 Local spectrum sensing

Local spectrum sensing is substantially a detection process conducted by each SU. It is based on local SU's observation and aims to sense whether the PU signal is present or not in a specific frequency band. Several local spectrum sensing techniques have been studied in the literature [26, 30]. Matched filter detection (MFD) is the optimal method when the PU signal is known [31, 32, 33, 34]. Cyclostationary feature detection (CFD) which requires a prior knowledge of the PU signal characteristics, is robust against noise uncertainty [32, 35, 36]. However, it needs a long observation time and complex computation in order to get a good detection performance. Energy detection (ED) is popular due to its low implementation complexity, but it suffers from the noise uncertainty and requires a large number of samples for achieving a high probability of detection [32, 37, 38, 39]. Waveform based sensing (WBS) as a simplified version of the MFD is also robust to the noise uncertainty, but it also needs a prior knowledge of the PU signal [40, 41, 42]. Eigenvalue based sensing (EBS) is not only robust to noise uncertainty, but also requires no prior information of the PU signal [43, 44, 45, 46, 47, 48, 49, 50]. Unfortunately, it suffers from the long sensing time and the high computational complexity. Goodness of fit (GoF) test based sensing presents an advantage under a small number of samples, which utilizes the distribution characteristics of the background noise and is able to obtain a high detection performance [51, 52, 53, 54, 55, 56, 57, 58]. In addition, wideband sensing has also attracted a lot of interests [22, 59, 60, 61].

Most common local spectrum sensing techniques, which are listed in Figure 2.3, will be briefly explained in the next sections.

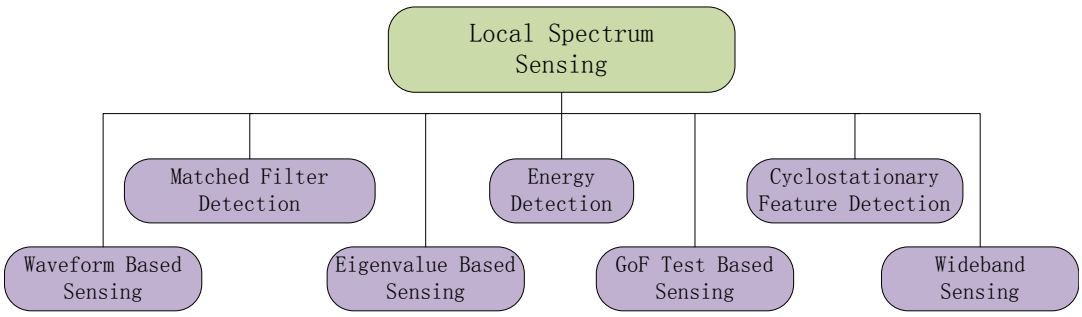

Figure 2.3 – Local spectrum sensing techniques.

2.2.1 Matched filter detection

The matched filter detection, which is a traditional coherent signal detection method, is known as the optimum method when transmitted signal is known at the receiver side [34]. Based on the signal model in (2.1), assume that $y[n]$ is the input to a finite impulse response (FIR) filter with impulse response $h[n]$, where $h[n]$ is nonzero for $n = 0, 1, \cdots, N_s - 1$, then the output at time n is

$$\text{Output}[n] = \sum_{k=0}^{n} h[n-k]y[n]. \tag{2.6}$$

Let the impulse response be a "flipped around" version of the signal $s[n]$ with power σ_s^2 or

$$h[n] = s[N_s - 1 - n] \quad n = 0, 1, \cdots, N_s - 1 \tag{2.7}$$

then

$$\text{Output}[n] = \sum_{k=1}^{n} s[N_s - 1 - (n-k)]y[k]. \tag{2.8}$$

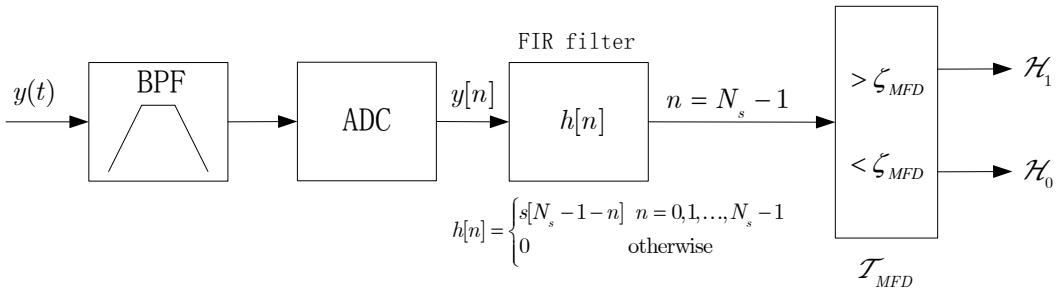

Figure 2.4 – Block diagram of matched filter detection [19].

Define the test statistic of the matched filter detection as the output at time $n = N_s - 1$, which is given by [19]

$$\mathcal{T}_{MFD} = \text{Output}[N_s - 1] = \sum_{k=0}^{N_s-1} s[k]y[k]. \tag{2.9}$$

By comparing this test statistic with a threshold ζ_{MFD}, a decision whether the PU signal is present or not can be made.

The block diagram of matched filter detection is illustrated in Figure 2.4. As shown in Figure 2.4, the received signal $y(t)$ goes through a band pass filter (BPF) to reject out of band noise and adjacent signals, and then Nyquist sampling analogy-to-digital converter (ADC), a FIR filter are applied to get the test statistic $\mathcal{T}_{MFD}$.

The test statistic $\mathcal{T}_{MFD}$ is proved to be Gaussian under either hypothesis [29]. Thus

$$\mathcal{T}_{MFD} \sim \begin{cases} \mathcal{N}(0, \sigma_w^2 \varepsilon), & \mathcal{H}_0 \\ \mathcal{N}(\varepsilon, \sigma_w^2 \varepsilon), & \mathcal{H}_1 \end{cases} \tag{2.10}$$

where $\mathcal{N}$ presents a Gaussian distribution and $\varepsilon = \sum_{n=0}^{N_s-1} s^2[n]$.

Then P_d and P_{fa} can be evaluated as:

$$P_d = Q\big(\frac{\gamma - \varepsilon}{\sqrt{\varepsilon \sigma_w^2}}\big) \tag{2.11}$$

and

$$P_{fa} = Q\big(\frac{\gamma}{\sqrt{\varepsilon \sigma_w^2}}\big), \tag{2.12}$$

respectively, where γ is the SNR at SU and $Q(x) = \int_x^\infty e^{-v^2/2} dv / \sqrt{2\pi}$.

The main advantage of this method is that it maximizes the output SNR for a given signal and needs less detection time because it requires only O(1/SNR) sample to meet a given probability of detection constraint [62]. The minimum number of samples is a function of the SNR $\gamma = \sigma_s^2/\sigma_w^2$, given by [29]

$$N_s = \big(Q^{-1}(P_{fa}) - Q^{-1}(P_d)\big)^2 \gamma^{-1} \tag{2.13}$$

However, in order to get high processing gain and less detection time, this method needs perfect knowledge of PU's signal feature such as bandwidth, modulation type, etc.. And as a coherent detection method, it requires synchronization with PU, which is an unreasonable assumption in most typical spectrum sensing scenarios. In addition, due to various signal types, the implementation complexity of sensing unit is high.

2.2.2 Cyclostationary feature detection

The cyclostationary feature detection is an effective detection method which is implemented based on the cyclostationary property of the received signal [63, 64, 65, 66, 67, 68]. In general, modulated signals are coupled with sine wave carriers, cyclic prefixes, etc., which result in built-in periodicity. Therefore, they can be characterized as cyclostationary. Since the noise is wide-sense stationary with no correlation, the cyclostationary feature based detection can be used for detecting the presence of PU signal. Furthermore, cyclostationary feature can be used for distinguishing among different types of transmissions and PUs [67].

For a cyclostationary process $s[n]$, its mean and autocorrelation are periodic in time. Thus, its cyclic autocorrelation function (CAF) $R^{\alpha}_{ss}[k] = E\big(s[n]s^*[n-k]e^{-j2\pi\alpha n}\big)$ and conjugate cyclic autocorrelation function (CCAF) $R^{\alpha}_{ss^*}[k] = E\big(s[n]s[n-k]e^{-j2\pi\alpha n}\big)$ are nonzero for a set of cyclic frequencies α ($\alpha \neq 0$); on the other hand, for a signal which does not exhibit cyclostationarity, i.e. white Gaussian noise, its CAF $R^{\alpha}_{ww}[k] = 0$ and CCAF $R^{\alpha}_{ww^*}[k] = 0$, $\forall\alpha \neq 0$. Therefore, according to the signal model in Equation (2.1), an estimation of the conjugate cyclic autocorrelation function of the observation samples at cyclic frequency α may be obtained using N_s observations as [67]:

$$\hat{R}^{\alpha}_{yy^*}[k] = \frac{1}{N_s}\sum_{n=1}^{N_s} y[n]y^*[n+k]e^{-j2\pi\alpha n} \tag{2.14}$$

$$= R^{\alpha}_{yy^*}[k] + \varepsilon^{\alpha}_{yy^*}[k] \tag{2.15}$$

where k is the lag parameter in the autocorrelation and $\varepsilon^{\alpha}_{yy^*}[k]$ is the estimation error which vanishes asymptotically as $N_s \to \infty$. In practice, due to the error $\varepsilon^{\alpha}_{yy^*}[k]$, the estimation $\hat{R}^{\alpha}_{yy^*}[k]$ is seldom exactly zero and a decision has to be made whether a given value of $\hat{R}^{\alpha}_{yy^*}[k]$ presents a zero or not [64].

In general, a vector of $\hat{R}^{\alpha}_{yy^*}[k]$ rather than a value is considered in order to check simultaneously for the presence of cycles in a set of lags k.

Let $k_1, k_2, \cdots, k_N$ be a fixed set of lags, α be a candidate cycle-frequency, $\mathcal{A}$ denote the set of cyclic frequencies of interest, and

$$\hat{\mathbf{r}}^{\alpha}_{yy^*} = \Big[\mathcal{R}_e\big\{\hat{R}^{\alpha}_{yy^*}[k_1]\big\}, \cdots, \mathcal{R}_e\big\{\hat{R}^{\alpha}_{yy^*}[k_N]\big\}, \mathcal{I}_m\big\{\hat{R}^{\alpha}_{yy^*}[k_1]\big\}, \cdots, \mathcal{I}_m\big\{\hat{R}^{\alpha}_{yy^*}[k_N]\big\}\Big] \tag{2.16}$$

denote a $1 \times 2N$ vector consisting of the estimated cyclic autocorrelations from (2.14) with $\mathcal{R}_e\{\}$ and $\mathcal{I}_m\{\}$ representing the real and imaginary parts, respectively. If the asymptotic (true) value of $\hat{\mathbf{r}}^{\alpha}_{yy^*}$ is given as $\mathbf{r}^{\alpha}_{yy^*}$

$$\begin{aligned}\mathbf{r}^{\alpha}_{yy^*} = \Big[&\mathcal{R}_e\{R^{\alpha}_{yy^*}[k_1]\}, \cdots, \mathcal{R}_e\{R^{\alpha}_{yy^*}[k_N]\}, \\ &\mathcal{I}_m\{R^{\alpha}_{yy^*}[k_1]\}, \cdots, \mathcal{I}_m\{R^{\alpha}_{yy^*}[k_N]\}\Big],\end{aligned} \tag{2.17}$$

then the estimation in Equation (2.15) becomes

$$\hat{\mathbf{r}}^{\alpha}_{yy^*} = \mathbf{r}^{\alpha}_{yy^*} + \boldsymbol{\varepsilon}^{\alpha}_{yy^*}, \tag{2.18}$$

where

$$\begin{aligned}\boldsymbol{\varepsilon}^{\alpha}_{yy^*} = \Big[&\mathcal{R}_e\{\varepsilon^{\alpha}_{yy^*}[k_1]\}, \cdots, \mathcal{R}_e\{\varepsilon^{\alpha}_{yy^*}[k_N]\}, \\ &\mathcal{I}_m\{\varepsilon^{\alpha}_{yy^*}[k_1]\}, \cdots, \mathcal{I}_m\{\varepsilon^{\alpha}_{yy^*}[k_N]\}\Big].\end{aligned} \tag{2.19}$$

Finally, by finding out whether there exists cyclic components in $\hat{\mathbf{r}}^{\alpha}_{yy^*}$, the hypothesis test in Equation (2.1) is reformulated in the following:

$$\begin{aligned}\mathcal{H}_0 : \quad &\forall \alpha \in \mathcal{A}, \forall \{k_n\}_{n=1}^{N} \quad \Longrightarrow \hat{\mathbf{r}}^{\alpha}_{yy^*} = \boldsymbol{\varepsilon}^{\alpha}_{yy^*} \\ \mathcal{H}_1 : \quad &\alpha \in \mathcal{A}, \text{for some} \{k_n\}_{n=1}^{N} \quad \Longrightarrow \hat{\mathbf{r}}^{\alpha}_{yy^*} = \mathbf{r}^{\alpha}_{yy^*} + \boldsymbol{\varepsilon}^{\alpha}_{yy^*}.\end{aligned} \tag{2.20}$$

The test statistic relying on the estimation $\hat{\mathbf{r}}^{\alpha}_{yy^*}$ is given by [64]

$$\mathcal{T}_{CFD} = N_s \hat{\mathbf{r}}^{\alpha}_{yy^*} \hat{\sum}_{2c}^{-1} (\hat{\mathbf{r}}^{\alpha}_{yy^*})^T \tag{2.21}$$

where $\hat{\sum}_{2c}$ is the covariance matrix of $\hat{\mathbf{r}}^{\alpha}_{yy^*}$, whose computation is given in Appendix A. Under the null hypothesis $\mathcal{H}_0$, $\mathcal{T}_{CFD}$ is asymptotically χ^2_{2N}-distributed. Thus, the probability of false alarm P_{fa} is derived:

$$P_{fa} = P(\mathcal{T}_{CFD} > \zeta_{CFD} | \mathcal{H}_0) = 1 - F_{\chi^2_{2N}}(\zeta_{CFD}), \tag{2.22}$$

where $F_{\chi^2_{2N}}$ is the cumulative distribution function of χ^2_{2N}-distribution and ζ_{CFD} is a threshold. Under the alternative hypothesis $\mathcal{H}_1$, it is proved that the test statistic $\mathcal{T}_{CFD}$

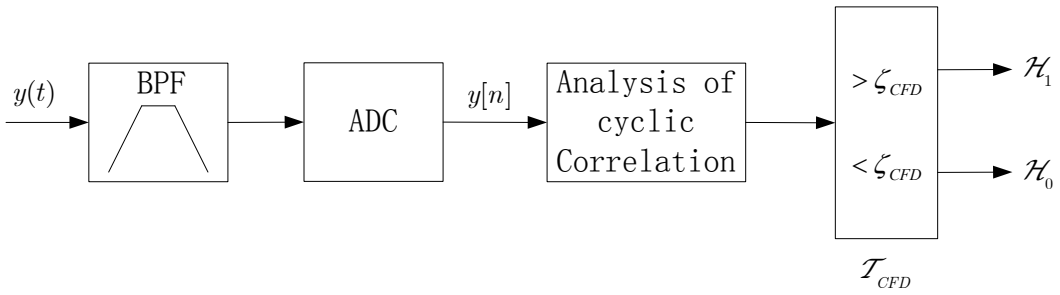

Figure 2.5 – Block diagram of cyclostationary feature detection.

for N_s large enough approximate a Gaussian distribution [64], as follows

$$\mathcal{T}_{CFD} \sim \mathcal{N}(N_s \mathbf{r}^{\alpha}_{yy^*} \sum\nolimits_{2c}^{-1} (\mathbf{r}^{\alpha}_{yy^*})^T, 4N_s \mathbf{r}^{\alpha}_{yy^*} \sum\nolimits_{2c}^{-1} (\mathbf{r}^{\alpha}_{yy^*})^T). \tag{2.23}$$

Therefore, after getting the threshold ζ_{CFD} by Equation (2.22), the probability of detection P_d can be evaluated by

$$P_d = P(\mathcal{T}_{CFD} > \zeta_{CFD} | \mathcal{H}_1) = Q\Big(\frac{\zeta_{CFD} - N_s \mathbf{r}^{\alpha}_{yy^*} \sum_{2c}^{-1} (\mathbf{r}^{\alpha}_{yy^*})^T}{4N_s \mathbf{r}^{\alpha}_{yy^*} \sum_{2c}^{-1} (\mathbf{r}^{\alpha}_{yy^*})^T}\Big). \tag{2.24}$$

The block diagram of cyclostationary feature detection is illustrated in Figure 2.5.

There are various implementations of cyclostationary feature detector in the literature. In [32], two detectors based on estimating the spectral correlation density and the magnitude squared coherence are proposed, which present a good performance in the low SNR. In addition, a hardware implementation of a cyclostationary feature detector is presented in [68], where a detection of 802.11g wireless regional access network (WLAN) signal from air is demonstrated by the cyclostationary feature detector. However, this method also requires a prior knowledge of the signal characteristics, and it needs a long observation time and complex computation.

2.2.3 Energy detection

Energy detection, which is a non-coherent detection method, has been demonstrated to be simple, blind and able to detect the PU signal based on the received energy. A block diagram of ED is shown in Figure 2.6.

In Figure 2.6, the received signal $y(t)$ goes through a BPF to reject out of band noise and adjacent signals, and then Nyquist sampling ADC, square-law device and integrator are applied to measure the signal power at SU, that is the test statistic $\mathcal{T}_{ED}$.

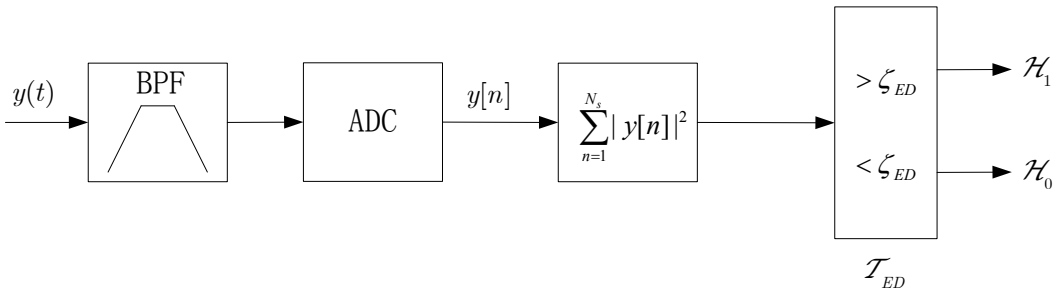

Figure 2.6 – Block diagram of energy detection.

As shown in the following equation:

$$\mathcal{T}_{ED} = \sum_{n=1}^{N_s} |y[n]|^2 \tag{2.25}$$

where $y[n]$ is the n-th sample of the received signal and N_s is the length of the sample.

In order to more comprehensively understand the performance of energy detection, two analyses of ED including exact performance and Gaussian approximation (GA) are considered as follows.

- **Exact performance**

  The test statistic $\mathcal{T}_{ED}$ in Equation (2.25) has been proven to follow a central chi-square (χ^2) distribution with N_s degrees of freedom when there is no signal transmission from PU. Otherwise, it follows a noncentral χ^2 distribution with N_s degrees of freedom and a non centrality parameter $N_s\gamma$ [37, 69]. Following the short-hand notations mentioned at the beginning of Section 2.1, the test statistic can be described as

$$\mathcal{T}_{ED} \sim \begin{cases} \chi^2_{N_s}, & \mathcal{H}_0 \\ \chi^2_{N_s}(N_s\gamma), & \mathcal{H}_1 \end{cases} \tag{2.26}$$

  where γ is the SNR of PU signal at SU.

  Hence, the probability of false alarm and detection can be generally computed

by [70, 71]

$$P_d = P(\mathcal{T}_{ED} > \zeta_{ED}|\mathcal{H}_1) = 1 - F_{\chi^2_{N_s}}\left(\frac{2\zeta_{ED}}{\sigma_x^2 + \sigma_w^2}\right) \tag{2.27}$$

$$P_{fa} = P(\mathcal{T}_{ED} > \zeta_{ED}|\mathcal{H}_0) = 1 - F_{\chi^2_{N_s}}\left(\frac{2\zeta_{ED}}{\sigma_w^2}\right) \tag{2.28}$$

where ζ_{ED} is a predetermined threshold, $F_{\chi^2_{N_s}}$ presents the cumulative distribution function (CDF) of χ^2 distribution with N_s degrees of freedom, σ_x^2 and σ_w^2 denotes the variance of $x[n]$ and $w[n]$.

According to Equations (2.27) and (2.28), by eliminating the threshold ζ_{ED}, the ROC can be obtained as

$$P_d = 1 - F_{\chi^2_{N_s}}\left(\frac{F^{-1}_{\chi^2_{N_s}}(1 - P_{fa})}{1 + \frac{\sigma_x^2}{\sigma_w^2}}\right) \tag{2.29}$$

where $\frac{\sigma_x^2}{\sigma_w^2} = \gamma$ is the SNR and $F^{-1}_{\chi^2_{N_s}}$ is the inverse function $F_{\chi^2_{N_s}}$.

In the exact performance analysis, in order to achieve a prescribed performance (P_{fa}, P_d) for a given SNR γ, the minimum number of samples N_s needs to be exactly calculated. Because N_s can not be obtained from Equation (2.29), it is necessary to execute multiple evaluations of two-dimensional functions such as $F_{\chi^2_N}$ and $F^{-1}_{\chi^2_N}$, which has a huge computational complexity in exact χ^2 distribution performance analysis [13].

- **Gaussian approximation**

  In order to use low-complexity analytical expressions about the required number of samples, it has been extensively shown that the test statistics $\mathcal{T}_{ED}$ can be well approximated as a Gaussian distribution $\mathcal{N}$. This is because the central limit theorem conditions are satisfied by the large number of the received samples (e.g. N_s >200). As a result, the following expressions are obtained.

$$\mathcal{T}_{ED} \sim \begin{cases} \mathcal{N}(N_s, 2N_s), & \mathcal{H}_0 \\ \mathcal{N}(N_s(\gamma+1), 2N_s(2\gamma+1)), & \mathcal{H}_1 \end{cases} \tag{2.30}$$

Then, in this case, the performance indicators P_d and P_{fa} can be written as

$$P_d = \frac{1}{\sqrt{2\pi}\sigma_1} \int_{\zeta_{ED}}^{\infty} \exp\Big(\frac{-(t-\mu_1)^2}{2\sigma_1^2}\Big) dt \tag{2.31}$$

$$= Q\big(\frac{\zeta_{ED} - \mu_1}{\sigma_1}\big) \tag{2.32}$$

and

$$P_{fa} = \frac{1}{\sqrt{2\pi}\sigma_0} \int_{\zeta_{ED}}^{\infty} \exp\Big(\frac{-(t-\mu_0)^2}{2\sigma_0^2}\Big) dt \tag{2.33}$$

$$= Q\big(\frac{\zeta_{ED} - \mu_0}{\sigma_0}\big), \tag{2.34}$$

respectively, where $\mu_0 = N_s$, $\mu_1 = N_s(\gamma + 1)$ and $\sigma_0^2 = 2N_s$, $\sigma_1^2 = 2N_s(2\gamma + 1)$ are the means and variances of the Gaussian distribution in Equation (2.30) under both hypotheses H_0 and H_1. Combining Equations (2.30), (2.32) and (2.34), Equation (2.29) becomes

$$P_d = Q\Big((1+\gamma)^{-1} Q^{-1}(P_{fa}) - \gamma(1+\gamma)^{-1}\sqrt{N_s}\Big) \tag{2.35}$$

where $Q(x) = \int_x^{\infty} e^{-v^2/2} dv/\sqrt{2\pi}$ and Q^{-1} is the inverse function of Q. Clearly, for a fixed P_{fa} in Equation (2.35), with the increasing of the samples N_s, the probability of detection P_d rises up at any SNR. That is to say, if the sensing time is arbitrarily long, $P_d \to 1$. However, in practice, this is typically not the case.

The Figure 2.7 shows the ROC comparison of ED for the exact χ^2 model and the Gaussian approximation model when the SNR γ = -5 dB. As shown, the classical GA in Equation (2.35) significantly deviates from the exact result in Equation (2.29). Conversely, with the increase of the number of samples from $N_s = 10$ to $N_s = 100$, the deviated distance is clearly reduced. This also verifies that the Gaussian approximation of ED is a good estimation only when the number of samples N_s is sufficiently high.

In addition, the effect of the uncertainty of noise power is also a disadvantage of ED. In ED, a decision whether the PU signal exists or not is simply made by comparing the statistic $\mathcal{T}_{ED}$ with the noise power. Thus, accurate knowledge of the noise power is necessary to get a reliable detection performance. However, in practice, the noise uncertainty is always present. Assume that the estimated noise power is $\hat{\sigma}_w^2 = \beta\sigma_w^2$

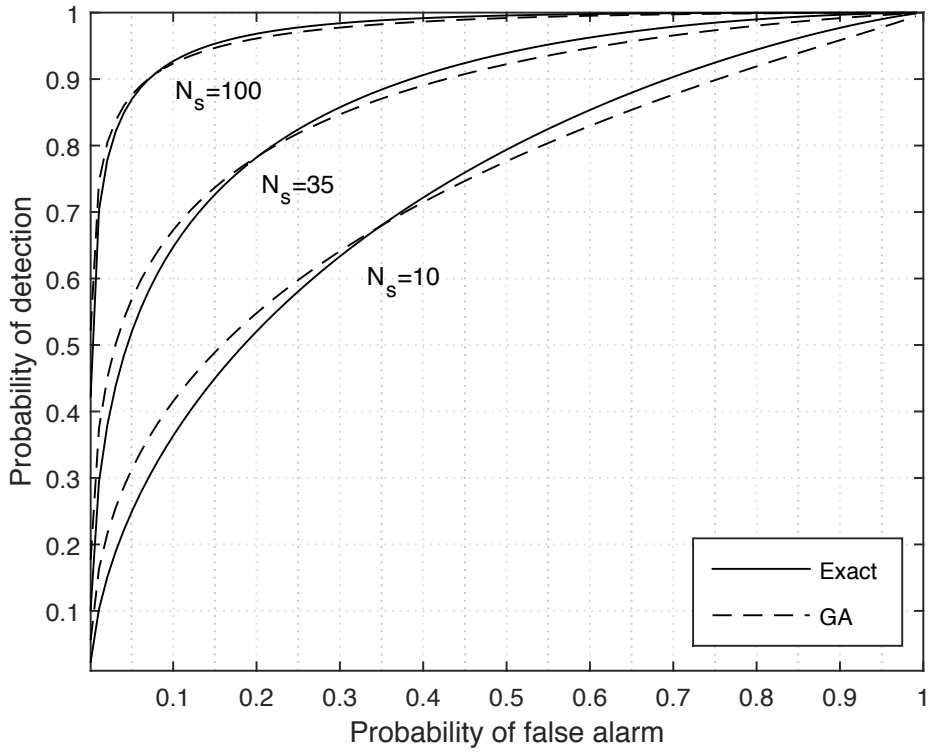

Figure 2.7 – The ROC comparison of ED for the exact chi-squared model and the Gaussian approximation model.

where β is called the noise uncertainty factor. The bound of the noise uncertainty (in dB) is defined as [72]

$$\mathcal{B} = \sup\left\{10\log_{10}\beta\right\}. \tag{2.36}$$

And β (in dB) is evenly distributed in an interval $[-\mathcal{B}, \mathcal{B}]$. When the noise uncertainty exists, ED is not a reliable sensing method [73]. However, ED still becomes one of the most popular sensing techniques in cooperative spectrum sensing because of its simple operations and no requirement on a prior knowledge of PU signals.

2.2.4 Waveform based sensing

Waveform-based sensing (WBS) aims to detect a prior known signals or sequences expected with the PU signal through correlation detection [21, 40, 41, 42], which is a simplified version of the matched filter detection where the exact PU signal is required. Many wireless systems introduce known pre-patterns such as preambles, transmitted pilot patterns, spreading sequences, etc. to assist synchronization or for other purposes. Correlation between the received signal and a known copy of itself can be used to detect the presence of a PU signal exhibiting this pattern. As shown in [40], waveform-based sensing has better detection performance and requires shorter sensing time over the energy detection. However, WBS needs to assume that a pattern exists in the PU signal, and SU must know and detect this information. Especially when a wide range of PU needs to be detected, the database of known pattern for SU may become large and complex to manage. Moreover, synchronisation is required between PU and SU and an error of synchronization can severely degrade the detection performance. Comparing with the matched filter detection, waveform based sensing has a lower complexity [21].

2.2.5 Eigenvalue based sensing

As a result of requiring no prior information of the PU signal or no noise variance, eigenvalue based detection has been widely investigated for blind spectrum sensing methods in CR [43, 44, 45, 46, 47, 48, 49, 50]. Those eigenvalue based methods usually utilize the correlation structure inherent in the received data for sensing, which results from the multipath propagation and/or oversampling of the PUs signal for a single-antenna receiver or the deterministic channel during the sensing period for a multiantenna receiver. It also involves that the statistical covariance matrices or the eigenvalues of the covariance matrix of signal and noise are different. Thus, the dif-

ference is used to differentiate the signal component from background noise in those eigenvalue based methods where the knowledge of the noise variance is not required.

Considering L (called "smoothing factor") consecutive samples and defining the following vectors:

$$\boldsymbol{y} \overset{\text{def}}{=} \begin{bmatrix} y[n] & y[n-1] & y[n-2] \dots y[n-L+1] \end{bmatrix}^T \tag{2.37}$$

$$\boldsymbol{x} \overset{\text{def}}{=} \begin{bmatrix} x[n] & x[n-1] & x[n-2] \dots x[n-L+1] \end{bmatrix}^T \tag{2.38}$$

$$\boldsymbol{w} \overset{\text{def}}{=} \begin{bmatrix} w[n] & w[n-1] & w[n-2] \dots w[n-L+1] \end{bmatrix}^T. \tag{2.39}$$

We can define the statistical covariance matrices of the received signal, the transmitted signal passing through a wireless channel and the corresponding noise as

$$\mathbf{R}_y = \mathrm{E}\big[\boldsymbol{y}\boldsymbol{y}^H\big], \tag{2.40}$$

$$\mathbf{R}_x = \mathrm{E}\big[\boldsymbol{x}\boldsymbol{x}^H\big], \tag{2.41}$$

$$\mathbf{R}_w = \mathrm{E}\big[\boldsymbol{w}\boldsymbol{w}^H\big]. \tag{2.42}$$

where $(\cdot)^H$ denotes the conjugate transpose and $\mathrm{E}[\cdot]$ is the mathematical expectation.

According to Equations (2.37 - 2.42), the hypothesis test in Equation (2.1) can be reformulated as follows:

$$\begin{aligned} \mathcal{H}_0 &: \mathbf{R}_y = \mathbf{R}_w \\ \mathcal{H}_1 &: \mathbf{R}_y = \mathbf{R}_x + \mathbf{R}_w, \end{aligned} \tag{2.43}$$

In practice, a finite number of samples can be obtained for calculating the statistical covariance matrix. Define the sample auto-correlations of the received signal as

$$\delta(k) = \lim_{N_s \to \infty} \frac{1}{N_s} \sum_{n=0}^{N_s-1} y[n]y[n-k], \qquad k = 0, 1, \dots, L-1. \tag{2.44}$$

where N_s is the number of collected samples.

Then, statistical covariance matrix $\mathbf{R}_{\boldsymbol{y}}$ can be approximated by the sample covari-

ance matrix defined as

$$\mathbf{R}_{\boldsymbol{y}}(N_s) = \begin{bmatrix} \delta(0) & \delta(1) & \cdots & \delta(L-1) \\ \delta(1) & \delta(0) & \cdots & \delta(L-2) \\ \vdots & \vdots & \ddots & \vdots \\ \delta(L-1) & \delta(L-2) & \cdots & \delta(0) \end{bmatrix} \tag{2.45}$$

where the sample covariance matrix is a Toeplitz matrix, and it is also symmetric. The eigenvalues of $\mathbf{R}_{\boldsymbol{y}}(N_s)$ are defined as $\lambda_1 \geq \lambda_2 \geq \ldots \geq \lambda_L$.

Depending on the difference of the statistical covariance matrices or its eigenvalue between signal and noise, several covariance matrix or eigenvalue based methods have been proposed in literature [50], such as the maximum-minimum eigenvalue (MME) method [14], the eigenvalue arithmetic-to-geometric mean (AGM) method [15], the covariance absolute value (CAV) method [16], the scaled largest eigenvalue (SLE) method [17] and the function of matrix based detection (FMD) method [18]. These methods will be explained in the following.

- **Maximum-minimum eigenvalue (MME) method:**
  The MME method firstly takes advantage of the ratio of the maximum over the minimum eigenvalue of the sample covariance matrix, that is, $\lambda_{max}/\lambda_{min}$, in order to decide that the PU signal is present or not. The test statistic of the MME method is given by [14]

$$\mathcal{T}_{MME} = \frac{\lambda_{max}}{\lambda_{min}} \underset{\mathcal{H}_0}{\overset{\mathcal{H}_1}{\gtrless}} \zeta_{MME}, \tag{2.46}$$

  where ζ_{MME} is the decision threshold. If $\lambda_{max}/\lambda_{min} > \zeta_{MME}$, the signal exists; otherwise, the signal does not exist. The MME method overcomes the noise uncertainty problem and can even perform better than the energy detection when the samples of the signal to be detected are highly correlated.

- **Arithmetic-to-geometric mean (AGM) method:**
  The AGM method is derived from a generalized likelihood ratio test (GLRT), which only depends on the observations through $\hat{\mathbf{R}}_{\boldsymbol{y}}(N_s)$. The test statistic is based on the ratio of the arithmetic mean over the geometric mean of the eigen-

values of the sample covariance matrix, which is given by [15]

$$\mathcal{T}_{AGM} = \frac{\frac{1}{L}\sum_{i=1}^{L}\lambda_i}{(\prod_{i=1}^{L}\lambda_i)^{\frac{1}{L}}} \underset{\mathcal{H}_0}{\overset{\mathcal{H}_1}{\gtrless}} \zeta_{AGM} \tag{2.47}$$

where $\lambda_1 \geq \lambda_2 \geq \ldots \geq \lambda_L$ are the decreasing sampling eigenvalues of $\hat{\mathbf{R}}_{\boldsymbol{y}}(N_s)$ and ζ_{AGM} is the decision threshold of the AGM method.

- **Covariance absolute value (CAV) method:**
  The CAV method makes use of the difference of the statistical covariances of the received signal and noise. When signal is not present, $\mathbf{R}_x = 0$. Hence, $\mathbf{R}_y = \mathbf{R}_w = \sigma_w^2\mathbf{I}_L$, its off-diagonal elements are all zeros. When there is a signal and the signal samples are correlated, $\mathbf{R}_x$ is not a diagonal matrix. Hence, $\mathbf{R}_y = \mathbf{R}_x + \sigma_w^2\mathbf{I}_L$, some of its off-diagonal elements should be nonzeros. According to this, the test statistic of the CAV method is given by [16]

$$\mathcal{T}_{CAV} = \frac{T_1}{T_2} \underset{\mathcal{H}_0}{\overset{\mathcal{H}_1}{\gtrless}} \zeta_{CAV} \tag{2.48}$$

  where ζ_{CAV} is the decision threshold of the CAV method, and the two values T_1 and T_2 are calculated by

$$T_1 = \frac{1}{L}\sum_{i=1}^{L}\sum_{j=1}^{L}|r_{i,j}| \tag{2.49}$$

$$T_2 = \frac{1}{L}\sum_{i=1}^{L}|r_{i,i}| \tag{2.50}$$

  where $r_{i,j}$ is the (i,j) entry of the sample covariance matrix $\hat{\mathbf{R}}_{\boldsymbol{y}}(N_s)$.

- **Scaled largest eigenvalue (SLE) method:**
  When the number of PUs (or rank) is a priori known, the accurate generalized likelihood ratio (GLR) method is proposed [17]. In the presence of a signal PU, the rank-1 GLR detector employs the SLE as its statistic, which is called the SLE method and is expressed as

$$\mathcal{T}_{SLE} = \frac{\lambda_1}{\frac{1}{L}\sum_{i=1}^{L}\lambda_i} \underset{\mathcal{H}_0}{\overset{\mathcal{H}_1}{\gtrless}} \zeta_{SLE} \tag{2.51}$$

- **Function of matrix based detection (FMD) method:**
  In the FMD method, the trace operation is utilized to distinguish the PU signal presence or absence, where the FMD method makes use of the monotonically increasing property of function of covariance matrix. For example, as known, the covariance matrix $\mathbf{R}_x$ is a positive semi-definite matrix with low rank, then $\mathbf{R}_x + \mathbf{R}_w > \mathbf{R}_w$. Based on the monotonically increasing property of trace operation, as a result $T_r(\mathbf{R}_x + \mathbf{R}_w) > T_r(\mathbf{R}_w)$ is obtained. Thus, the existence of PU can be detected. The test statistic of the FMD method is given by [18]

$$\mathcal{T}_{FMD} = T_r(\mathbf{R}_y) \underset{\mathcal{H}_0}{\overset{\mathcal{H}_1}{\gtrless}} \zeta_{FMD}, \tag{2.52}$$

  where $T_r(\cdot)$ is the trace operation and ζ_{FMD} is the threshold of the FMD method. The FMD method does not require the prior information of structure of PU signal, and it is able to work under extremely low SNR with limited sample data.

Algorithm 2.1 Pseudo code of eigenvalue based sensing

$\zeta \leftarrow$ Set the decision threshold
$\mathbf{y} \leftarrow$ Receive the sensing segment
$\hat{\mathbf{R}}_{\mathbf{y}}(N_s) \leftarrow$ Compute the sample covariance matrix according to Equation (2.45)
$\lambda_i \ (i = 1, 2, \cdots, L) \leftarrow$ Obtain the eigenvalue of the matrix $\hat{\mathbf{R}}_{\mathbf{y}}(N_s)$
$\mathcal{T} \leftarrow$ Calculate the test statistic
if $\mathcal{T} > \zeta$ **then**
    PU signal exists
else
    PU signal does not exist
end if

Considering the mentioned methods above, the pseudo code of eigenvalue based method is given in Algorithm 2.1.

In Algorithm 2.1, the decision threshold ζ can be determined by solving $F(\zeta) = 1 - P_{fa}$, where $F(x)$ is the cumulative density function (CDF) of the statistic under $\mathcal{H}_0$. The CDF can be determined via theoretical derivation or Monte Carlo simulation. Note that the major computational complexity of eigenvalue based sensing comes from computation of the covariance matrix, the eigenvalue decomposition (EVD) of the covariance matrix and computation of the test statistic $\mathcal{T}$. According to this, various methods present different complexity. The computational complexity of MME, AGM, CAV, SLE and FMD are summarized in Table 2.1 [50].

As mentioned above, numerous covariance matrix or eigenvalue based detection

Table 2.1 – Number of flops required in different eigenvalue based methods [50].

Method	Calculation of $\hat{\mathbf{R}}_y(N_s)$	EVD of $\hat{\mathbf{R}}_y(N_s)$	Norm of $\hat{\mathbf{R}}_y(N_s)$	Total
MME AGM SLE	L^2N_s	$\mathcal{O}(L^3)$	–	$L^2N_s + \mathcal{O}(L^3)$
CAV	L^2N_s	–	L^2	$L^2(N_s+1)$
FMD	L^2N_s	–	–	L^2N_s

methods have been proposed, which overcome the noise uncertainty problem and can even perform better than the energy detection. Moreover, there are no requirement of the prior information of the PU signal. In addition to these advantages, most of them have also some limits: the long sensing time (large sample size) and the high computational complexity mainly resulting from the computation of the covariance matrix and the eigenvalue decomposition of the covariance matrix. These limits hinder the eigenvalue based detection to be applied in some practical applications. Therefore, in order to overcome these problems, some new eigenvalue based method with small sample size are proposed [50, 74, 75]. In [74], based on the latest development in multivariate analysis of variance, the distribution of the largest eigenvalue of finite sample covariance matrix is approximated as the form of sum of two gamma random variables referring to the moment generating function of the distribution of the largest eigenvalue and confluent form of Lauricella function. It is shown that the proposed approximation can obtain a better detection performance for finite number of samples. In [75], a cumulative spectrum sensing method with small data sets is proposed, where oracle-approximating shrinkage estimation is utilized to get an accurate estimate of the true covariance matrix. Concentration inequalities of statistics is also adopted to demonstrate that the proposed method can work in a lower SNR with small data sets.

2.2.6 GoF test based sensing

In order to get a practical approach, the GoF test based detection is proposed which utilizes the distribution characteristics of the background noise and can be easily extended to make use of the empirical cumulative density function, thus resulting in a high detection performance [51, 52, 53, 54].

In the GoF test based detection, let $y[n]$ $(n = 1, 2, \cdots, N_s)$ denote N_s local time-domain observation samples at SU. Without loss of generality, each $y[n]$ is assumed

to be real-valued; otherwise, replace $y[n]$ by its real and imaginary parts. In situations when there is no signal transmission from the primary user, $y[1], \ldots, y[N_s]$ are only the noise samples. In this case, they can be regarded as an independent and identically distribution (i.i.d.) sequence with common cumulative distribution function $F_0(y)$. However, on basis of the kind of modulation and the channel characteristics, the observations $y[1], \ldots, y[N_s]$ may not come from the distribution function $F_0(y)$ when there is a signal from the primary user. Therefore, the spectrum sensing problem is now equivalent to testing the null hypothesis

$$\mathcal{H}_0 : y \text{ is an i.i.d sequence drawn with distribution } F_0(y) \tag{2.53}$$

against the general alternative that y is not an i.i.d. sequence drawn with distribution $F_0(y)$. In other words, for the GoF test based detection, the binary hypotheses of spectrum sensing at the beginning of this section can be formulated as follows:

$$\mathcal{H}_0 : F(y) = F_0(y), \tag{2.54}$$

$$\mathcal{H}_1 : F(y) \neq F_0(y). \tag{2.55}$$

where $F(y)$ is the empirical CDF of the observation samples and can be calculated by

$$F(y) = |\{i : Y_i \leq y, 1 \leq i \leq N_s\}|/N_s, \tag{2.56}$$

where for any finite set $\mathcal{S}$, $|\mathcal{S}|$ denotes the cardinality of $\mathcal{S}$. Note that in this GoF test formula, there is no need of the knowledge of any information about the PU signal and arbitrary noise distribution $F_0(y)$ can be assumed.

Depending on how to measure the distance between two distributions $F(y)$ and $F_0(y)$, many GoF tests have been proposed in literature [24, 76], such as Shapiro-Wilk (SW) test, Kolmogorov-Smirnov (KS) test, Cramer-Von Mises (CM) test and Anderson-Darling (AD) test. In the following, KS test, CM test and AD test are briefly explained, which all perform well with small sample sizes [77].

- **Kolmogorov-Smirnov (KS) Test:**
  In KS test, relying on the empirical CDF of the observation samples and the reference CDF, the largest absolute distance between the two CDFs is used as the GoF test statistic given by

$$\mathcal{T}_{\text{KS}} = \sup\{|F(y) - F_0(y)| : -\infty < y < \infty\}, \tag{2.57}$$

where $\sup\{\cdot\}$ is a supremum function which denotes the maximum element of the set.

- **Cramer-Von Mises (CM) Test:**
  The CM test is an alternative to the KS test, whose statistic is defined by

$$\mathcal{T}_{\text{CM}} = N_s \int_{-\infty}^{\infty} \big(F(y) - F_0(y)\big)^2 dF_0(y). \tag{2.58}$$

  According to [24], and by breaking the integral into N_s parts, $\mathcal{T}_{\text{CM}}$ can be approximated as

$$\mathcal{T}_{\text{CM}} = \frac{1}{12N_s} + \sum_{n=1}^{N_s} \big(F_0(y[n]) - \frac{2n-1}{2N_s}\big)^2. \tag{2.59}$$

- **Anderson-Darling (AD) Test:**
  As shown in Equation (2.59), the CM test statistic $\mathcal{T}_{\text{CM}}$ does not give enough weight to the tails of the distribution $F_0(y)$. Thus, Anderson and Darling generalized the CM test statistic in order to enhance the difference between the lower and upper tails of the distribution. By introducing a weight function, the AD test statistic is proposed as follows:

$$\mathcal{T}_{\text{AD}} = N_s \int_{-\infty}^{\infty} \big(F(y) - F_0(y)\big)^2 \phi(F_0(y)) dF_0(y), \tag{2.60}$$

  where $\phi(t)$ is a non-negative weight function defined over $0 \leq t \leq 1$. As the AD statistic, the weight function $\phi(t)$ is selected to be $\phi(t) = 1/(t(1-t))$.

  The expression of $\mathcal{T}_{\text{AD}}$ can be also simplified to:

$$\mathcal{T}_{\text{AD}} = -N_s - \frac{1}{N_s} \sum_{n=1}^{N_s} (2n-1)(\ln Z_n + \ln(1 - Z_{N_s+1-n})), \tag{2.61}$$

  where $Z_n = F_0(y[n])$.

After obtaining the GoF test statistic $\mathcal{T}$ (that is one of $\mathcal{T}_{KS}, \mathcal{T}_{CM}$ and $\mathcal{T}_{AD}$), if $\mathcal{T} > \zeta$, reject the null hypothesis H_0 and agree with the presence of signal transmission; otherwise, declare that the channel is vacant. Algorithm 2.2 gives the pseudo code of the GoF test based sensing.

Each kind of GoF test is appropriate to a specific distribution and various GoF test based methods are proposed [78, 79]. In [80], the AD test based detection is pro-

Algorithm 2.2 Pseudo code of GoF test based sensing

```
ζ ← Set the decision threshold according to the reference [24]
y[n] (n = 1, 2, ··· , N_s) ← Obtain the observation samples
Sort the sequence y[n] in increasing order such as y[1] ≤ y[2] ≤ ··· ≤ y[N_s]
T ← Calculate the test statistic
if T > ζ then
    PU signal exists
else
    PU signal does not exist
end if
```

posed, where both analysis and simulation results show that under the same detection conditions and channel environments, the detection performance of the AD test based method outperforms ED, especially with a low SNR at SU. In [81], the KS test based spectrum sensing method offers superior detection performance and faster detection than ED and eigenvalue based detection. In [57], a new GoF test with a unilateral alternative hypothesis for spectrum sensing is proposed, which is able to obtain an improvement of the detection performance under low computational complexity. And it also evaluates that the superiority of the AD test based methods over the KS and CM test based methods. In summary, most GoF test based spectrum sensing methods show the similar advantages that there is no requirements of the prior knowledge of PU signal, the computational complexity is low and a better detection performance can be obtained even under the small number of samples.

In the end, a basic comparison of the various local spectrum sensing methods mentioned in this section is presented in Figure 2.8. It is evident that matched filter detection has highest accuracy and waveform based sensing has the second highest accuracy. It results from the coherent processing from using deterministic signal component, but a prior information about PU signal's characteristics should be known in advance. Similarly, energy detection is least accurate compared to other approaches, as shown in Figure 2.8. That is because the performance of energy detection is limited by the noise uncertainty. But it is still one of the most popular methods in cooperative spectrum sensing because of the least complexity of implementation. For other approaches, cyclostationary feature detection can get a higher accuracy than energy detection under the condition of non-stationary noise. In addition, eigenvalue based sensing and GoF test based sensing have obviously higher accuracy then energy detection, and they do not need a prior knowledge of PU signal.

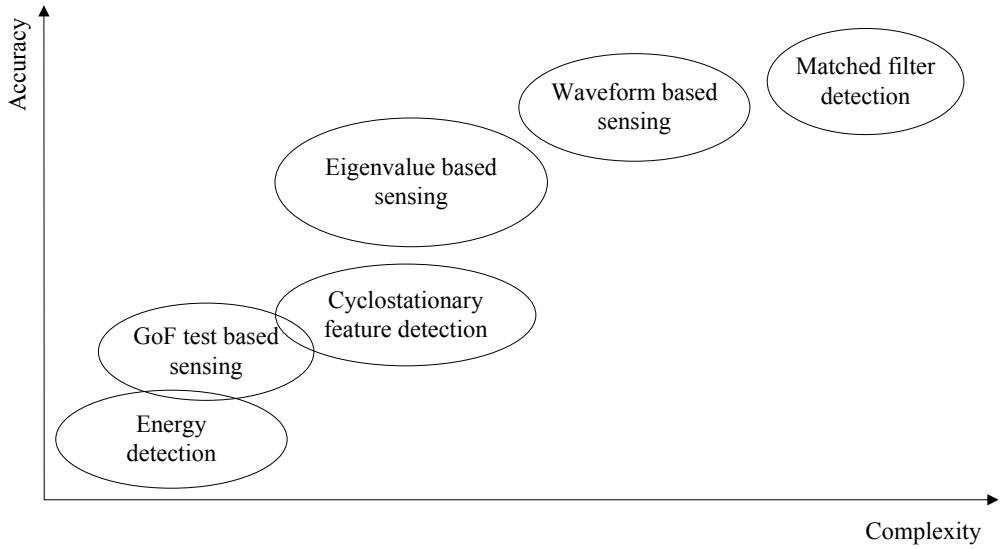

Figure 2.8 – Sensing accuracy and complexity of various sensing methods [20, 21].

2.3 Wideband spectrum sensing

Wideband spectrum sensing aims to find more spectral opportunities over a wide frequency range, for example, the ultra-high-frequency (UHF) TV band (between 300 MHz and 3 GHz), and achieve higher opportunistic aggregate throughput. According to the difference of sampling rate, wideband sensing can be broadly categorized into two types: traditional Nyquist wideband sensing and sub-Nyquist wideband sensing.

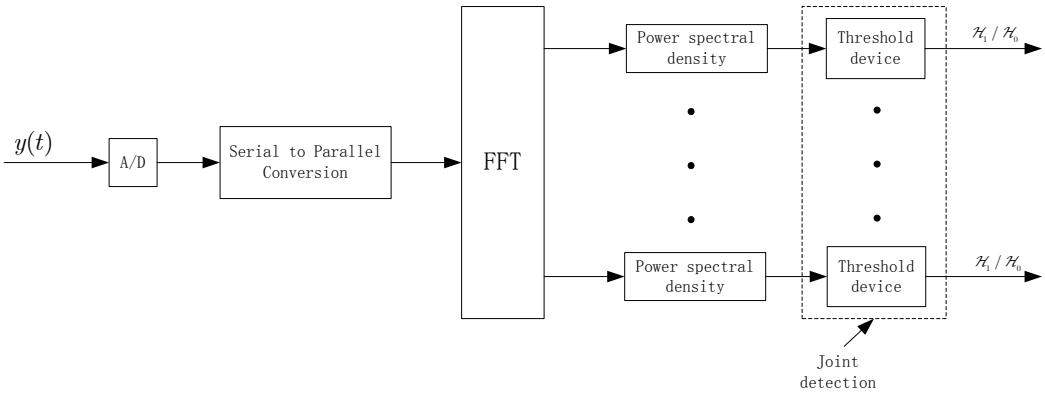

Figure 2.9 – Block diagrams of traditional Nyquist wideband sensing based on multi-band joint detection [22].

- **Traditional Nyquist wideband sensing**

  Traditional Nyquist wideband sensing usually acquires the wideband signal us-

ing a standard ADC at or above the Nyquist rate and then utilizes signal processing techniques to detect spectral opportunities. For example, a multiband joint detection method is proposed in [22] which is based on a simple detection structure (Figure 2.9) and can sense the PU signal over multiple frequency bands. However, it's worth noting that sampling signals in the traditional Nyquist wideband sensing follow Shannon's theorem: the sampling frequency should be at least twice the highest frequency contained in the signal to avoid aliasing. It is very difficult to achieve such sampling frequency when the frequency band to be detected is too wide. For example, if the wideband signal has frequency rang $5 \sim 10$ GHz, the sampling rate should be at least 20 GHz, which is a significant challenges for the implementation of the high-rate ADC.

- **Sub-Nyquist wideband sensing**
  Facing the disadvantages of high sampling rate in the traditional Nyquist wideband sensing, sub-Nyquist based wideband sensing methods are proposed that mainly include two methods: multichannel sub-Nyquist wideband sensing referring to the processing of dividing the wideband channel into multiple and jointly sensing transmission opportunities on those channels, and compressive sensing based wideband sensing focusing on the sparsity of the signal to be exploited. In the following, some discussions and comparisons regarding these methods are presented.

  — **Compressive sensing based wideband sensing**
  Due to the inherent sparsity of the wideband spectrum, compressive sensing becomes a promising candidate to realize wideband sensing. The compressive sensing is able to efficiently acquire a signal using relatively few measurements and reconstruct it [82]. Authors of [59] introduce compressive sensing theory for wideband spectrum, where sub-Nyquist rate samples are utilized to detect and classify frequency bands via a wavelet-based edge detector. The robustness to noise is improved since spectrum location estimation takes priority over fine-scale signal reconstruction. Moreover, considering the acquisition cost and the implementation of compressive sensing in the analog domain, [83] and [60] propose a distributed compressive wideband sensing, which are based on a decentralized consensus optimization algorithm, and an analog-to-information converter relying on a new type of data acquisition system called a random demodulator, respectively.

— **Multichannel sub-Nyquist wideband sensing**
The multiband sensing problem can be reduced to a binary hypothesis test if all subchannels are independent. However, in practice the primary user occupancy can be correlated [84]. In this case, the detection problem becomes a composite hypothesis test and a huge complexity of the optimal detector appears with the increasing of the number of subchannels. Therefore, many multichannel sub-Nyquist wideband sensing methods have considered joint spectrum sensing and efficient resource utilization. In [61], an asynchronous multirate wideband sensing method is proposed where sub-Nyquist sampling is induced in each sampling branch to wrap the sparse spectrum occupancy map to itself. The sensing requirements are therefore significantly reduced.

In a word, various wideband sensing methods have been proposed, which are able to obtain more spectral opportunities over a wide frequency range. And each wideband sensing method mentioned above has some advantages and disadvantages. A summary of these wideband sensing methods is shown in Table 2.2.

Table 2.2 – Summary of wideband sensing methods with advantages and disadvantages.

Type	Traditional Nyquist WS	Compressive sensing based WS	Multichannel sub-Nyquist WS
Advantage	Simple structure	Low sampling rate, signal acquisition cost	Low sampling rate, robust model mismatch
Disadvantage	High sampling rate, energy cost	Sensitive to design imperfections	Require multiple sampling channels

2.4 Cooperative spectrum sensing

Local spectrum sensing has a number of limitations. First of all, the detection sensitivity of a single detector can not meet the requirement of PU signal because of the limits of processing and energy. Furthermore, local spectrum sensing can miss the detection of PU who experiences a deep fading. Moreover, the SU who is shadowed might not detect the PU signal, and then may try to utilize the frequency band of PU when in the presence of PU. That is known as the hidden terminal problem. In order

to effectively improve the detection sensitivity of SS and make it more robust against depth attenuation, multipath shadows and the hidden terminal, cooperative spectrum sensing is considered.

Cooperative spectrum sensing generally utilizes more than one detectors and combines their results to make a more reliable decision. According to the different collaboration model, cooperative spectrum sensing technology is classified into two categories: centralized cooperative spectrum sensing and distributed cooperative spectrum sensing.

- **Centralized cooperative spectrum sensing**
  In centralized cooperative spectrum sensing techniques, multiple sensor nodes (SUs) distributed in different locations firstly independently sense the local environment, and then transmit the sensing information to a central unity called fusion center (FC), finally the FC makes the decision whether PU is present or not on basis of the received information and diffuses the decision back to each SU. The diagram of the centralized cooperative spectrum sensing is shown in Figure 2.10.

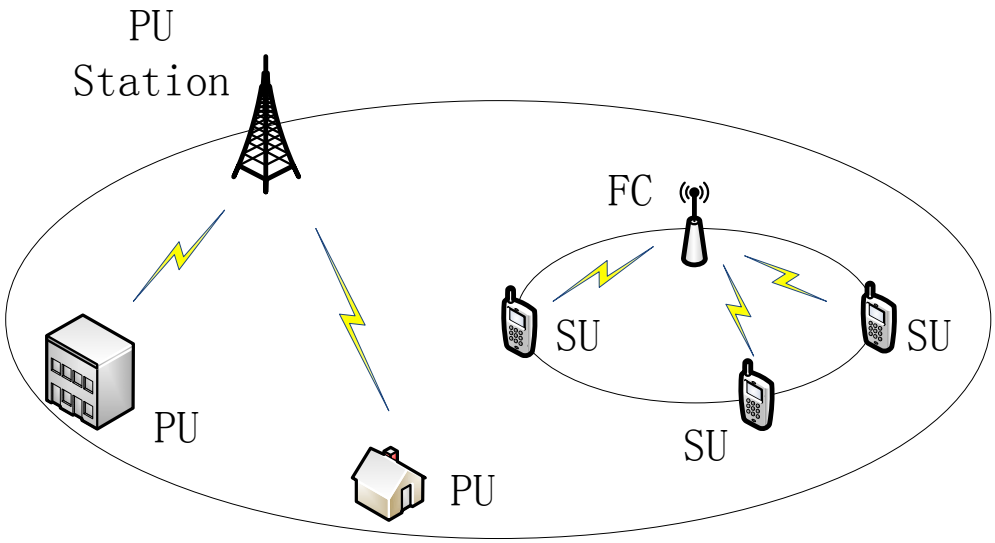

Figure 2.10 – The diagram of centralized cooperative spectrum sensing.

- **Distributed cooperative spectrum sensing**
  In distributed cooperative spectrum sensing, due to lack of a central cooperator, it works in a distributed manner. The SUs share their information among themselves and update periodically on the spectrum information table in order

to reach an unanimous collaborative decision, which thus occupies more storage and consumes more energy than those nodes in the centralized CSS. The diagram of the distributed cooperative spectrum sensing is shown in Figure 2.11.

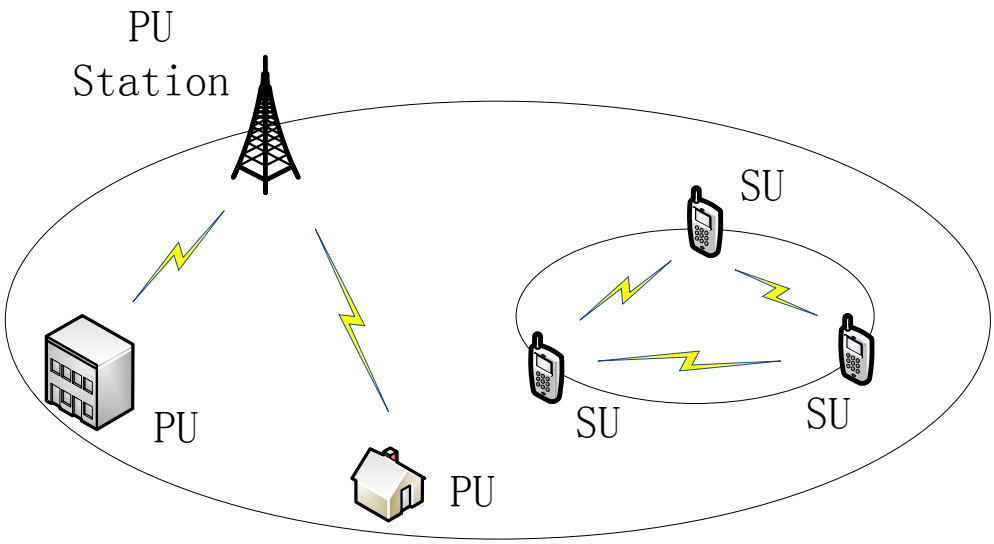

Figure 2.11 – The diagram of distributed cooperative spectrum sensing.

Based on the discussion above, for the centralized and distributed cooperative spectrum sensing, the final decision which is made by SU or FC depends on data fusion. According to the way of fusing information, cooperative spectrum sensing techniques can also be grouped into hard-decision combining or soft-decision combining. If SU is sending signal characteristic about the presence or absence of the PU by using 1 bit of information, this is called hard-decision combining. If SU directly transmits the received information or the test statistics calculated from its local observation, this is called soft-decision combining.

2.4.1 Hard-decision combining data fusion schemes

In the hard-decision combining data fusion schemes, the final decision is made by taking into consideration only the individual decisions reported by each SU. The main advantage of the method is that it is simple and has small transmission overhead. In order to simplify the explanations, some notation will be introduced first: $P_{d,i}$, $P_{fa,i}$ and $P_{m,i}$ denote the probability of detection, the probability of false alarm and the probability of miss of the i-th SU in cooperative spectrum sensing scheme, respectively.

Whereas their global representatives will be denoted as P_D, P_{FA} and P_M.

In [85], three classic hard-decision combining methods, which are very simple, are shown as follows:

- **"And" Rule**
  The FC makes use of the way of logic "And" to merge the local detection results ($P_{d,i}$ and $P_{fa,i}$) from all N_{su} SUs, which results in the cooperative detection results (P_D and P_{FA}) as follows.

$$P_D = \prod_{i=1}^{N_{su}} P_{d,i} \tag{2.62}$$

$$P_{FA} = \prod_{i=1}^{N_{su}} P_{fa,i} \tag{2.63}$$

- **"Or" Rule**
  Similarly, the way of logic "Or" is used in the FC. That is, the FC makes decision that the PU is present if at least one of the SU decides for the presence of PU, otherwise the PU is absent. Then, the cooperative probability of detection P_D and probability of false alarm P_{FA} can be obtained in the following:

$$P_D = 1 - \prod_{i=1}^{N_{su}} (1 - P_{d,i}) \tag{2.64}$$

$$P_{FA} = 1 - \prod_{i=1}^{N_{su}} (1 - P_{fa,i}) \tag{2.65}$$

- **"K order" Rule**
  The FC makes a decision that the PU is present if more than K users in N_{su} SUs decide the PU is present, otherwise it is absent. This is the general form of the "And" rule and "Or" rule, when $K = N_{su}$ and $K = 1$, respectively. Then the corresponding probability of detection and probability of false alarm are

$$P_D = \sum_{j=K}^{N_{su}} \sum_{\sum D_i = j} \prod_{i=1}^{N_{su}} (P_{d,i})^{D_i} (1 - P_{d,i})^{1-D_i} \tag{2.66}$$

$$P_{FA} = \sum_{j=K}^{N_{su}} \sum_{\sum D_i = j} \prod_{i=1}^{N_{su}} (P_{fa,i})^{D_i} (1 - P_{fa,i})^{1-D_i} \tag{2.67}$$

In addition, [86] studies the optimization of cooperative spectrum sensing based

on hard-decision combining data fusion for energy detection with equal SNR for all SUs. In this case, it has been found that the optimal decision voting rule to minimize the total error probability is the half-voting rule. Then, optimal decision threshold and minimal number of SUs are derived, where optimality refers to the global probability of error $P_{FA} + P_M$.

2.4.2 Soft-decision combining data fusion schemes

Due to only 1 bit information transmitted from SU to FC in hard-decision combining data fusion scheme, the reliability of detection is low and can not always satisfy requirements. Thus, in order to improve the detection performance and reduce the probability of false alarm, soft-decision combining data fusion schemes are proposed. In soft-decision combining, observations from the local SU are delivered to the FC to provide high level of information, but this increases the volume of communication data.

Cooperative spectrum sensing scheme based on energy detection is considered in [87], where soft-decision combining of the observed energy values from different SUs is investigated. In this case, the observation energies from N_{su} cooperative SUs are scaled by weight factor and added up. The test statistic results of the weighted sum and is given by

$$\mathcal{T} = \sum_{i=1}^{N_{su}} \mathrm{w}_i E_i \tag{2.68}$$

where E_i is the observed energy of the i-th SU and w_i denotes the weighted factor corresponding to the i-th SU.

Based on the different evaluation of the weights, two soft-decision combining schemes including maximal ratio combination (MRC) and equal gain combination (EGC) are proposed.

- **MRC soft-decision combining scheme**
  In MRC soft-decision combining scheme, the weight coefficients are defined as

$$\mathrm{w}_{MRC,i} = \frac{\gamma_i}{\sqrt{\sum_{j=1}^{N_{su}} \gamma_j^2}}, \quad 1 \leq i \leq N_{su} \tag{2.69}$$

  where γ_i denotes the instantaneous SNR of the i-th SU. After normalizing the weights and assigning them to each SU, nodes with strong signals are further am-

plified, while weak signals are attenuated. It is proved that MRC is the optimal combination in the low SNR case, but it requires an estimation of the channel gains.

- **EGC soft-decision combining scheme**
  In EGC soft-decision combining scheme, the weight coefficients are calculated as

$$\mathrm{w}_{EGC,i} = \frac{1}{N_{su}}, \quad 1 \leq i \leq N_{su} \tag{2.70}$$

  Note that the weights of EGC soft-decision combining scheme only depend on the number of cooperative SUs N_{su}. It is considered as the best choice for a combination under the limitation of the channel state information of SUs.

Moreover, an extension of this research is proposed based on a softened hard combination scheme with 2-bit overhead for each SU, but it has a much lower spectrum sensing performance than the MRC and further requires a complicated computation for the quantization threshold at each SU whenever the network size is changed.

In addition, there are substantial data fusion schemes, which are widely studied in [88, 89, 90]. In the next sections, four data fusion mechanisms which enable both hard and soft decision methods are described. They mainly include Bayesian fusion rule, Neyman-Pearson criterion, Fuzzy fusion rule and Dempster-Shafer theory of evidence. Some knowledge of these approaches are provided in the following.

2.4.3 Bayesian fusion rule

In Bayesian fusion rule, considering that there are N_{su} local nodes (SUs), the observations at each SU are denoted by $\mathbf{y}_i$, $(i = 1, \cdots, N_{su})$ and $\mathbf{y} = \{\mathbf{y}_1, \mathbf{y}_2, \cdots, \mathbf{y}_{N_{su}}\}$. The observations at the individual SUs are assumed to be statistically independent. The Bayesian criterion allows to determine the decision rule so that the expected cost E[C], also known as Bayes risk $\mathfrak{R}$, is minimized. The expected cost is calculated by:

$$\mathfrak{R} = \mathrm{E[C]} = \sum_{i=0}^{1} \sum_{j=0}^{1} \mathrm{C}_{ij} P(\mathcal{H}_i|\mathcal{H}_j) P(\mathcal{H}_j). \tag{2.71}$$

where C_{ij} is the cost if deciding $\mathcal{H}_i$ but $\mathcal{H}_j$ is true. $P(\mathcal{H}_0)$ and $P(\mathcal{H}_1)$ are the prior probabilities of hypotheses $\mathcal{H}_0$ and $\mathcal{H}_1$, respectively. $P(\mathcal{H}_i|\mathcal{H}_j)$ is the conditional probability that indicates the probability of deciding $\mathcal{H}_i$ when $\mathcal{H}_j$ is true, which is defined

by:

$$P(\mathcal{H}_i|\mathcal{H}_j) = \int_{R_i} p(\mathbf{y}|\mathcal{H}_j)d\mathbf{y} \tag{2.72}$$

where $R_i = \{\mathbf{y} : \text{decide} \quad \mathcal{H}_i\}$, $(i = 0, 1)$ is termed the critical region of deciding $\mathcal{H}_i$ hypothesis, and $p(\mathbf{y}|\mathcal{H}_j)$ is the probability density function (PDF) of $\mathbf{y}$ when hypothesis $\mathcal{H}_j$ is true. By taking Equation (2.72) into (2.71), the Bayes risk is determined by:

$$\begin{aligned}\mathfrak{R} =& \mathrm{C}_{00}P(\mathcal{H}_0)\int_{R_0} p(\mathbf{y}|\mathcal{H}_0)d\mathbf{y} + \mathrm{C}_{01}P(\mathcal{H}_1)\int_{R_0} p(\mathbf{y}|\mathcal{H}_1)d\mathbf{y} \\ &+ \mathrm{C}_{10}P(\mathcal{H}_0)\int_{R_1} p(\mathbf{y}|\mathcal{H}_0)d\mathbf{y} + \mathrm{C}_{11}P(\mathcal{H}_1)\int_{R_1} p(\mathbf{y}|\mathcal{H}_1)d\mathbf{y}\end{aligned} \tag{2.73}$$

And

$$\int_{R_0} p(\mathbf{y}|\mathcal{H}_i)d\mathbf{y} = 1 - \int_{R_1} p(\mathbf{y}|\mathcal{H}_i)d\mathbf{y} \tag{2.74}$$

since R_0 and R_1 partition the entire space. Substitute Equation (2.74) into (2.73), the Bayes risk can be simplified to

$$\begin{aligned}\mathfrak{R} =& \mathrm{C}_{00}P(\mathcal{H}_0) + \mathrm{C}_{01}P(\mathcal{H}_1) \\ &+ \int_{R_1} \Big(\big(\mathrm{C}_{10}P(\mathcal{H}_0) - \mathrm{C}_{00}P(\mathcal{H}_0)\big)p(\mathbf{y}|\mathcal{H}_0) \\ &\qquad + \big(\mathrm{C}_{11}P(\mathcal{H}_1) - \mathrm{C}_{01}P(\mathcal{H}_1)\big)p(\mathbf{y}|\mathcal{H}_1)\Big)d\mathbf{y}.\end{aligned} \tag{2.75}$$

Consequently, only if the integrand is negative, include $\mathbf{y}$ in R_1. That is to say, we decide $\mathcal{H}_1$ if

$$\big(\mathrm{C}_{10} - \mathrm{C}_{00}\big)P(\mathcal{H}_0)p(\mathbf{y}|\mathcal{H}_0) < \big(\mathrm{C}_{01} - \mathrm{C}_{11}\big)P(\mathcal{H}_1)p(\mathbf{y}|\mathcal{H}_1), \tag{2.76}$$

otherwise, we decide $\mathcal{H}_0$. Therefore, the decision rule from the Bayesian criterion is the likelihood ratio test as follows:

$$\frac{p(\mathbf{y}|\mathcal{H}_1)}{p(\mathbf{y}|\mathcal{H}_0)} \underset{\mathcal{H}_0}{\overset{\mathcal{H}_1}{\gtrless}} \frac{(\mathrm{C}_{10} - \mathrm{C}_{00})P(\mathcal{H}_0)}{(\mathrm{C}_{01} - \mathrm{C}_{11})P(\mathcal{H}_1)} \tag{2.77}$$

Define the likelihood ratio (LR) $\mathcal{L}(\mathbf{y})$ by

$$\mathcal{L}(\mathbf{y}) = \frac{p(\mathbf{y}|\mathcal{H}_1)}{p(\mathbf{y}|\mathcal{H}_0)} = \frac{p(\mathbf{y}_1, \cdots, \mathbf{y}_{N_{su}}|\mathcal{H}_1)}{p(\mathbf{y}_1, \cdots, \mathbf{y}_{N_{su}}|\mathcal{H}_0)} \tag{2.78}$$

Since the observations at each SU are independent, the LR can be simplified as follows:

$$\begin{aligned}\mathcal{L}(\mathbf{y}) &= \frac{p(\mathbf{y}_i|\mathcal{H}_1)\cdots p(\mathbf{y}_{N_{su}}|\mathcal{H}_1)}{p(\mathbf{y}_1|\mathcal{H}_0)\cdots p(\mathbf{y}_{N_{su}}|\mathcal{H}_0)} \\ &= \prod_{i=1}^{N_{su}} \frac{p(\mathbf{y}_i|\mathcal{H}_1)}{p(\mathbf{y}_i|\mathcal{H}_0)} \\ &= \prod_{i=1}^{N_{su}} \mathcal{L}(\mathbf{y}_i)\end{aligned} \tag{2.79}$$

Substituting Equation (2.79) into (2.77) and simplifying, the log likelihood ratio (LLR) test is obtained as follows:

$$\mathcal{T} = \sum_{i=1}^{N_{su}} \Lambda_i \underset{\mathcal{H}_0}{\overset{\mathcal{H}_1}{\gtrless}} \zeta \tag{2.80}$$

where ζ is the Bayes optimal threshold to make a final decision and Λ_i denote the LLR value of the i-th SU which is calculated by

$$\Lambda_i = \log\mathcal{L}(\mathbf{y}_i) = \log\left(\frac{p(\mathbf{y}_i|\mathcal{H}_1)}{p(\mathbf{y}_i|\mathcal{H}_0)}\right). \tag{2.81}$$

The threshold ζ minimizing the expected cost is determined by

$$\zeta = \log\frac{(\mathrm{C}_{10} - \mathrm{C}_{00})P(\mathcal{H}_0)}{(\mathrm{C}_{01} - \mathrm{C}_{11})P(\mathcal{H}_1)} \tag{2.82}$$

Usually, when the minimum probability of error criterion P_e is assumed, that is, $\mathrm{C}_{00} = \mathrm{C}_{11} = 0$, and $\mathrm{C}_{10} = \mathrm{C}_{01} = 1$, the threshold reduces to

$$\zeta = \log\frac{P(\mathcal{H}_0)}{P(\mathcal{H}_1)}. \tag{2.83}$$

Based on the Bayesian fusion rule mentioned above, an optimal data fusion scheme is proposed in [91] where a global decision is made by combining the individual SUs while minimizing the overall probability of error and individual decisions are weighted according to the reliability of the SU. However, the main problem of this method is that

it requires that priori probabilities $P(\mathcal{H}_1)$ and $P(\mathcal{H}_0)$ to be known in advance.

2.4.4 Neyman-Pearson criterion

In the Neyman-Pearson test, the objective is to guarantee a target probability of false alarm $P_{FA} = \alpha$ while maximizing the probability of detection P_D. This method is also based on calculating the LLR test and comparing the result with a threshold, as shown in the following expression:

$$\mathcal{T}(\mathbf{y}) = \prod_{i=1}^{N_{su}} \frac{p(\mathbf{y}_i|\mathcal{H}_1)}{p(\mathbf{y}_i|\mathcal{H}_0)} \underset{\mathcal{H}_0}{\overset{\mathcal{H}_1}{\gtrless}} \zeta \tag{2.84}$$

where the threshold ζ is found from

$$P_{FA} = \int_{\{\mathbf{y}:\mathcal{T}(\mathbf{y})>\zeta\}} p(\mathbf{y}|\mathcal{H}_0)d\mathbf{y} = \alpha. \tag{2.85}$$

Unfortunately, each SU in the cooperative sensing processing, experiences different reception conditions, thresholds can not be obtained analytically and their numerical evaluation is an NP-complete problem. In contrast to Bayesian fusion rule, this method does not require the prior probabilities of the hypotheses $\mathcal{H}_0$ and $\mathcal{H}_1$. However, it still requires the knowledge of a priori probability of $\mathbf{y}_i$ $(i = 1, \cdots, N_{su})$ when the global decision is $\mathcal{H}_1$ or $\mathcal{H}_0$.

2.4.5 Fuzzy fusion rule

Fuzzy reasoning is able to deal with imperfect data, which introduces the novel notion of partial set membership enabling imprecise reasoning [92].

A fuzzy set $\mathcal{F} \subseteq \mathcal{U}$ is defined by the gradual membership function $\mu_{\mathcal{F}}(u)$ in the interval [0,1] as below:

$$\mu_{\mathcal{F}}(u) \in [0, 1] \quad \forall u \in \mathcal{U} \tag{2.86}$$

where the higher the membership degree is, the more u belongs to $\mathcal{F}$. Thus, fuzzy data fusion is able to utilize fuzzy rules and combine the fuzzy data which is produced by vague sensing data with a gradual membership function.

There are two classifications in fuzzy fusion rule, which mainly include conjunctive and disjunctive fuzzy fusion as follows:

- **Conjunctive fuzzy fusion**
  When the sources are homogeneous and the fusion data from the sources are equally reliable, conjunctive fuzzy fusion rule is appropriate. Two examples are shown in the following:

$$\mu_{A\cap B}(x) = \min\big(\mu_A(x), \mu_B(x)\big) \tag{2.87}$$
$$\mu_{A\cap B}(x) = \mu_A(x) \cdot \mu_B(x), \tag{2.88}$$

  where A and B are fuzzy sets that $A, B \in \mathcal{U}$, x is an element in the $\mathcal{U}$ universe. Equations (2.87) and (2.88) represent the standard intersection and product of two fuzzy sets, respectively.

- **Disjunctive fuzzy fusion**
  When high conflict among the data from the sources exists, disjunctive fuzzy fusion is applied. Two examples are given by:

$$\mu_{A\cup B}(x) = \max\big(\mu_A(x), \mu_B(x)\big) \tag{2.89}$$
$$\mu_{A\cup B}(x) = \mu_A(x) + \mu_B(x) - \mu_A(x) \cdot \mu_B(x), \tag{2.90}$$

  which represent the standard union and algebraic sum of two fuzzy sets, respectively.

Accordingly, fuzzy fusion rule is well suitable for modelling the fuzzy membership of a target in a vague class. Unfortunately, it requires prior membership functions for different fuzzy sets.

2.4.6 Dempster-Shafer theory of evidence

The Dempster-Shafer theory of evidence, which was first introduced by Dempster and was later extended by Shafer, is a mathematical theory of evidence which allows to combine evidence from different sources and evaluate the credibility of system state [93].

According to the D-S theory of evidence, denote Ω a finite set of mutually exclusive and exhaustive hypotheses, and let 2^Ω be its power set. A function m: $2^\Omega \mapsto [0, 1]$ named basic probability assignment (BPA) is defined to quantify the candidate propo-

sition as follows:

$$m(\emptyset) = 0 \tag{2.91}$$

$$\sum_{A \subset 2^{\Omega}} m(A) = 1 \tag{2.92}$$

where, for any set $A \subset 2^{\Omega}$, $m(A) > 0$ which provides the body of confidence that proposition A is true. In D-S theory of evidence, there are two functions named belief (bel) and plausibility (pl) that define the upper and lower bounds of a probability interval from the mass assignment in the following:

$$bel(A) \leq P(A) \leq pl(A). \tag{2.93}$$

These two functions, derived from the mass values, are respectively defined as a map from set of hypotheses to an interval $[0, 1]$ as follows:

$$bel(A) = \sum_{B \subseteq A} m(B) \tag{2.94}$$

and

$$pl(A) = \sum_{A \cap B \neq \emptyset} m(B), \tag{2.95}$$

where $bel(A)$ can be interpreted as the minimum or necessary support of one's belief that hypothesis A is true, while $pl(A)$ may be viewed as the maximum or potential support for that hypothesis.

In order to combine different sets of probability mass assignments from different information sources, Dempster's rule of combination is used. It makes use of the orthogonal sum for multiple mass functions and then yields a new mass function. Specially, the new joint mass function m is calculated from the two mass functions m_1 and m_2 in the following manner:

$$m(\emptyset) = 0 \tag{2.96}$$

$$\begin{aligned} m(A) &= (m_1 \oplus m_2)(A) \\ &= \frac{1}{1-\kappa} \sum_{B \cap C = A} m_1(B) m_2(C) \end{aligned} \tag{2.97}$$

where

$$\kappa = \sum_{B \cap C = \emptyset} m_1(B) m_2(C). \tag{2.98}$$

κ is often interpreted as a measure of conflict among different mass functions.

According to the D-S theory of evidence, several efficient cooperative spectrum sensing methods have been proposed in order to make a reliable decision in the literatures. In [88], the credibility of the channel condition between PU and SU is quantified by the basic probability assignment (BPA) estimation and D-S theory of evidence is firstly applied into FC in order to fuse the different detection from each SU. That turns out to be better than the traditional logic fusion "And" and "Or" rules. The authors in [94] reduce the reporting bandwidth and keep the performance by utilizing special characteristics of hypothesis and employing the Lloyd-Max quantization method. In [95], an enhanced D-S theory cooperative spectrum sensing algorithm is proposed against spectrum sensing data falsification attack by removing the lowest reliable SU, which is evaluated by considering the Max-Min similarity degree between any two SUs. In [96], the authors evaluate the trustworthiness degree from the current and historical aspects, and establish a "soft update" approach for the reputation value maintenance, which results in obtaining a better detection performance compared with other spectrum sensing methods.

Table 2.3 – Comparison of different data fusion schemes.

Method	Pros	Cons
“And” rule “Or” rule “K order” rule	Simple implementation, small transmission overhead	Low reliability, low robustness
MRC EGC	Considering a weight factor, improving reliability	Increasing transmission overhead
Bayesian fusion rule	Calculating a decision cost, optimal fusion rule	Requiring prior probabilities
Neyman-Pearson criterion	Guaranteeing a target probability of false alarm	Requiring prior probabilities
Fuzzy fusion rule	Intuitive approach to deal with vague data	Requiring membership functions
D-S theory of evidence	Fusing uncertain data, high reliability	High computational complexity

In the end, a comparison of different data fusion schemes given in this section is presented in Table 2.3, where the pros and cons of each data fusion scheme are summarized.

2.5 Summary

In this chapter, some developed spectrum sensing techniques are summarized. At the beginning, the classification of spectrum sensing is shown and performance indicators of spectrum sensing are given. Then, in local spectrum sensing, energy detection, eigenvalue based sensing and GoF test based sensing are primarily introduced. In cooperative spectrum sensing, the Bayesian fusion rule and Dempster-Shafer theory of evidence are introduced in detail. Based on the observations of the spectrum sensing techniques in the literature and considering the limits of current methods such as the long sensing time and high energy consumption, we propose new efficient spectrum sensing methods, which are introduced in the next chapters.

3

Proposed local spectrum sensing technique

As described in previous chapter, wireless sensors in CWSNs have hardware constraints in terms of computational power, memory storage and energy. One way to solve the problem, reducing the sampling brings an important advantage in CWSN applications. It is usually able to reduce the storage requirements and the computational power consumption. Sometimes small sample size also means shorter time in real-time data processing. This is particularly true when SU has only a single-radio architecture, the time of sampling and observing the channel is expected to be as short as possible. In the literature many spectrum sensing methods are limited by the number of samples and has low reliability of detection. For example, energy detection, as the most popular technique, is able to achieve a good detection performance only when the sample size is sufficiently large [13]. Thus, several goodness-of-fit test based methods are proposed for the small number of samples [24], which rely on the Kolmogorov-Smirnov test [81], the Cramer-Von Mises test [51], the Anderson-Darling test [80] and other statistical tests. These GoF test based methods can obtain better probability of detection than ED. However, in these cases, the GoF test is only performed to assess the rejection (or not) of the null hypothesis (the absence of PU signal). It seems reasonable to think that the detection performance could be improved by considering both hypotheses of presence and absence of the PU signal.

Considering the challenges mentioned above, we propose an efficient local spectrum sensing method, which is able to get a high reliability of detection under small number of samples. Firstly, in order to deal with the small sample size at SU, spectrum sensing is reformulated into a student's t-distribution test problem, which is popular in situations where the sample size is small. Besides, based on the characteristics of student's t-distribution, new basic probability assignment functions are proposed for estimating the presence or not of PU. However, due to the small number of samples, the estimation of SU's belief has inevitably a lack of reliability. In order to improve the reliability, the D-S theory of evidence is used to make a final decision. In our scheme, in order to fully exploit the collected sample, both hypotheses of presence or absence of PU are assessed.

The remainder of this chapter is organized as follows. In Section 3.1, we give a simplified system model for local spectrum sensing. The proposed local spectrum sensing scheme with small sample size is presented in Section 3.2, where a statistical model based on student's t-distribution is firstly proposed to deal with the received small samples, then new BPA functions are proposed to estimate the SU's reliability and finally a reliable decision is made by D-S theory of evidence. Simulations and conclusions are respectively presented in Section 3.3 and Section 3.4.

3.1 System model

In this part of the work, in order to focus on how to cope with small sample size and improve the reliability of spectrum sensing, we do not consider realistic radio channel conditions, which means there is no path loss, no multipath and no shadowing. Thus, we assume a simple system model similar to [80] and [53]. Let $y[n]$ $(n = 1, 2, \cdots, N_s)$ denotes the observation sample set made locally at the SU, where N_s is the number of samples. Without loss of generality, we assume that each sample $y[n]$ is real-valued. Then spectrum sensing for PU signal detection in Equation (2.1) can be simplified as follows

$$y[n] = \begin{cases} w[n], & \mathcal{H}_0 \\ s_t + w[n], & \mathcal{H}_1 \end{cases} \tag{3.1}$$

where $\mathcal{H}_0$ and $\mathcal{H}_1$ respectively represent the hypothesis of absence and presence of PU signal. $w[n]$ is an additive white Gaussian noise with zero mean and σ_w^2 variance,

the transmitted signal $s_t = 1$ is assumed such as in [80]. This assumption can be considered realistic for static signals, which can be found in the event detection of a WSN, or in the case of the very high sampling rate. In these cases, the spectrum sensing problem refers to a standard scenario with Gaussian distributions with equal variance and different means under each hypothesis.

3.2 Proposed LSS with small sample size

The proposed local spectrum sensing method relies on a fusion processing using the D-S theory and a new set of basic probability assignments (BPA). BPA definition and evaluation are the key points of the D-S fusion. In most applications, it is generally assumed that a sufficiently large number of samples is available in order to correctly estimate BPAs and perform a reliable fusion. But in this work, we consider that the SU is very limited in terms of sample size. Hence, we propose to define a new BPA relying on the student's t-distribution.

3.2.1 Statistical model of the received samples

Considering the small number of samples and the special sensing scenario about detecting non-zero PU signal in a zero mean noise, it is demonstrated that the optimal test in signal detection is the student's t-test [55]. In order to construct the test statistic in accordance with the student's t-distribution, after collecting the sample data $y[n]$ ($n = 1, 2, \cdots, N_s$) at the SU, we divide the samples into N_g groups where each group has L ($L > 1$) samples, that is $N_g = N_s/L$. Let define $\bar{Y_j}$ and S_j^2 as the mean and variance of the samples in the j-th group, respectively. Then, just as in [53],

$$\bar{Y_j} \triangleq \sum_{k=0}^{L-1} \frac{y[Lj-k]}{L} \tag{3.2}$$

and

$$S_j^2 \triangleq \sum_{k=0}^{L-1} \frac{(y[Lj-k]-\bar{Y_j})^2}{L-1} \tag{3.3}$$

where $j = 1, 2, \cdots, N_g$.

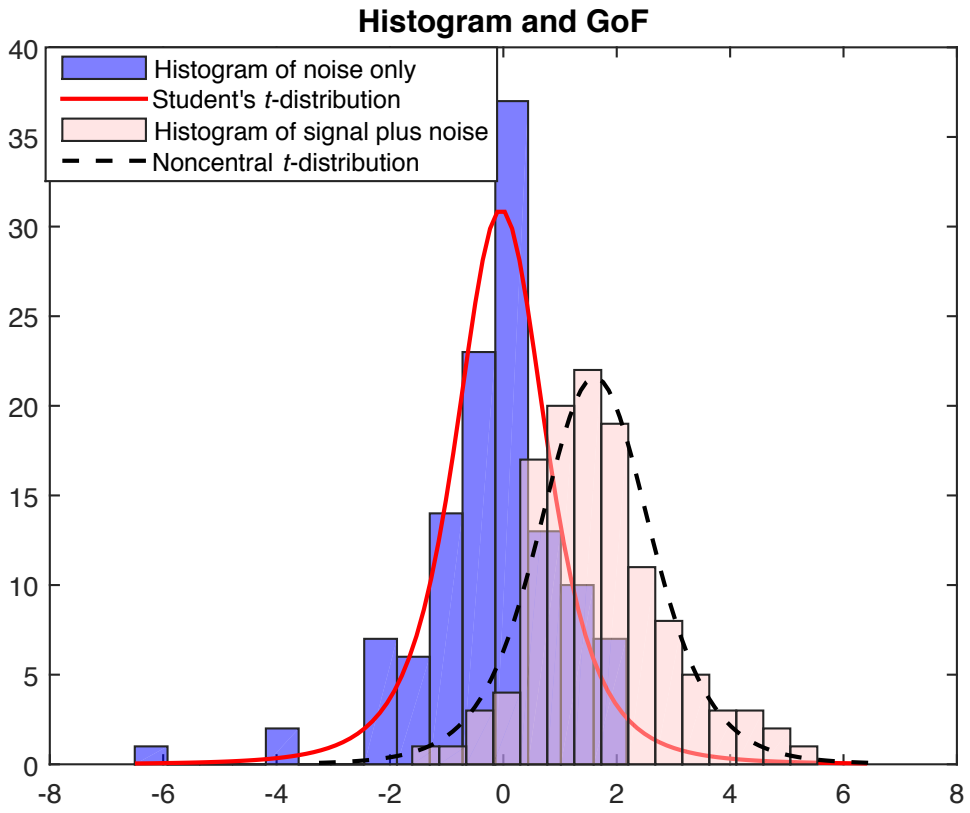

Figure 3.1 – Histogram and the GoF of Z_j under $\mathcal{H}_0$ hypothesis with only noise and $\mathcal{H}_1$ hypothesis with signal plus noise.

As a result, a new variable Z_j can be defined as:

$$Z_j \triangleq \frac{\bar{Y}_j}{S_j/\sqrt{L}}, \quad j = 1, 2, \cdots, N_g. \tag{3.4}$$

Under $\mathcal{H}_0$ hypothesis, there is no signal transmission from PU, $y[n] \sim \mathcal{N}(0, \sigma_w^2)$, thus Z_j is proved to follow a student's t-distribution with degree $v = L-1$. Otherwise, under $\mathcal{H}_1$ hypothesis, the received signal samples include the PU signal and the noise, then $y[n] \sim \mathcal{N}(\mu, \sigma_w^2)$, where $\mu = s_t$ in our case. It comes that Z_j has then a noncentral student's t-distribution with $v = L-1$ degrees of freedom and non-centrality parameter $\delta = \sqrt{L\mu^2/\sigma_w^2}$, μ^2/σ_w^2 is the SNR [53]. The histograms and the GoFs of the variable Z_j under $\mathcal{H}_0$ and $\mathcal{H}_1$ hypotheses are shown in Figure 3.1, where the number of samples $N_s = 64$ and SNR = -2 dB. We can see that the histograms of only noise and signal plus noise fit the student's t-distribution and the noncentral t-distribution, respectively. It is also obvious that the position of the curve of the noncentral t-distribution moves a little to the right relative to the student's t-distribution with the same degree of freedom.

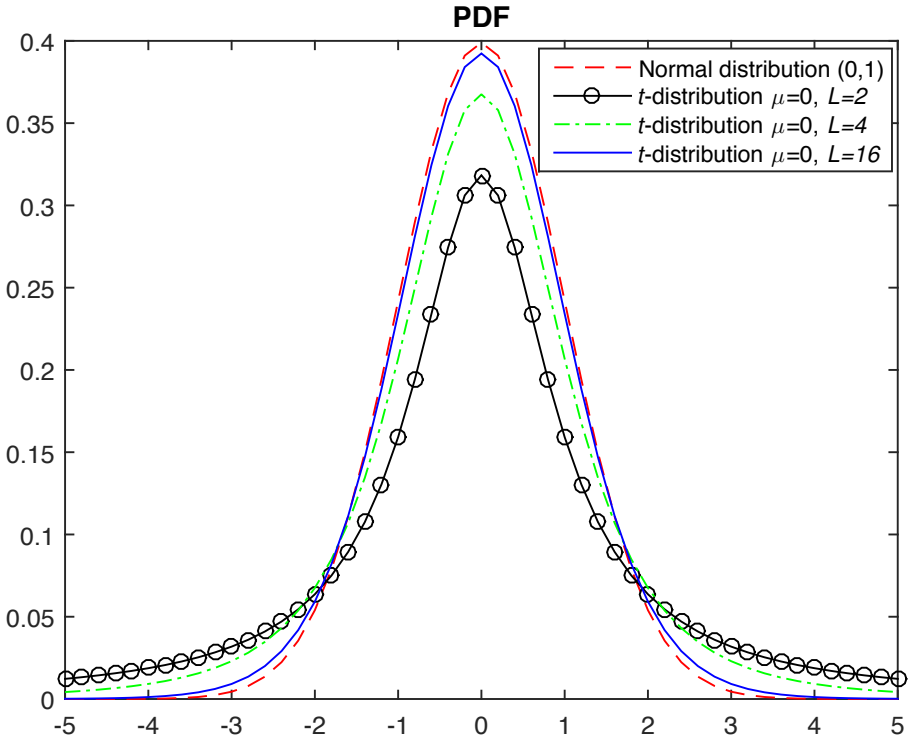

Figure 3.2 – The impact of the different degrees of freedom $v = L - 1$ for the probability density function (PDF) of student's t-distribution.

Moreover, the shape of the probability density function of the student's t-distribution resembles the bell shape of a normally distributed variable with mean 0 and variance 1, except that it is a bit lower and wider. The larger L is, the more the student's t-distribution approaches the standard normal distribution. Conversely, when L is small, the tail of that student's t-distribution is much heavier than those of the normal distribution, as shown in Figure 3.2. Hence for small L, it results that the variable Z_j in Equation (3.4) is prone to getting values that fall far from their statistical mean. This leads to an unreliable BPA estimation and a poor detection performance. Therefore, we propose to calculate N_g variable Z_j and combine them by the D-S theory of evidence for a reliable decision. In addition, in order to estimate the SU's belief, the cumulative distribution functions (CDF) of Z_j under $\mathcal{H}_0$ and $\mathcal{H}_1$ denoted by $F_0(z)$ and $F_1(z)$ are applied, which are given respectively in Equation (3.5) and Equation (3.6) [97], where $a_j = \frac{2j}{2j+1} a_{j-1}$, $a_0 = 1$, $b_j = \frac{2j-1}{2j} b_{j-1}$, $b_0 = 1$, and I is the regularized incomplete beta function.

$$F_0(z) = \begin{cases} \frac{1}{2} + \frac{1}{\pi}\tan^{-1}(z), & v = 1, \\ \frac{1}{2} + \frac{z}{2\sqrt{v+z^2}} \sum_{j=0}^{(v-2)/2} \frac{b_j}{(1+\frac{z^2}{v})^j}, & v \geq 2 \quad even, \\ \frac{1}{2} + \frac{1}{\pi}\tan^{-1}(\frac{z}{\sqrt{v}}) + \frac{z\sqrt{v}}{\pi(v+z^2)} \sum_{j=0}^{(v-3)/2} \frac{a_j}{(1+\frac{z^2}{v})^j}, & v \geq 3 \quad odd, \end{cases} \tag{3.5}$$

$$F_1(z) = \begin{cases} \frac{1}{2}\sum_{j=0}^{\infty} \frac{1}{j!}(-\delta\sqrt{2})^j e^{-\frac{\delta^2}{2}} \frac{\Gamma(\frac{j+1}{2})}{\sqrt{\pi}} \times I(\frac{v}{v+z^2}; \frac{v}{2}, \frac{j+1}{2}), & y \geq 0, \\ 1 - \frac{1}{2}\sum_{j=0}^{\infty} \frac{1}{j!}(-\delta\sqrt{2})^j e^{-\frac{\delta^2}{2}} \frac{\Gamma(\frac{j+1}{2})}{\sqrt{\pi}} \times I(\frac{v}{v+z^2}; \frac{v}{2}, \frac{j+1}{2}), & y < 0. \end{cases} \tag{3.6}$$

Note that in this statistical model we reformulate the received sample $\mathbf{y}$ into a new form $Z = \{Z_j\}_{j=1}^{N_g}$, which has a student's t-distribution and noncentral t-distribution under $\mathcal{H}_0$ and $\mathcal{H}_1$ hypotheses, respectively. As shown in Equation (3.5), the CDF $F_0(z)$ of Z_j under $\mathcal{H}_0$ hypothesis only refers to the degrees of freedom v, while $F_1(z)$ in Equation (3.6) is related to the parameter $\delta = \sqrt{L \times \text{SNR}}$. Thus we assume that the noise variance σ_w^2 is known, such as in ED based methods. For the D-S fusion, we assume that Z_j has at least 2 values, that is $N_g \geq 2$. Moreover, for the proposed method, as explained in the next section, the PU signal detection is done by evaluating the reliabilities of both $\mathcal{H}_0$ and $\mathcal{H}_1$ hypothesis, which is a beneficial feature that is not used in the conventional GoF test based methods.

3.2.2 Basic probability assignment estimation

After collecting small number of samples $\mathbf{y}$ and reformulating it into the new value $Z = \{Z_j\}_{j=1}^{N_g}$, Z_j from the j-th group sample is used to estimate a SU's self-assessed decision credibility. According to D-S theory of evidence shown in Section 2.4.6, Ω denotes the universal set, and let 2^Ω be its power set. The BPA function $m : 2^\Omega \mapsto [0, 1]$ is able to quantify the candidate proposition as follows:

$$m(\emptyset) = 0 \tag{3.7}$$

$$\sum_{A \subset 2^\Omega} m(A) = 1. \tag{3.8}$$

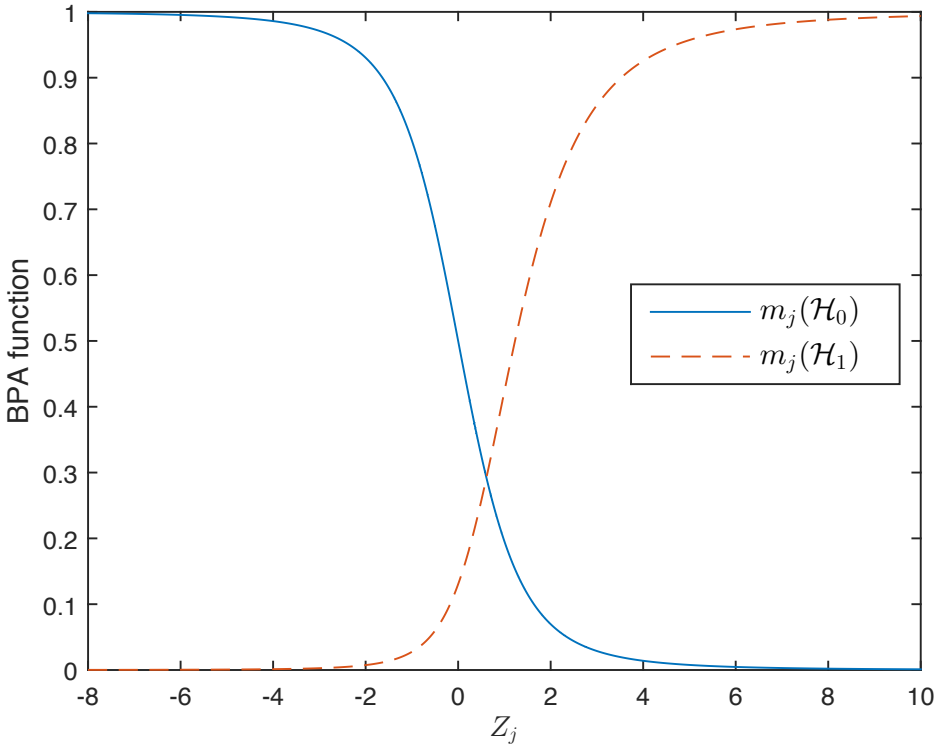

Figure 3.3 – The tendency of the BPA functions of Z_j including $m_j(\mathcal{H}_0)$ under $\mathcal{H}_0$ hypothesis and $m_j(\mathcal{H}_1)$ under $\mathcal{H}_1$ hypothesis.

where, for any set $A \subset 2^{\Omega}$, $m(A) > 0$. Then, in our framework, $\Omega = \{\mathcal{H}_0, \mathcal{H}_1\}$ and $2^{\Omega} = \{\emptyset, \{\mathcal{H}_0\}, \{\mathcal{H}_1\}, \Omega\}$.

In order to estimate a SU's credibility, we propose two new BPA functions $m_j(\mathcal{H}_0)$ and $m_j(\mathcal{H}_1)$ for $\mathcal{H}_0$ and $\mathcal{H}_1$ hypotheses, which are given by

$$m_j(\mathcal{H}_0) = 1 - F_0(Z_j) \tag{3.9}$$

$$m_j(\mathcal{H}_1) = F_1(Z_j). \tag{3.10}$$

Importantly, these BPA functions state the credibility for hypotheses $\mathcal{H}_0$ and $\mathcal{H}_1$ to be true. For example, the larger of the value of Z_j results in the larger $m_j(\mathcal{H}_1)$ and the smaller $m_j(\mathcal{H}_0)$, and vice versa, as shown in Figure 3.3. Thus we can make a decision whether the PU signal is present or not by comparing $m_j(\mathcal{H}_0)$ and $m_j(\mathcal{H}_1)$. If $m_j(\mathcal{H}_1) > m_j(\mathcal{H}_0)$, signal exists; otherwise, it is do not.

However, since the total number of samples N_s is small, it is obvious to tell that Z_j has been obtained with a very few number of them, i.e. L samples. This causes a big uncertainty and increase the conflict between $m_j(\mathcal{H}_0)$ and $m_j(\mathcal{H}_1)$. Then a third BPA

function is defined as follows:

$$m_j(\Omega) = 1 - m_j(\mathcal{H}_0) - m_j(\mathcal{H}_1) \tag{3.11}$$

where $\Omega = \{\mathcal{H}_1, \mathcal{H}_0\}$ denotes that both hypothesis could be true and $m_j(\Omega)$ indicates the total uncertainty of the jth group of samples. In order to improve the probability of detection and reduce the influence of the conflict evidence, we make a final reliable decision by fusing all BPA functions obtained from the N_g groups of samples.

3.2.3 D-S fusion and final decision

In order to improve the reliability of detection, we need to combine the N_g BPA functions and make a final decision. Then, according to the basic D-S theory of evidence and Equations (3.9), (3.10) and (3.11), two new combined BPA functions can be obtained in the following:

$$m(\mathcal{H}_0) = \frac{1}{1-\kappa} \sum_{\substack{\cap A_j = \mathcal{H}_0, A_j \subset 2^\Omega \\ j \in \{1,\ldots,N_g\}}} \prod_{j=1}^{N_g} m_j(A_j) \tag{3.12}$$

$$m(\mathcal{H}_1) = \frac{1}{1-\kappa} \sum_{\substack{\cap A_j = \mathcal{H}_1, A_j \subset 2^\Omega \\ j \in \{1,\ldots,N_g\}}} \prod_{j=1}^{N_g} m_j(A_j) \tag{3.13}$$

where κ is a measure of the amount of conflict among the mass sets:

$$\kappa = \sum_{\substack{\cap A_j = \emptyset, A_j \subset 2^\Omega \\ j \in \{1,\ldots,N_g\}}} \prod_{j=1}^{N_g} m_j(A_j). \tag{3.14}$$

Finally, based on all N_g groups of samples, the decision is made by comparing the ratio between $m(\mathcal{H}_1)$ and $m(\mathcal{H}_0)$ as follows:

$$\frac{m(\mathcal{H}_1)}{m(\mathcal{H}_0)} \underset{\mathcal{H}_0}{\overset{\mathcal{H}_1}{\gtrless}} \zeta \tag{3.15}$$

where ζ is the decision threshold. According to the constant false alarm rate (CFAR) criterion, we can acquire in advance the threshold ζ corresponding to a given probability of false alarm by Monte Carlo approach.

Algorithm 3.1 Proposed SS method with small sample size

1: Initialization: $j = 0$
2: $\zeta \leftarrow$ Set the decision threshold
3: $\mathbf{y} = \left[y[1]y[2]\cdots y[N_s]\right]^T \leftarrow$ Get the received sample
4: Divide $\mathbf{y}$ into N_g groups (each group has L elements)
5: **while** $j \leq N_g$ **do**
6: $\quad j \leftarrow j + 1$
7: $\quad Z_j \leftarrow$ Construct the new statistics using Equation (3.4)
8: $\quad F_0(Z_j), F_1(Z_j) \leftarrow Z_j$
9: $\quad m_j(\mathcal{H}_0), m_j(\mathcal{H}_1), m_j(\Omega) \leftarrow F_0(Z_j), F_1(Z_j)$
10: **end while**
11: D-S fusion $(m(\mathcal{H}_0), m(\mathcal{H}_1)) \leftarrow$ Calculate the final BPA functions using Equation (3.12) and Equation (3.13)
12: **if** $\frac{m(\mathcal{H}_1)}{m(\mathcal{H}_0)} > \zeta$ **then**
13: $\quad$ PU signal exists
14: **else**
15: $\quad$ PU signal does not exist
16: **end if**

Consequently, the pseudo code of the proposed spectrum sensing method with small sample size is given as Algorithm 3.1. Note that the computational complexity of the proposed method mainly comes from two parts: the construction of the statistics Z_j (in Step 7 in Algorithm 3.1) and the D-S fusion (in Step 11 in Algorithm 3.1). For the first part, the statistics Z_j is constructed by Equations (3.2), (3.3) and (3.4). Hence $N_g(3L-2)$ additions and $N_g(L+3)$ multiplications are needed. For the second part, the computational complexity generally increases rapidly with the number of elements in the frame of discernment (Ω) and the number of groups N_g, as shown in Equation (3.12) and Equation (3.13). However, since the frame of discernment consists in only two elements $\{\mathcal{H}_0, \mathcal{H}_1\}$ for the spectrum sensing, the combination of two mass functions require the computation of 2×2 intersections [98]. Thus, $(2^{N_g} - 1) - 1$ additions and $(N_g - 1) \times (2^{N_g} - 1)$ multiplications are sufficient for the computation of the second part. Moreover, in the proposed scheme, the small number of samples N_s is considered. And due to dividing N_s samples into N_g ($N_g \geq 2$) groups, a large L leads to a small N_g, which also reduces the number of BPA functions participating in combination in order to simplify the computation of the D-S fusion. Above all, under the same small number of samples N_s, the less the number of groups N_g is, the lower the total computational complexity is.

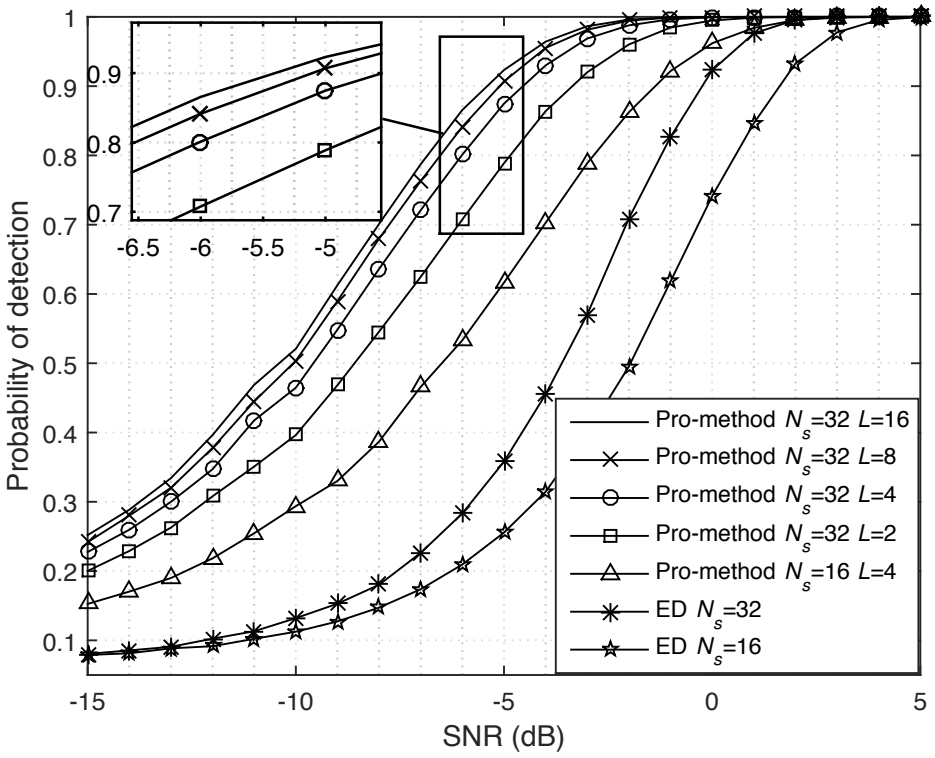

Figure 3.4 – Probability of detection versus SNR for the proposed method and ED with different sampling numbers.

3.3 Simulation results and analysis

In this section, performance comparison among the proposed method, the method based on GoF test [53] [58] and ED method [37] are given for different SNR and numbers of sample, when the PU signal is not known. The noise power σ_w^2 is assumed to be known in ED method and in the proposed method.

Figure 3.4 presents the probability of detection of the proposed method with different sample numbers $N_s = 16, L = 4$ and $N_s = 32, L = 2, 4, 8, 16$, where the probability of false alarm is set to 0.05 for different SNR. As can be seen, with the increase of the SNR, the probability of detection of the proposed method with $N_s = 32$ and $N_s = 16$ rises up quickly which is better than the trend of the curves of ED method with $N_s = 32$ and $N_s = 16$. For the proposed method, when the sample numbers $N_s = 32$, the detection performance with $L = 2$ is the worst among all tests. As an example, consider a SNR of -5 dB with the parameters used in the given comparison. As shown in the magnified parts of Figure 3.4, when the number of samples $N_s = 32$, the probability of detection with $L = 2, 4, 8, 16$ is $0.7887, 0.8748, 0.9069$ and 0.9233,

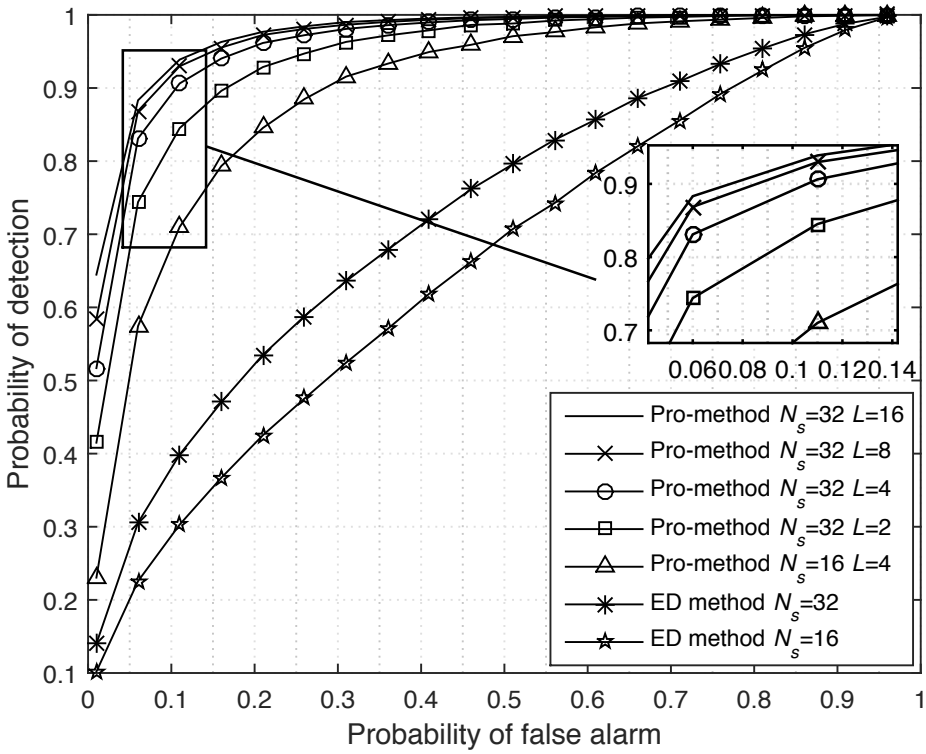

Figure 3.5 – ROC curves of the proposed method and ED with different sampling numbers at SNR= -6 dB.

respectively. This also verifies that a large L results in a more reliable BPA estimation and finally obtains a higher detection probability. In order to clearly reveal the proposed method, the receiver operating characteristic (ROC) curves are shown in Figure 3.5 when the SNR = -6 dB. It is obvious that the performances of the proposed method and ED are improved with the increase of the number of samples from $N_s = 16$ to 32. More specifically, as shown in the magnified parts of Figure 3.5, when the probability of false alarm P_{fa} is 0.11 with $N_s = 16, L = 4$ and $N_s = 32, L = 2, 4, 8, 16$, the corresponding detection probability of the proposed method P_d reach 0.7100 and $0.8451, 0.9062, 0.9299, 0.9389$, respectively. We can see that the performance of the proposed method with $L = 16$ is the best under the number of samples $N_s = 32$. And noting that $N_g = 2$ when $N_s = 32, L = 16$, the computational complexity is also the lowest. Therefore, for the proposed method, when a small number of samples is received, it should be divided into 2 groups to obtain the highest detection performance and the lowest computational complexity.

Likewise, Figure 3.6 shows the ROC curves of the proposed method, the GoF method in [53] with a number of samples of $N_s = 16$ and $L = 4$, the method in

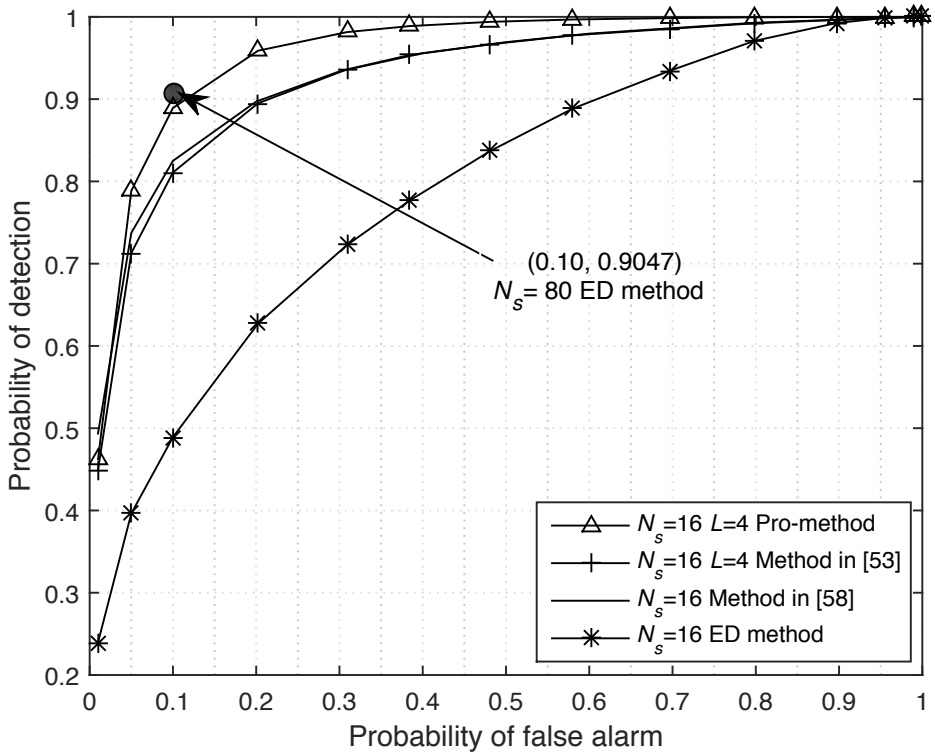

Figure 3.6 – ROC curves comparison among different spectrum sensing methods with $N_s = 16$ samples.

[58] and ED method with $N_s = 16$ at SNR= -3 dB. As it can be observed, the proposed method and the GoF methods [53] [58], are better than ED when 16 samples are used. When the probability of false alarm is equal to 0.10 and $N_s = 16$, the detection probability of our method is 0.8926. This is about 7% better than the detection probability of its counterparts (the GoF methods [53] [58]). Besides, the ED technique with $N_s = 16$ samples shows much less performances. In addition, in order to facilitate comparisons with other methods, we determine the number of samples required by the ED technique to achieve a similar performance. Thus, in Figure 3.6, it can be observed that the black dot $(P_{fa}, P_d) = (0.10, 0.9047)$ associated to the ED technique using 80 samples is close to the position $(P_{fa}, P_d) = (0.10, 0.8926)$ connected with the proposed method using only 16 samples. Finally, reducing the number of samples without sacrificing the detection performance is a very attractive feature in practice, because it brings an economy in terms of computational burden, sensing time and energy consumption.

3.4 Conclusion

In this chapter, we propose a local spectrum sensing method with small sample size for small devices used in WSN. The advantage of the proposed technique compared to the traditional energy detection is that only small number of samples is required. In this work, the samples are fully exploited with a statistical model more suitable to the small sample size case. New BPA functions based on a statistical model are constructed and used in a D-S fusion process, which reduces the conflict from different sample groups and improves the detection performance. Simulation results show that the proposed method achieves a higher probability of detection than other compared methods with small sample size. Therefore, as a local spectrum sensing method, the proposed method can be efficiently employed in cooperative spectrum sensing framework.

However, there are also many limiting conditions in the proposed method. For example, in order to focus on dealing with the small number of samples based on the student's t-distribution, channel conditions are not considered in the system model in this chapter. Unfortunately, it is demonstrated that the radio channel conditions seriously affect the detection reliability of local spectrum sensing methods. When a SU practically experiences path loss, multipath, shadowing due to obstacles and possibly non-line-of-sight between SU and PU, it is difficult for the SU to make a reliable decision only on its own measurement. It is thus obvious that a stand-alone decision about the fact that a PU is emitting or not, made independently by each SU, is not reliable enough. In that context it is much more preferable to use a cooperative spectrum sensing strategy, which is introduced in Chapter 4.

4

Cooperative spectrum sensing technique

As described in the previous Chapter, when considering the channel conditions such as path loss, multipath and shadowing fading, the detection reliability of local spectrum sensing method decreases. In order to solve this problem, cooperative spectrum sensing has attracted a lot of attention [10, 11] and has been shown to be an effective technique to improve the detection performance by exploiting spatial diversity. In cooperative spectrum sensing scheme, several distributed SUs in an area are cooperatively involved in the spectrum sensing, which allows to mitigate the channel effects. A fusion center (FC) is then in charge of merging information collected by the SUs and making a final decision about the spectrum occupancy. Unfortunately cooperative sensing can incur additional computation and cost; i.e. delay, fusion processing and overhead transmissions. In order to mitigate the impact of these issues, and not to increase the overall computation cost of the cooperative spectrum sensing (CSS) process at an unbearable level, a part of the solution is to reduce the sample size at each SU.

As mentioned previously, when CSS is expected to get energy-efficient, a significant reduction of sample size at each SU would be worthwhile. Although, an efficient local spectrum sensing method based on GoF test is proposed to cope with small sample size in Chapter 3, it is still a big challenge to apply those methods into cooperative

spectrum sensing. On the one hand, the transmitted signal in spectrum sensing method based on GoF test is assumed as $s_t = 1$, which is only suitable for some cases in practical applications. On the other hand, we do not consider the channel conditions between the transmitter of PU signal and the receiver of SU in the spectrum sensing method based on GoF test. Thus, in order to solve the problems, spectrum sensing techniques based on the eigenvalue analysis of the samples covariance matrix have been proposed recently. These methods make use of the statistics of the largest eigenvalue of the covariance matrix of the observation that is a Tracy-Widom law, and exhibit appealing performance [17, 18, 45, 50]. Since our ambition is to massively reduce the number of samples used for the spectrum detection, we introduce an appropriate approximation of the Tracy-Widom distribution to characterize the largest eigenvalue in the very small sample size case.

Therefore, in this chapter, considering the channel conditions and relaxing the limit of the PU signal compared with the PU signal in spectrum sensing method based on GoF test, we propose a new method for coping with the small number of samples in cooperative spectrum sensing. The method is based on an appropriate approximation of the Tracy-Widom distribution and D-S theory of evidence. Firstly, according to the small number of samples at each SU, a more reasonable Tracy-Widom approximation compared to other eigenvalue-based spectrum sensing techniques [17, 18, 45, 50], is utilized to form a thin observation matrix, which allows to get a small dimension covariance matrix. Then, we propose some new BPA functions based on the largest eigenvalue of the received sample covariance matrix, which considers the credibility of local spectrum sensing and is applied to the D-S theory of evidence. Finally, a more reliable final decision is made. Simulation results verify the effectiveness of the proposed method for different scenarios.

The remainder of the chapter is as follows. In Section 4.1, the local SS system model based on the covariance matrix of received signal is introduced. The proposed cooperative spectrum sensing scheme with small sample size is presented in Section 4.2, where a suited Tracy-Widom approximation is introduced and a thin observation matrix is formed, then some new BPA functions are constructed at the local sensing side, and finally the D-S fusion is applied at the FC. Simulations and conclusions are respectively presented in Section 4.3 and Section 4.4.

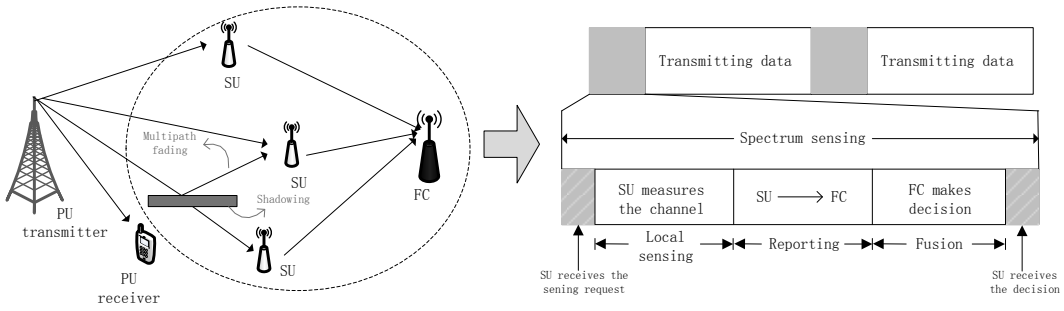

Figure 4.1 – Scenario and framework of cooperative spectrum sensing in CWSNs.

4.1 System model

In our work, we consider a centralized CSS based on D-S theory of evidence. As shown in Figure 4.1, our system includes one PU, one FC and N_{su} SUs, where each SU is equipped with one antenna. Then, each SU senses the channel and sends the acquired information to the FC. This latter makes a final decision and returns the results to each SU. In detail, Figure 4.1 shows the CSS framework where spectrum sensing is periodically executed before data transmissions [94]. Firstly SU receives the sensing request from the FC and measures the channel, then each SU reports its sensing or processed information to the FC, finally the FC makes a decision whether the PU is present or not, and broadcasts the result to each SU. Therefore, in the following we present the system model in local sensing at SU.

For presentation convenience and without loss of generality, we consider the local spectrum sensing with a discrete model. Then, spectrum sensing can be formulated as a binary hypothesis test between the following two hypotheses:

$$\mathcal{H}_0 : \quad y[nT_s] = w[nT_s] \tag{4.1}$$

$$\mathcal{H}_1 : \quad y[nT_s] = \boldsymbol{h}^T \boldsymbol{s}[nT_s] + w[nT_s] \tag{4.2}$$

where T_s is the sampling period, $\boldsymbol{h} = [h[0], h[T_c], \ldots, h[(N_c - 1)T_c]]^T$ stands for N_c taps of the multipath discrete channel impulse response which includes the transmission filter, the channel itself and the receiver filter. The length of each tap is T_c, $T_h = N_c T_c$ being the maximum length of the impulse response. Here, we consider that the received signal of a SU is sampled at a low rate $T_s > T_h$ (under-sampling). This aims to assume that the observation samples are uncorrelated, which plays an important role in next largest eigenvalue analysis. For practicality and without loss of generality, we consider the channel $\boldsymbol{h}$ as the Clarke's Rayleigh fading model which is a

baseline filtered white Gaussian noise (FWGN) model [99, 100]. In the Clarke model, isotropic scattering and linear relationship between input and output are assumed, and it includes two branches, one for a real part and the other for an imaginary part. The random process of Clarke's fading model with N_m multipaths can be described as the sum-of-sinusoid as follows:

$$h_I[lT_c] = \frac{1}{\sqrt{N_m}} \sum_{i=1}^{N_m} \cos\{2\pi f_D \cos[\frac{(2i-1)\pi + \theta}{4N_m}]lT_c + \alpha_i\} \tag{4.3}$$

$$h_Q[lT_c] = \frac{1}{\sqrt{N_m}} \sum_{i=1}^{N_m} \sin\{2\pi f_D \sin[\frac{(2i-1)\pi + \theta}{4N_m}]lT_c + \beta_i\} \tag{4.4}$$

$$h[lT_c] = h_I[lT_c] + jh_Q[lT_c] \tag{4.5}$$

where θ, α_i and β_i are uniformly distributed over [0, 2π) for all l and are mutually distributed, f_D is the maximum Doppler spread. $\boldsymbol{s}[nT_s] = [s[nT_s], s[nT_s - T_c], \ldots, s[nT_s - (N_c - 1)T_c]]^T$ is the discrete model of the PU signal. The noise signal $w[nT_s]$ is assumed to be complex white Gaussian with zero mean and σ_w^2 variance. Furthermore, it is assumed that noise and signal are uncorrelated.

In order to create a covariance matrix of observations, each SU collects N_s frames $\boldsymbol{y}_{i=0,1,\ldots,N_s-1}$ of L consecutive samples which is a stationary random vector. As shown in the next section, the local spectrum sensing operation can rely on the eigenvalue decomposition of this matrix. Then the following matrices can be defined:

$$\mathbf{Y} \overset{\text{def}}{=} [\boldsymbol{y}_0, \boldsymbol{y}_1, \ldots, \boldsymbol{y}_i, \ldots, \boldsymbol{y}_{N_s-1}] \tag{4.6}$$

$$\mathbf{S} \overset{\text{def}}{=} [\boldsymbol{s}_0, \boldsymbol{s}_1, \ldots, \boldsymbol{s}_i, \ldots, \boldsymbol{s}_{N_s-1}] \tag{4.7}$$

$$\boldsymbol{w} \overset{\text{def}}{=} [\boldsymbol{w}_0, \boldsymbol{w}_1, \ldots, \boldsymbol{w}_i, \ldots, \boldsymbol{w}_{N_s-1}] \tag{4.8}$$

where, $\boldsymbol{y}_i$, $\boldsymbol{s}_i$, and $\boldsymbol{w}_i$ denote the $L \times 1$ received random vector, the $LN_c \times 1$ PU signal vector $\boldsymbol{s}_i = [\boldsymbol{s}[iLT_s]^T \boldsymbol{s}[(iL+1)T_s]^T \ldots \boldsymbol{s}[((i+1)L-1)T_s]^T]^T$, and the $L \times 1$ random noise vector, respectively.

When there is no PU emitting

$$\boldsymbol{y}_i = \boldsymbol{w}_i \tag{4.9}$$

When the PU is present,

$$\boldsymbol{y}_i = \begin{bmatrix} y[iLT_s] \\ y[(iL+1)T_s] \\ \vdots \\ y[((i+1)L-1)T_s] \end{bmatrix} \tag{4.10}$$

$$= \begin{bmatrix} \boldsymbol{h}_1^T \boldsymbol{s}[iLT_s] + w[iLT_s] \\ \boldsymbol{h}_2^T \boldsymbol{s}[(iL+1)T_s] + w[(iL+1)T_s] \\ \vdots \\ \boldsymbol{h}_L^T \boldsymbol{s}[((i+1)L-1)T_s] + w[((i+1)L-1)T_s] \end{bmatrix} \tag{4.11}$$

$$= \mathbf{H}_i \boldsymbol{s}_i + \boldsymbol{w}_i \tag{4.12}$$

where $\mathbf{H}_i$ is a $L \times LN_c$ channel matrix defined as:

$$\mathbf{H}_i \overset{\text{def}}{=} \begin{bmatrix} \boldsymbol{h}_1^T & \mathbf{0} & \cdots & \mathbf{0} \\ \mathbf{0} & \boldsymbol{h}_2^T & \cdots & \mathbf{0} \\ \vdots & \vdots & \ddots & \vdots \\ \mathbf{0} & \mathbf{0} & \cdots & \boldsymbol{h}_L^T \end{bmatrix} \tag{4.13}$$

Statistical covariance matrix of the received signal, the PU signal and the noise can be respectively defined as:

$$\mathbf{R}_\mathbf{Y} = \mathrm{E}[\boldsymbol{y}_i \boldsymbol{y}_i^\dagger] \tag{4.14}$$

$$\mathbf{R}_\mathbf{S} = \mathrm{E}[\mathbf{H}_i \boldsymbol{s}_i \boldsymbol{s}_i^\dagger \mathbf{H}_i^\dagger] \tag{4.15}$$

$$\mathbf{R}_{\boldsymbol{w}} = \mathrm{E}[\boldsymbol{w}_i \boldsymbol{w}_i^\dagger] \tag{4.16}$$

where $\boldsymbol{y}_i$, $\boldsymbol{s}_i$ and $\boldsymbol{w}_i$ are assumed to be zero-mean stochastic stationary processes.

Then the binary hypothesis, (4.1) and (4.2), can be rewritten in a matrix form as

$$\mathcal{H}_0 : \quad \mathbf{R}_\mathbf{Y} = \mathbf{R}_{\boldsymbol{w}} \tag{4.17}$$

$$\mathcal{H}_1 : \quad \mathbf{R}_\mathbf{Y} = \mathbf{R}_{\boldsymbol{S}} + \mathbf{R}_{\boldsymbol{w}} \tag{4.18}$$

However, in practice we only can get a finite number of samples. Thus, the sample covariance matrix $\mathbf{R}_\mathbf{Y}$ can be estimated as

$$\hat{\mathbf{R}}_\mathbf{Y} = \frac{1}{N_s} \mathbf{Y}\mathbf{Y}^\dagger \tag{4.19}$$

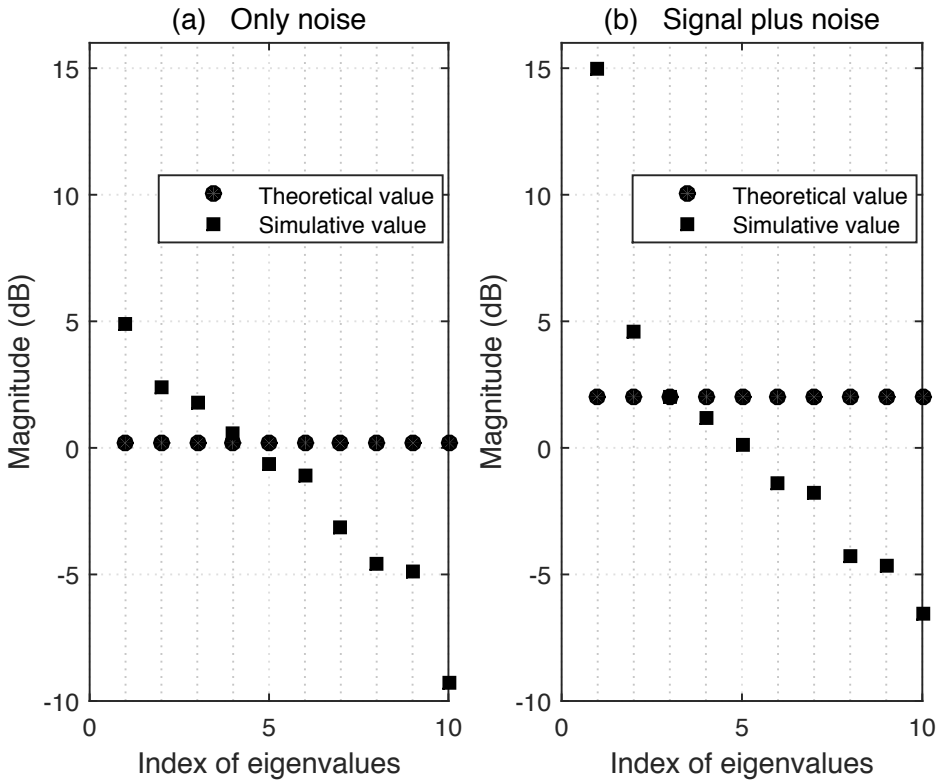

Figure 4.2 – Comparison of eigenvalues between theoretical value and simulative value where there are a finite number of samples. (a) Only noise in $\mathcal{H}_0$ hypothesis. (b) Signal plus noise in $\mathcal{H}_1$ hypothesis.

As mentioned previously, noise is a white Gaussian process. In case of the presence of a PU, whose signal is obviously not correlated to the noise, the sampling period has been set sufficiently large ($T_s > T_h$) to assume that the observation samples $\mathbf{Y}$ are independent and identically distributed random variables. Then in the $\mathcal{H}_0$ case (no PU), the mean power of the observed signal $\mathbf{Y}$ is given by the noise power $P = \sigma_w^2$, and in the $\mathcal{H}_1$ case (a PU is present) the asymptotical mean power samples is $P = \sigma_s^2$ + σ_w^2 where σ_s^2 is the received PU signal power through the channel. In Figure 4.2, we illustrate that the asymptotical eigenvalues of covariance matrix $\mathbf{R_Y}$ under $\mathcal{H}_0$ or $\mathcal{H}_1$ hypotheses are the same, and the asymptotical eigenvalues σ_w^2 in Figure 4.2(a) are smaller than the asymptotical eigenvalues $\sigma_s^2 + \sigma_w^2$ in Figure 4.2(b). Moreover, the simulative/sample eigenvalues of the estimated sample covariance matrix $\hat{\mathbf{R}}_\mathbf{Y}$ with $N_s = 20$ and $L = 10$ are also presented in Figure 4.2. As shown in Figure 4.2(a) and Figure 4.2(b), the simulative/sample eigenvalues are blurring relative to the theoretical eigenvalues when there is a finite number of samples. Therefore, the eigenvalue distribution of the sample covariance matrix $\hat{\mathbf{R}}_\mathbf{Y}$ becomes very complicated [101, 102], no

closed form expression has been found for the marginal probability density function (PDF) of ordered eigenvalues. In the following, the latest random matrix theory referring to the largest eigenvalue is introduced to propose an efficient spectrum sensing method for small sample size.

4.2 CSS with small sample size

The proposed CSS strategy relies on a fusion process using the D-S theory and a new set of basic probability assignments(BPA) functions. BPA function definition and evaluation is the key point of the D-S fusion. In most applications, it is generally assumed that a sufficiently large number of samples is available in order to correctly estimate BPAs and perform a reliable fusion. But in this work, we consider that the SU are very limited in terms of sample size. Following the effectiveness of the utilization of the D-S fusion [93] in CSS, we propose to define new reliable BPA functions by using eigenvalues of the covariance matrix of the observation, enabling to have a small number of collected samples.

4.2.1 Largest eigenvalue analysis

Whether a PU signal is present or not in the collected samples at a SU, according to the statistical properties of the samples, the observation covariance matrix $\hat{\mathbf{R}}_{\mathbf{Y}}$ in Equation (4.19) can be considered as a Whishart matrix [101]. In such a case, according to [102], when the number of samples is high enough, the largest eigenvalue of the matrix $\mathbf{R}_{\mathbf{Y}}$ is ruled by the Tracy-Widom (TW) distribution. Parameters of the distribution can be defined as functions of N_s, L and the dimensions of the observation matrix $\mathbf{Y}$. The following theorem allows to establish the parameters of the Tracy-Widom distribution when the number of samples is large (or in the asymptotic case).

Theorem 4.1 *Assume that the received signal is real. Let* $\boldsymbol{A} = \frac{N_s}{P}\hat{\boldsymbol{R}}_{\boldsymbol{Y}}$, $\phi = (\sqrt{N_s - 1} + \sqrt{L})^2$, *and* $\upsilon = (\sqrt{N_s - 1} + \sqrt{L})(1/\sqrt{N_s - 1} + 1/\sqrt{L})^{1/3}$. *Then,* $\frac{\lambda_1(\boldsymbol{A}) - \phi}{\upsilon}$ *converges to the Tracy-Widom distribution of order 1 (*W_1*) [102].*

The Tracy-Widom distribution which was found by Tracy and Widom (1996) is considered as the limiting law of the largest eigenvalue of certain random matrices [103]. The cumulative distribution function (CDF) of the Tracy-Widom distribution of

Table 4.1 – Some values of CDF of the Tracy-Widom distribution of order 1.

t	-3.90	-3.18	-2.78	-1.91	-1.27	-0.59	0.45	0.98	2.02
$F_1(t)$	0.01	0.05	0.10	0.30	0.50	0.70	0.90	0.95	0.99

order 1 F_1 is defined as

$$F_1(t) = \exp\Big(-\frac{1}{2}\int_t^\infty \big(q(u) + (u-t)q^2(u)\big)du\Big), \tag{4.20}$$

where $q(u)$ is the solution of the nonlinear Painleve II differential equation

$$q''(u) = uq(u) + 2q^3(u). \tag{4.21}$$

Because there is no closed form expression for the distribution function F_1, it is difficult to evaluate it. Fortunately, there are have been tables for the functions [102]. The values of F_1 at some points are given in Table 4.1.

However, since Theorem 4.1 is based on a large number of samples, reducing the number of samples (small $N_s \times L$ product) means that definitions of $\phi(N_s, L)$ and $\upsilon(N_s, L)$ in Theorem 4.1 are no longer well suitable. Recently in [104] it has been found that when facing with thin observation matrix $\mathbf{Y}$, namely when L is as small as 2, more appropriate parameters of the Tracy-Widom distribution should be chosen. Then, according to [104] when L is very small, and referring to Theorem 4.1, the largest eigenvalue λ_1 is considered to be ruled by the Tracy-Widom distribution of order 1, with the following mean and variance parameters:

$$\mu = \frac{P}{N_s}(\sqrt{N_{s-}} + \sqrt{L_-})^2 \tag{4.22}$$

$$\sigma^2 = (\frac{P}{N_s})^2(\sqrt{N_{s-}} + \sqrt{L_-})^2(\frac{1}{\sqrt{N_{s-}}} + \frac{1}{\sqrt{L_-}})^{2/3} \tag{4.23}$$

where $N_{s-} = N_s - \frac{1}{2}$ and $L_- = L - \frac{1}{2}$. It is also called adjusted TW distribution, which is able to achieve improved accuracy for a small number of samples.

This is illustrated in Figure 4.3, where the comparison of the theoretical CDF of the maximum eigenvalue, TW distribution and adjusted TW distribution with $N_s = 50$ and $L = 4$ is presented. It is evident that the curves of the TW distribution and the adjusted TW distribution of the largest eigenvalue both match the theoretical CDF ap-

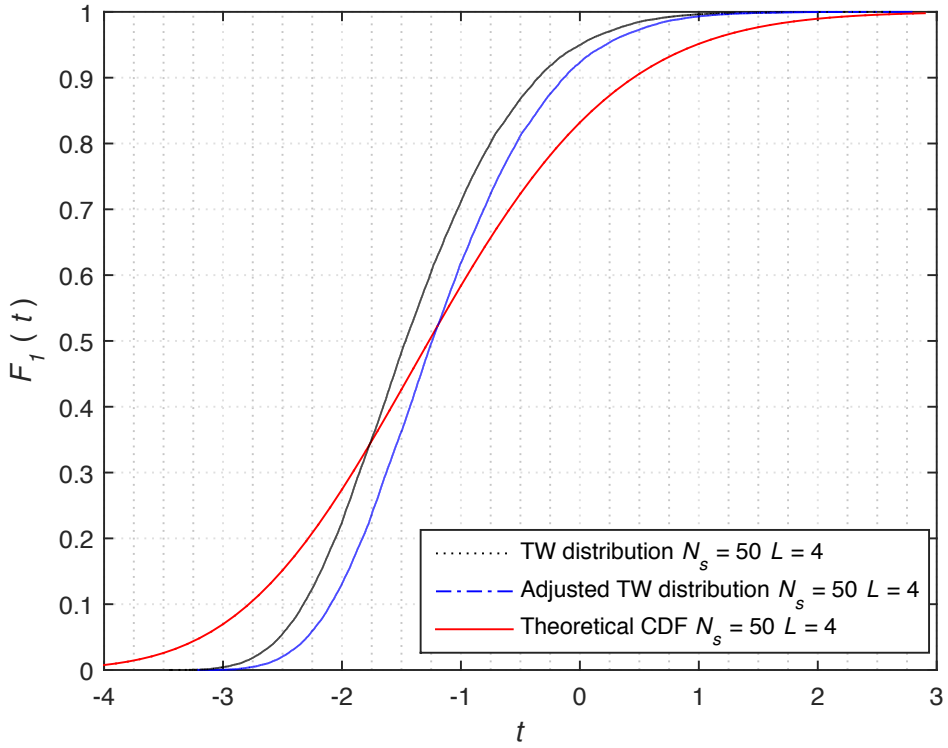

Figure 4.3 – Comparison of the theoretical CDF of the maximum eigenvalue, TW distribution and adjusted TW distribution with $N_s = 50$ and $L = 4$.

proximately. Moreover, it is clear that the adjusted TW distribution of the maximum eigenvalue converges closely to the theoretical CDF than the TW distribution in Theorem 4.1 but still with significant deviation when there is a finite number of samples. In addition, the mean power P in Equation (4.22) and Equation (4.23) is respectively equal to σ_w^2 or $\sigma_s^2 + \sigma_w^2$ if the PU is present or not. We assume that in both cases, the value of P is known at each SU. When L is small, the matrix $\mathbf{Y}$ of collected samples is what we can call a thin observation matrix and the inherited small size of the covariance matrix $\hat{\mathbf{R}}_\mathbf{Y}$ eigenvalue calculation requires less complexity. This last feature is of great importance in the framework of our applications.

According to the local spectrum sensing system model above, it is obvious that each SU acquires the sensing information through stochastic channel condition, thus each SU indicates its own credibility, and small sample size at each SU increases the uncertainty of observing and reduces the credibility of its sensing. Hence, in order to improve the detection performance and reduce the uncertainty, we propose some new BPA functions for evaluating the reliability of each SU.

4.2.2 Basic probability assignment evaluation

D-S theory of evidence allows to combine evidence from different sources and evaluate the credibility of each source with small sample size. In order to make a final decision by applying D-S theory of evidence, we propose some new basic probability assignment functions of each SU based on the largest eigenvalue λ_1 of the received sample covariance matrix $\hat{\mathbf{R}}_{\mathbf{Y}}$. The BPA functions are able to estimate SUs' self-assessed decision credibility.

The proposed BPA functions at the ith SU (i = 1, 2, ..., N_{su}) are based on the integral of the probability density function of the Tracy-Widom distribution of order 1, and are defined as:

$$\begin{aligned} m_i(\mathcal{H}_0) &= \int_{\lambda_{1i}}^{+\infty} W_1\left(\frac{x-\mu_{0i}}{\sigma_{0i}}\right)\mathrm{d}x \\ &= 1 - F_1\left(\frac{\lambda_{1i}-\mu_{0i}}{\sigma_{0i}}\right) \end{aligned} \tag{4.24}$$

and

$$\begin{aligned} m_i(\mathcal{H}_1) &= \int_{-\infty}^{\lambda_{1i}} W_1\left(\frac{x-\mu_{1i}}{\sigma_{1i}}\right)\mathrm{d}x \\ &= F_1\left(\frac{\lambda_{1i}-\mu_{1i}}{\sigma_{1i}}\right), \end{aligned} \tag{4.25}$$

where $m_i(\mathcal{H}_0)$, $m_i(\mathcal{H}_1)$ are the BPA of hypotheses $\mathcal{H}_0$ and $\mathcal{H}_1$ of the ith SU, which presents respectively credibility for hypotheses $\mathcal{H}_0$ and $\mathcal{H}_1$ to be true. W_1 and F_1 denote the probability density function and the cumulative distribution function for the distribution of Tracy-Widom of order 1 [103] [105]. λ_{1i} is the largest eigenvalue of the received sample covariance matrix $\hat{\mathbf{R}}_{\mathbf{Y}}$ of the ith SU. μ_{0i} and σ_{0i} are respectively equal to μ and σ in Equation (4.22) and Equation (4.23) with $P = \sigma_w^2$. μ_{1i} and σ_{1i} are respectively equal to μ and σ in Equation (4.22) and Equation (4.23) with $P = \sigma_s^2$ + σ_w^2.

The third BPA function is

$$m_i(\Omega) = 1 - m_i(\mathcal{H}_0) - m_i(\mathcal{H}_1) \tag{4.26}$$

where $\Omega = \{\mathcal{H}_1, \mathcal{H}_0\}$ denotes that either hypothesis could be true, and $m_i(\Omega)$ is the

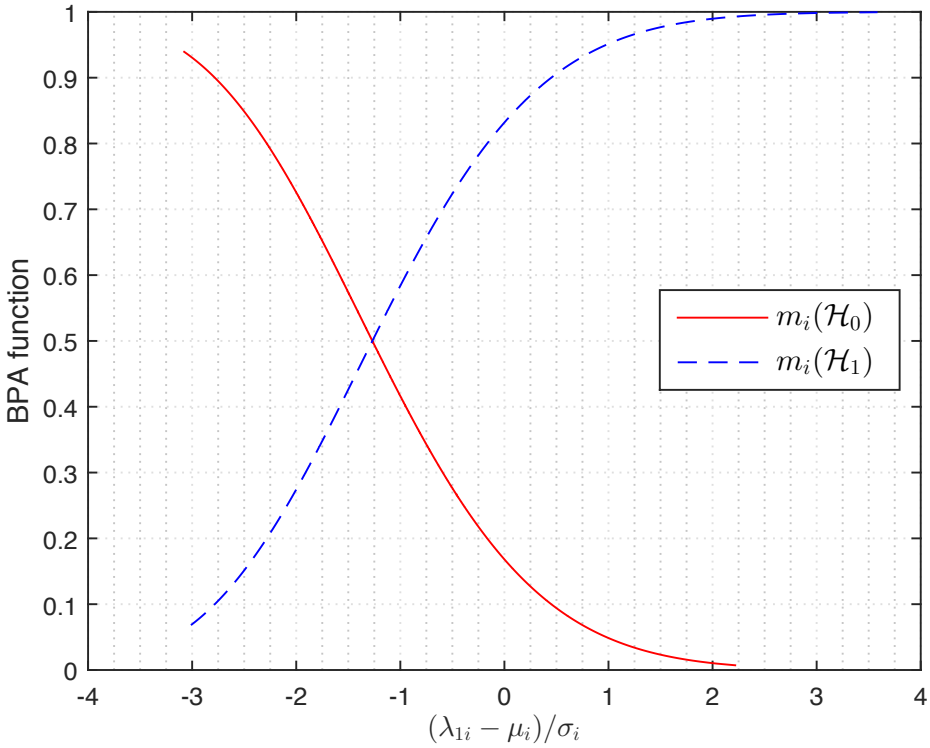

Figure 4.4 – The tendency of the BPA functions of $(\lambda_{1i} - \mu_i)/\sigma_i$ under $\mathcal{H}_0$ and $\mathcal{H}_1$ hypotheses.

total uncertainty of the ith SU.

Roughly speaking, if the calculated λ_{1i} turns out to be small, the BPA function $m_i(\mathcal{H}_0)$ will get a larger value than $m_i(\mathcal{H}_1)$, which will give more credit to the $\mathcal{H}_0$ hypothesis. Conversely if λ_{1i} is large, the $\mathcal{H}_1$ hypothesis will get a much higher probability than the $\mathcal{H}_0$ hypothesis. This is illustrated in Figure 4.4 where the tendency of the BPA functions under $\mathcal{H}_0$ and $\mathcal{H}_1$ hypotheses are presented. As shown in Figure 4.4, the dashed line indicating the BPA function $m_i(\mathcal{H}_1)$ goes up with the increasing of the value of $(\lambda_{1i} - \mu_{1i})/\sigma_{1i}$, whereas the solid line presenting the BPA function $m_i(\mathcal{H}_0)$ declines when the value of $(\lambda_{1i} - \mu_{0i})/\sigma_{0i}$ increases.

These BPA functions are evaluated at each SU relying on their own observations. Due to the problem of path loss, multipath and shadowing fading, single node can not make a reliable decision by its own evaluation. Each SU sends the information of BPA functions to the FC, and this latter will make a final decision by running the D-S based fusion process.

4.2.3 D-S fusion

According to D-S theory of evidence and the above new BPA functions (Equations (4.24), (4.25) and (4.26)), two new BPA functions can be obtained at the FC as follows:

$$\begin{aligned} m(\mathcal{H}_0) &= (m_1 \oplus m_2 \oplus \cdots \oplus m_{N_{su}})(\mathcal{H}_0) \\ &= \frac{1}{1-\kappa} \sum_{\substack{\cap A_i = \mathcal{H}_0, A_i \subset 2^\Omega \\ i \in \{1,\ldots,N_{su}\}}} \prod_{i=1}^{N_{su}} m_i(A_i) \end{aligned} \tag{4.27}$$

$$\begin{aligned} m(\mathcal{H}_1) &= (m_1 \oplus m_2 \oplus \cdots \oplus m_{N_{su}})(\mathcal{H}_1) \\ &= \frac{1}{1-\kappa} \sum_{\substack{\cap A_i = \mathcal{H}_1, A_i \subset 2^\Omega \\ i \in \{1,\ldots,N_{su}\}}} \prod_{i=1}^{N_{su}} m_i(A_i) \end{aligned} \tag{4.28}$$

where $2^\Omega = \{\emptyset, \{\mathcal{H}_0\}, \{\mathcal{H}_1\}, \Omega\}$, $\oplus$ is the logical operation of exclusive disjunction, and κ is a measure of the amount of conflict among the mass sets defined as:

$$\kappa = \sum_{\substack{\cap A_i = \emptyset, A_i \subset 2^\Omega \\ i \in \{1,\ldots,N_{su}\}}} \prod_{i=1}^{N_{su}} m_i(A_i) \tag{4.29}$$

Finally, the decision is made at the FC by simply comparing $m(\mathcal{H}_0)$ and $m(\mathcal{H}_1)$ as follows:

$$\mathcal{H}_1 \text{ is true} \quad \text{if } m(\mathcal{H}_1) > m(\mathcal{H}_0) \tag{4.30}$$

$$\mathcal{H}_0 \text{ is true} \quad \text{otherwise} \tag{4.31}$$

4.3 Simulation results and analysis

In the following simulations a captured DTV signal in [106] is considered to be transmitted by the PU, with a 0.5 probability of being present. Its center frequency is 545 MHz with a 6 MHz bandwidth. The observed passband signal is frequency-shifted and turned into the baseband signal. It is then sampled at $1/T_s$=100 KHz rate. This sampling rate is much lower than the 6 MHz bandwidth of the PU signal. The channel impulse response duration is set to $T_h = 1\mu s$. In this condition ($T_s > T_h$), collected samples are totally uncorrelated. With this setting, 0.5 ms is required to collect 50 samples. Channels between the PU and the SUs are generated according to the Clark

Table 4.2 – DTV signal parameters and simulation setup.

Center frequency	545 MHz
Bandwidth	6 MHz
Sampling period	10 μs
Channel model	Clark model
Channel impulse response duration	1 μs
Maximum doppler spread	1 KHz
Number of SU	6
Number of PU	1
Number of FC	1

Rayleigh fading model in Equation (4.5), where the maximum Doppler spread f_D is set to 1 KHz. The DTV signal parameters and the simulation setup are summarized in Table 4.2. In addition, an additive, white and Gaussian noise (AWGN) channel is considered and it exists a FC which combines evidences from each SU and makes the final decision.

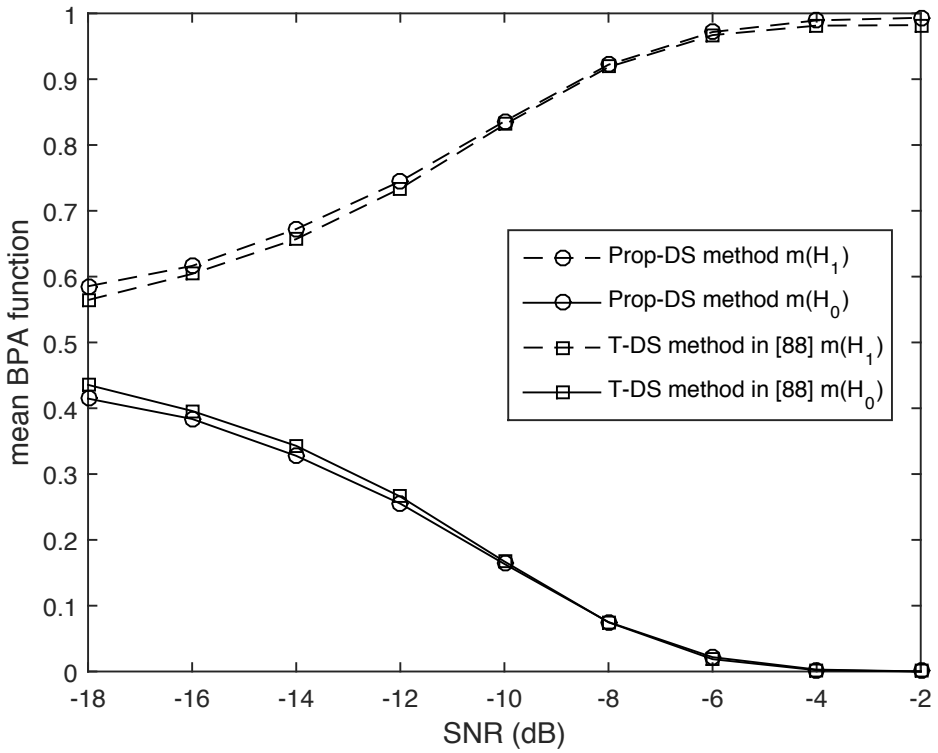

Figure 4.5 – The variation trend of the BPA functions with the increasing of SNR when PU is present using 200 samples.

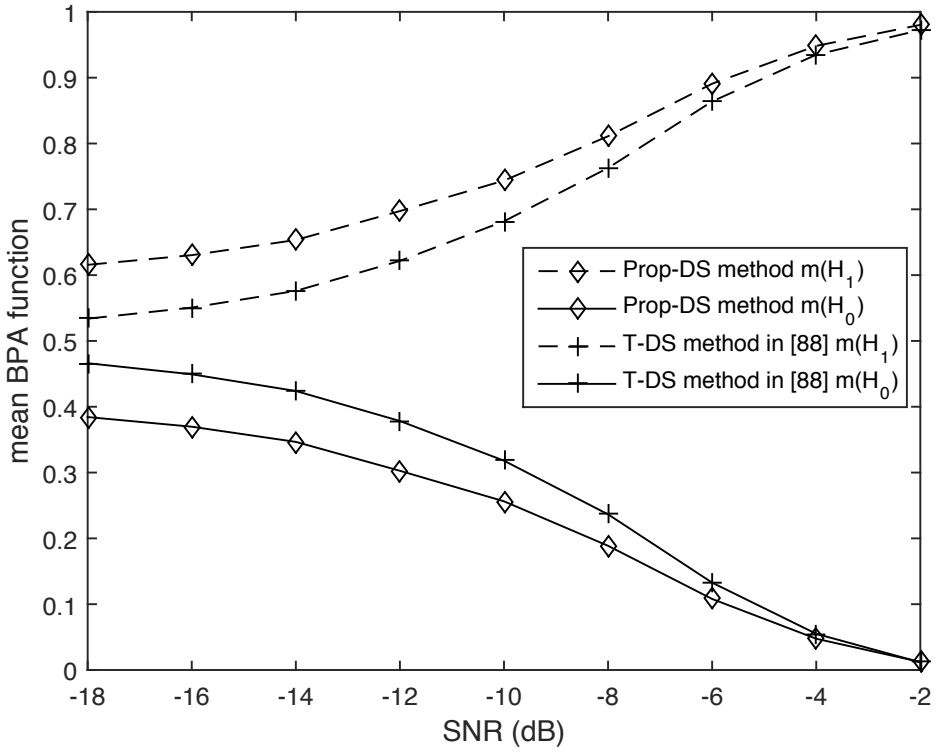

Figure 4.6 – The variation trend of the BPA functions with the increase of SNR when PU is present using 50 samples.

As the first part of simulation, we show the mean behavior of the BPA functions when SNR is varying in Figure 4.5 and Figure 4.6 where the number of sampling is respectively 200 and 50. Since the BPA function of the traditional D-S (T-DS) fusion in [88] is based on the central limit theorem, it is a good estimate of SUs' self-assessed decision credibility only when the number of samples is sufficiently high [13]. Therefore, it is not suitable for small sample size. According to the Equation (4.24) and Equation (4.25), we know that $m_i(\mathcal{H}_0)$ decreases and $m_i(\mathcal{H}_1)$ increases with the increasing of the largest eigenvalue λ_{1i} when a PU is present. Then after D-S fusion in Equation (4.27) and Equation (4.28), the BPA functions $m(\mathcal{H}_0)$ and $m(\mathcal{H}_1)$ also should have a declining and increasing trends, respectively. As shown in Figure 4.5, when the number of sample is large, i.e. 200 samples, for the proposed method, that is (N_s, L)=(100,2), the BPA functions in Equation (4.24) and Equation (4.25) of the proposed method are very similar to the BPA functions in T-DS [88]. Conversely, when the number of samples is small, the BPA function of the proposed method is still suitable. Figure 4.6 shows that the BPA functions of the proposed method with small sample size, with 50 samples that is (N_s, L)=(25,2), has a similar tendency compared

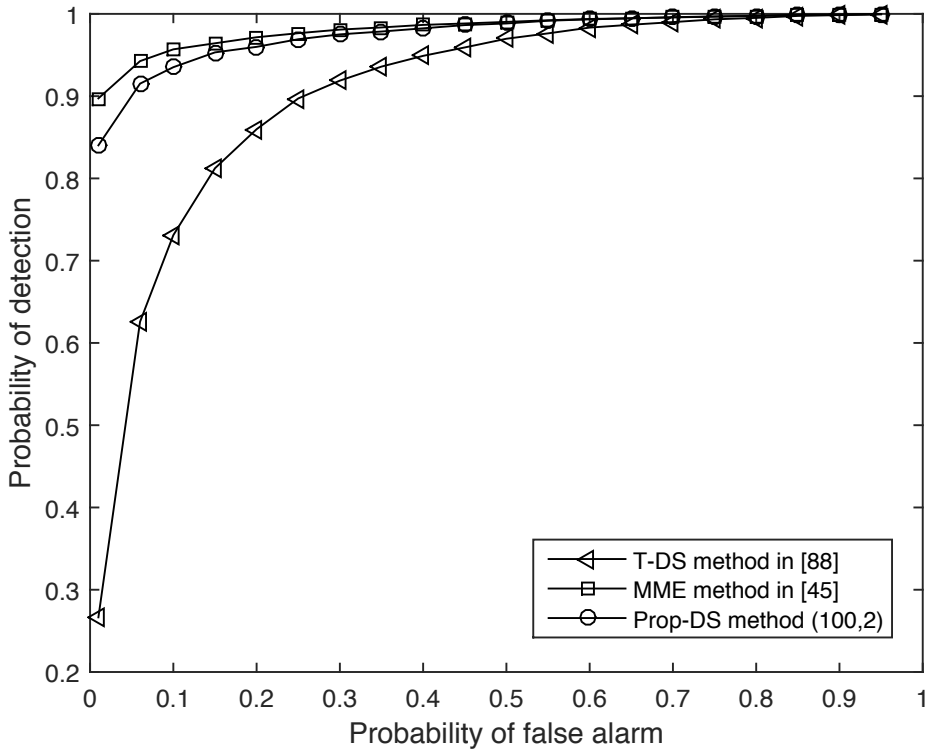

Figure 4.7 – ROC curves of the compared methods using 200 samples at each SU.

to the large sample size, which is not true for T-DS. We can see that the proposed DS (Prop-DS) method has about 5% improvement over T-DS with small sample size.

Therefore, in order to show the behaviour of the compared methods in a more general scenario, we assume now that each of the six SUs experiences different channel conditions. 100000 Monte Carlo simulations have been run where SNR at each SU is a random variable with a uniform distribution on the interval [-20 dB, 0 dB]. Based on this setting, Figure 4.7 and Figure 4.8 present the ROC curves of the proposed method and the other methods in [88] and [45]. When the sample number is 200, as shown in Figure 4.7, the proposed method (the circular curve) has a litter bit lower detection probability than the maximum-minimum eigenvalue (MME) method in [45]. As expected when the number of samples is large, the approximated Tracy-Widom distribution is no longer well adapted to characterize the BPA function. This is why the proposed method shows little less attractive performance in that case. Besides with 200 samples, it can be observed that the two eigenvalue-based methods perform much better than the T-DS one. Most importantly, when the sample number is 50, as shown in Figure 4.8, it is very obvious that the probability of detection of all methods decline compared with 200 samples. However, the proposed method shows better performance

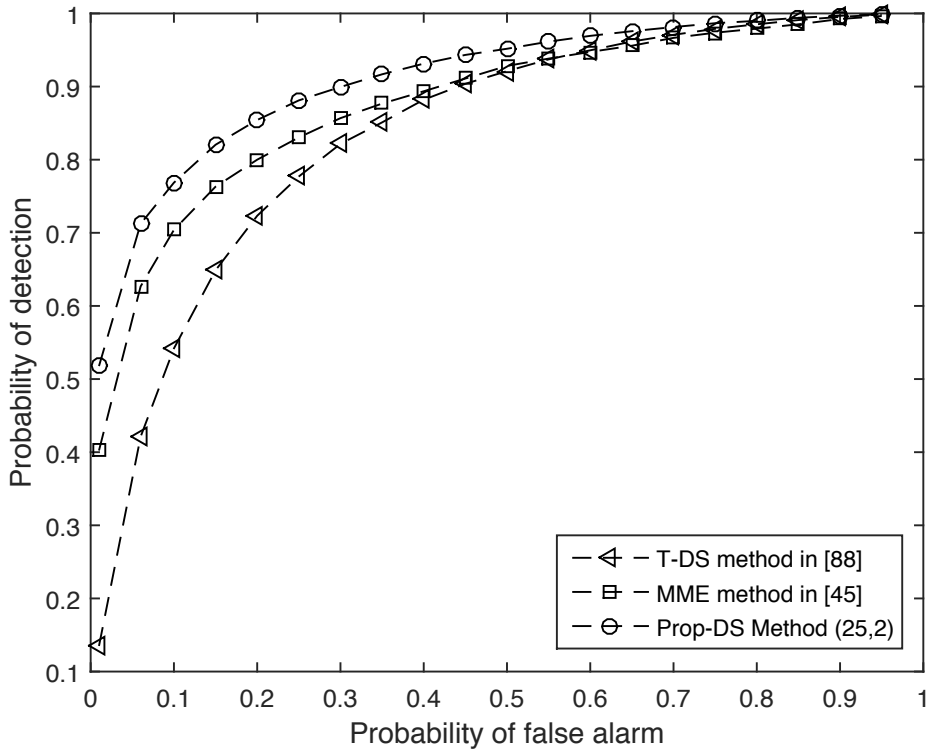

Figure 4.8 – ROC curves of the compared methods using 50 samples at each SU.

than its counterparts. It can be observed that the ROC curve of the proposed method with 50 samples is even partly above the one of the T-DS method in [88] with 200 samples.

In addition, for evaluating the performance of the proposed method with small sample size according to the number of SUs engaged in the process, we show in Figure 4.9 the ROC curves of the proposed method when the number of SUs is 10, 8, 6 and 4. The sample size at each SU is 50, and Monte Carlo simulations have been run where the SNR at each SU is randomly chosen in the interval [-20 dB, 0 dB], exactly in the same way as for the previous experiments. As shown in Figure 4.9, the detection performance brings up with the increasing number of SU. When the number of SU is 10, the proposed method can obtain about 0.9 probability of detection with 0.1 probability of false alarm. And due to the small sample size 50, with L=2, the proposed method keep on exhibiting a very low computational cost, mainly because of the eigenvalue decomposition. It is very suitable in practical CWSNs applications when dealing with constrained power devices.

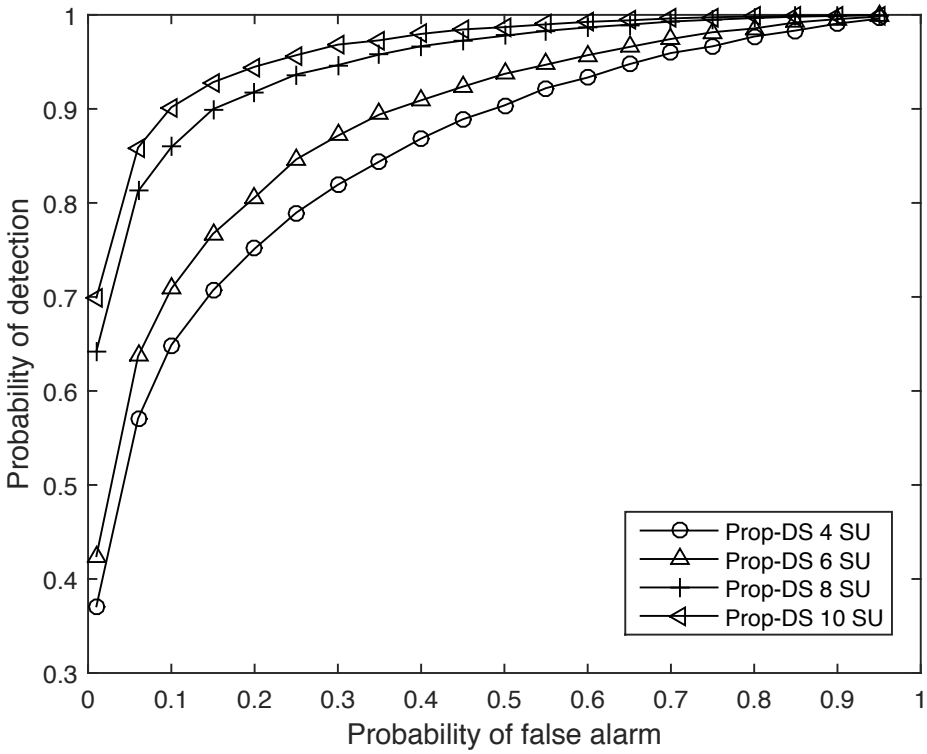

Figure 4.9 – ROC curves of our proposed scheme with different numbers of SU when the sample number is 50.

4.4 Conclusion

In this chapter, considering the channel conditions, an efficient cooperative spectrum sensing with small sample size is presented. The advantage of the proposed technique compared to other eigenvalue-based spectrum sensing techniques is that we form a thin observation matrix, which allows to get a small dimension covariance matrix. In that case the eigenvalue decomposition has a negligible cost. Then, a new BPA function is constructed and used in D-S fusion rule, which reduces the conflict of evidence from different SUs. Simulation results have shown that our method can achieve a higher probability of detection than other methods in small sample size situation.

However, in order to focus on the research of small sample size in spectrum sensing, previous schemes assume that all SUs always work normally, which means there are not any security issue for SU in the sensor network. Unfortunately, it is not very practical. Therefore, we will consider the cooperative spectrum sensing where faulty nodes are existing in the next chapter.

5

Robust and energy efficient CSS

In order to deal with the energy efficiency of a complete network, we propose a cluster-based CSS scheme in CWSNs where all SUs are separated into clusters and one "cluster head" is set as the FC to collect the sensing information and make the cluster decision. This is motivated by the energy consumption of sensor nodes, especially for the mobile ones, where the communication unit consumes the most power [107, 108] and the location of sensor node is changed. When applying the cluster algorithm into CSS, the energy consumption of the communications unit for the SU will be extremely reduced because most of them are closer to their own cluster head than the other FC and less power is needed to transmit local decisions. In addition, for the whole network, the cluster head makes its own decision whether the PU is present or not in each cluster, which remarkably improves the spectrum utilization of the spectrum hole.

On the other hand, reliability of the spectrum sensing decision in CR becomes a very important challenge when the WSNs is dealing with low-power and even low-cost SU nodes [109]. Among the SUs in the cluster, sometimes some of them inevitably fail in sending to the FC (that is the cluster head) a reliable information about the spectrum. Many reasons can lead to a node dysfunction such as battery depletion, electronic device under harsh environment or even errors in data transmissions. Taking the reliability problem into account, we propose to make the decision more robust against faulty nodes effects. We then propose a method that allows to consider simultaneously the reliability of each SU in the cluster and the mutually supportive degree among the

whole set of SUs in the cluster. This is what we call the double reliability evaluation in the rest of this chapter. Finally, after removing the nodes of low credibility, that are supposed to be faulty, the energy efficiency and reliability of each cluster is improved. Simulation results show that the proposed CSS scheme clearly allows to save energy and provides a more robust decision under faulty nodes situation.

The rest of this chapter is organized as follows. In Section 5.1, we present the system description with some background on cooperative spectrum sensing. The proposed robust and energy efficient CSS scheme in CWSNs is given in Section 5.2, where the cluster technique is adopted in CSS scheme and the double reliability evaluation is proposed in D-S fusion. Simulation results are shown in Section 5.3. Finally, the conclusions are drawn in Section 5.4.

5.1 System model

As illustrated in Figure 5.1, we consider a CWSNs where all SUs are separated into K clusters. These clusters are formed by running the K-means clustering algorithm presented in Section 5.2.1. Each cluster includes one FC and some SUs where potentially faulty sensor nodes exist. At first, each SU measures its input signal energy and calculates the evidence of its reliability according to the D-S theory. Then the information is sent to the FC in the cluster. After receiving the data, the FC calculates the supportive degree of every sensor node, removes the node of low reliability, combines the remaining evidences and makes the final decision for its cluster. This process is conducted in each cluster in parallel.

In this scheme, on basis of local observation, each SU in the cluster executes the local spectrum sensing. Thus, for each SU, the spectrum sensing problem in Equation (2.1) can be simplified in the following:

$$\begin{aligned} \mathcal{H}_0 &: y_i[n] = w_i[n] \\ \mathcal{H}_1 &: y_i[n] = x_i[n] + w_i[n] \end{aligned} \tag{5.1}$$

where $y_i[n]$ represents the received data at i-th SU_i. In our scheme, each SU_i applies energy detection to measure the PU's signal energy in one sensing period, as shown in Section 2.2.3. When the number of sampling is relatively large (e.g. $N_s > 200$), the observation energy follows a normal distribution as in Equation (2.30).

After local spectrum sensing, each SU will process this information and transmit

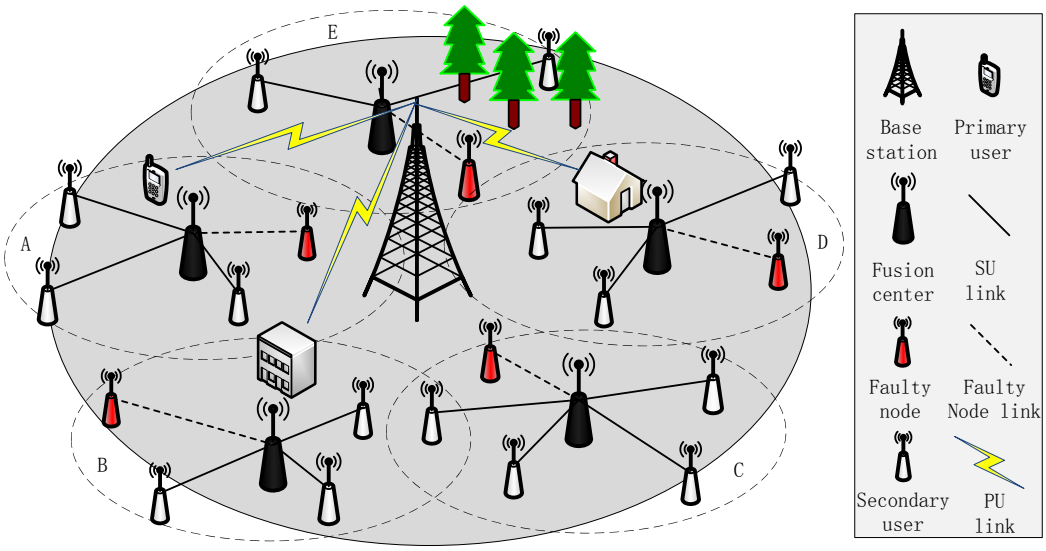

Figure 5.1 – Cluster-based cooperative spectrum sensing in CWSNs where some faulty nodes are existing.

them to the FC where the final decision is made. In Section 2.4.6, we introduce the D-S theory of evidence in order to make the final decision. In our spectrum sensing context, let $\Omega = \{\mathcal{H}_0, \mathcal{H}_1\}$ be the set representing all possible states of the system under consideration, called the frame of discernment. Then 2^{Ω} is the set of all subsets of Ω, including the empty set $\emptyset$. In our framework, $2^{\Omega} = \{\emptyset, \{\mathcal{H}_0\}, \{\mathcal{H}_1\}, \Omega\}$. In this case, the BPA functions for each SU_i, which estimate the SU's self-assessed credibility, are given by

$$m_i(\mathcal{H}_0) = \int_{\mathcal{T}(y_i)}^{+\infty} \frac{1}{\sqrt{2\pi}\sigma_{0i}} \exp\Big(- \frac{(x-\mu_{0i})^2}{\sigma_{0i}^2}\Big) dx \tag{5.2}$$

$$m_i(\mathcal{H}_1) = \int_{-\infty}^{\mathcal{T}(y_i)} \frac{1}{\sqrt{2\pi}\sigma_{1i}} \exp\Big(- \frac{(x-\mu_{1i})^2}{\sigma_{1i}^2}\Big) dx \tag{5.3}$$

and

$$m_i(\Omega) = 1 - m_i(\mathcal{H}_0) - m_i(\mathcal{H}_1), \tag{5.4}$$

where $i \in \{1, 2, \cdots, N_{su}\}$ and N_{su} is the number of SUs introduced in the CSS process. $\mathcal{T}(y_i)$ denotes the test statistic of the i-th SU as in Equation (2.25). μ_{0i}, μ_{1i} and σ_{0i}^2, σ_{1i}^2 are the mean and variance of the statistic test $\mathcal{T}(y_i)$ under hypotheses $\mathcal{H}_0$ and

$\mathcal{H}_1$, respectively. Finally, according to the so-called D-S rule of combination shown in Equation (2.97), for $B_j \subset 2^{\Omega}$, a new BPA function $m(B_j)$ is yielded by N_{su} BPA functions at FC as:

$$m(B_j) = (m_1 \oplus m_2 \oplus \cdots \oplus m_{N_{su}})(B_j) \tag{5.5}$$

In order to reduce the energy dissipation of sensor nodes as in the broadcast CSS scheme and to improve the detection reliability of CSS when faulty nodes are existing, we introduce the clustering into CSS and propose the double reliability evaluation algorithm.

5.2 Efficient and reliable CSS scheme

In this section, we propose a robust and energy efficient CSS scheme where a clustering technique is introduced to CSS. Thus all SUs are separated into K clusters. One cluster head is chosen in each cluster. Clustering is a common data analysis method which is widely applied to machine learning, pattern recognition and image analysis. Clustering is the task of grouping similar objects, which have similar characteristics. Here, clustering is introduced into CSS in order to separate all SUs into different groups. The idea is to reduce the distance between each SU and its associated FC who is in charge to make the CSS decision. The cluster head is the FC in the cluster. This strategy allows to reduce the energy consumption of transmission from each SU to its cluster head. At the same time, in order to take into account the possible existing faulty nodes in clusters, we propose the double reliability evaluation method that allows to consider simultaneously the reliability of each SU and the mutually supportive degree among the whole set of SUs in each cluster. At the end, we remove the node of low reliability in the cluster, which does not only provide more robust decision but also reduce the global energy consumption of the cluster.

5.2.1 K-means clustering algorithm

The usual clustering algorithms are respectively partitioning clustering algorithm, hierarchical clustering algorithm, density-based clustering algorithm, grid-based clustering algorithm and model-based clustering algorithm [110, 111]. Among these algorithms, the K-means algorithm is very simple and can be easily implemented in solving many practical problems. At the same time, we know that K-means clustering algo-

rithm can divides some sensor nodes into K clusters and the average distance from every sensor node to the cluster head is minimized in each cluster. Therefore, CSS based on K-means clustering algorithm can save energy consumption, especially for mobile cognitive sensor nodes. We mainly study the K-means clustering algorithm in the following, but other approaches can be studied.

K-means clustering algorithm is an efficient clustering algorithm based on partition. It assigns objects (SU) to the nearest cluster by distance and divides ultimately N_{tot} SUs into K clusters. The process is that firstly choose K SUs, regularly distributed in the whole network, as the center of each cluster, then assign the remaining SUs to a cluster according to the distance from the SU to the center of each cluster, and calculate the average value of each cluster again until convergence [112]. Here we use a squared error criterion:

$$V = \sum_{i=1}^{K} \sum_{\mathbf{x}_j \in \mathbf{S}_i} ||\mathbf{x}_j - \mathbf{v}_i||^2 \tag{5.6}$$

where $\mathbf{x}_j$ is vector of coordinate of the j-th SU, and $\mathbf{v}_i$ is the mean coordinate vector of the SU in the i-th cluster, which is defined as

$$\mathbf{v}_i = \frac{1}{card(\mathbf{S}_i)} \sum_{\mathbf{x}_j \in \mathbf{S}_i} \mathbf{x}_j, \tag{5.7}$$

where $\mathbf{S}_i$ is the set of position vectors of SUs of the i-th cluster.

The steps of K-means clustering algorithm are:

1 : Choose K SUs regularly distributed in the whole network as the center of the K clusters;

2 : Define the sets of SU for the K clusters by assigning each SU into the cluster with the nearest center;

3 : Calculate the average coordinate vector $\mathbf{v}_i$ ($i = 1, 2, \cdots, K$) of each cluster, and define $\mathbf{v}_i$ as the new center of the i-th cluster;

4 : Calculate the function V in Equation (5.6);

5 : Repeat Step 2 to Step 4 until the function value V is not varying.

Then, for every cluster, the FC is finally chosen as the nearest SU to the center of the cluster, $\mathbf{x}_{\text{FC},i} = \min_{\mathbf{x}_j \in \mathbf{S}_i} ||\mathbf{x}_j - \mathbf{v}_i||$. Obviously we have to mention here that this technique requires to know the position of every SU.

5.2.2 Energy consumption of CSS based on K-means clustering algorithm

For simplicity and without loss of generality, we only consider the energy consumption of the communication unit in the sensor node. In addition, we know that the transmitting power is relative to the distance between the emitting and the receiving node.

In order to compare the energy consumption of the CSS based on clustering with the energy consumption of the broadcast approach, we assume that each sensor node knows the position of the other ones. First of all, we consider that some sensor nodes are randomly scattered in a certain area. In the broadcast CSS scheme, each SU sensor node transmits its own sensing result to every other SU in the whole network. The energy consumption of the broadcast cooperative spectrum sensing approach is given by:

$$\begin{aligned} E_{\text{broadcast}} &= E_{T_x} + E_{R_x} \\ &= (\sum_{i=1}^{N_{tot}} P_{dis-farthest-user,i} + N_{tot}(N_{tot}-1)P_{R_x})T \end{aligned} \tag{5.8}$$

where E_{T_x} and E_{R_x} are respectively the total transmitting energy and the total receiving energy in the network. The range of the broadcast is the farthest distance, N_{tot} is the total number of sensor nodes, T is the time of transmitting and receiving. P_{R_x} is the power consumption of a SU in the receiving mode, $P_{dis-farthest-user,i}$ is the power consumption of the i-th SU in the emitting mode, which is ruled by the distance with the farthest SU in the network.

Similarly, the energy consumption of the CSS based on K-means clustering algorithm is given by:

$$E_{\text{K-means}} = E_{T_x} + E_{R_x} \tag{5.9}$$

However, other than the broadcast CSS scheme, in our cluster-based scheme the communication distance is bounded to the cluster dimension, and we consider only the transmission from the SU to the FC. Thus, the Equation (5.9) can be turned into the

Equation (5.10) [113, 114]

$$E_{\text{K-means}} = \Big(\sum_{j=1}^{K} \sum_{i=1}^{N_{node,j}-1} P_{i,\text{CH}_j} + (N_{tot} - K)P_{R_x}\Big)T, \tag{5.10}$$

where $N_{node,j}$ is the number of sensor nodes in the j-th cluster, K is the number of clusters, P_{i,CH_j} is the transmitting power from the i-th node to the j-th cluster head, P_{R_x} is the receiving power and T is the time required to transmit or receive the report for the CSS. Note that in each cluster we assume that the cluster head is the FC. It receives the data information from the SUs in the cluster and makes its own decision whether the PU is present or not, which is able to improve the spectrum utilization in the whole network.

For comparing the energy consumption of the different approaches, we introduce the energy ratio which is the ratio between the energy consumption of the CSS based on K-means clustering algorithm and the energy consumption of the broadcast CSS. According to the Equation (5.8) and Equation (5.10), we calculate the energy ratio as follows:

$$\eta = \frac{E_{\text{K-means}}}{E_{\text{broadcast}}} \tag{5.11}$$

Note that in cooperative spectrum sensing based on K-means clustering algorithm, we need to select a suitable value for the parameter K in order to keep balance between reducing the energy consumption of the whole sensor networks and increasing the reliability of each cluster. For example, when the total number of sensor node is 100, the parameter K is set to 8. But providing an optimized value of K is not obvious, it relies on many parameters, such as area to be covered, mean distance between nodes, mobility of node and transmission rate. That is out of the scope of this thesis but it could be part of future works. In addition, because of the imbalanced energy consumption between FC and other nodes, a battery level threshold for the FC is set in order to ensure the reliability. When the battery level of the FC is lower than the threshold, the next nearest node to the center $\mathbf{v}_i$ is elected as the new FC. Moreover, according to the mobility of nodes in the network, it has to be mentioned that the K-means clustering algorithm needs to be recalculated periodically.

5.2.3 Double reliability evaluation algorithm

In the previous subsection, we consider the energy consumption of CSS. Then, in this subsection, we will focus on the reliability of spectrum sensing in CWSNs. For one cluster including N_{su} (equal to $N_{node,j}$ in the j-th cluster) nodes in the network, we need to consider the reliability of evidence before using D-S theory of evidence and fusing them, and then make a more reliable decision only according to the reliable evidence. So we propose the double reliability evaluation algorithm in order to evaluate more accurately the reliability of each SU by simultaneously considering the source reliability and the mutual supportive degree among the SUs.

The source reliability can be evaluated by Equation (5.12) [115]:

$$\mathrm{w}_i = \frac{\gamma_i}{\max(\gamma_1, \gamma_2, \cdots, \gamma_{N_{su}})} \tag{5.12}$$

where γ_i is the SNR of the PU at the i-th SU. And then, combining with the Equations (5.2) and (5.3), the new BPA functions are obtained with corresponding weight w_i as follows:

$$m_i^{'}(\mathcal{H}_0) = \mathrm{w}_i m_i(\mathcal{H}_0) \tag{5.13}$$

$$m_i^{'}(\mathcal{H}_1) = \mathrm{w}_i m_i(\mathcal{H}_1) \tag{5.14}$$

$$m_i^{'}(\Omega) = 1 - m_i^{'}(\mathcal{H}_0) - m_i^{'}(\mathcal{H}_1) \tag{5.15}$$

According to the reliability resource evaluation in Equations (5.12) - (5.15), the effect of low reliable node (lower SNR) is decreased thanks to the weighting. However, in realistic environment some SUs may inevitably fail in sending a reliable information about the spectrum due to node dysfunctions, such as low battery or electronic device under harsh environment.

In realistic environment, SUs experience different surroundings and their credibility degrees are not the same. Especially when some SUs are not working as expected and send erroneous data, the evidences are different from other SUs. That is to say, if the evidence of one SU is similar to the other ones, this SU acquires a high supportive degree. Otherwise, if one SU's evidence is obviously different from the other SUs, it gets a less supportive degree from the other SUs. Then this node is considered as not reliable and is removed from the fusing process. As a result, the similarity degree between SU_i and SU_j based on BPA function can be described by the following

formulation:

$$sim(i,j) = \frac{\sum_{k=1}^{card(2^{\Omega})} \min(m_i'(A_k), m_j'(A_k))}{\frac{1}{2}\sum_{k=1}^{card(2^{\Omega})} (m_i'(A_k) + m_j'(A_k))} \tag{5.16}$$

where $card(2^{\Omega})$ denotes the cardinality of 2^{Ω}.

Then the supportive degree of SU_i with respect to other SUs can be evaluated by Equation (5.17):

$$Sup(i) = \sum_{j=1}^{N_{su}} sim(i,j), \qquad j \neq i, \quad i = 1, 2, \ldots, N_{su}. \tag{5.17}$$

If a node is not working as expected, its supportive degree $Sup(i)$ will be very low, and vice versa.

Thus, the normalization of the supportive degree evaluation can be written as:

$$Rel(i) = \frac{Sup(i)}{\max\limits_{j \in \{1,2,\ldots,N_{su}\}} (Sup(j))}, \qquad i = 1, 2, \ldots, N_{su}. \tag{5.18}$$

In order to make a more reliable decision, we have to consider the highest reliability of SUs. So we should remove the data with low reliability caused from faulty node which can disturb the final decision. Hence, we need to define the evaluation threshold F that is able to decide whether we should remove the data. For accuracy and effectiveness, we set the evaluation threshold F to 0.5. When the supportive degree $Rel(i)$ is lower than 0.5, SU_i is considered as not reliable and is removed, otherwise, the evidence is saved and applied for the fusion. In addition to the faults in the node, the proposed method also allows to remove the unreliable sensing due to channel experiences.

Finally, after removing the unreliable evidence, we get the reliable and accurate BPA function of M remaining SUs (with $1 \leq M \leq N_{su}$), and the final BPA function

is obtained based on the D-S theory in the Equations (5.19) and (5.20),

$$m(\mathcal{H}_0) = \frac{1}{1-\kappa} \sum_{A_1 \cap A_2 \cap \cdots \cap A_M = \mathcal{H}_0} \prod_{i=1}^{M} m_i^{'}(A_i) \tag{5.19}$$

$$m(\mathcal{H}_1) = \frac{1}{1-\kappa} \sum_{A_1 \cap A_2 \cap \cdots \cap A_M = \mathcal{H}_1} \prod_{i=1}^{M} m_i^{'}(A_i) \tag{5.20}$$

where

$$\kappa = \sum_{A_1 \cap A_2 \cap \cdots \cap A_M = \emptyset} \prod_{i=1}^{M} m_i^{'}(A_i) \tag{5.21}$$

After getting the final combination results $m(\mathcal{H}_0)$ and $m(\mathcal{H}_1)$, the final decision is made upon the following rule:

$$\begin{aligned} \mathcal{H}_0 : \quad & m(\mathcal{H}_1) < m(\mathcal{H}_0) \\ \mathcal{H}_1 : \quad & m(\mathcal{H}_1) > m(\mathcal{H}_0) \end{aligned} \tag{5.22}$$

Note that in the double reliability evaluation algorithm, we remove the node of low reliability from the cluster in order to improve the detection probability. Hence, the cluster head (FC) will not ask any information to the faulty node for the next round of CSS. The consequence is that less energy will be required because the cluster head does not need to communicate anymore with those faulty nodes. In Section 5.3, we present the energy consumption benefit obtained thanks to the removal of faulty nodes.

5.3 Simulation results and analysis

In this section, performance of the proposed scheme is evaluated by simulations. The simulation of the proposed efficient and reliable CSS scheme in CWSNs is conducted under the following assumptions:

- The PU signal is DTV signal as in [116].
- The probability of PU appearing is 0.5.
- The bandwidth of the PU signal is 6 MHz.
- The local sensing time is 50 μs, and an AWGN channel is considered.
- Each cluster head is the FC of the cluster.

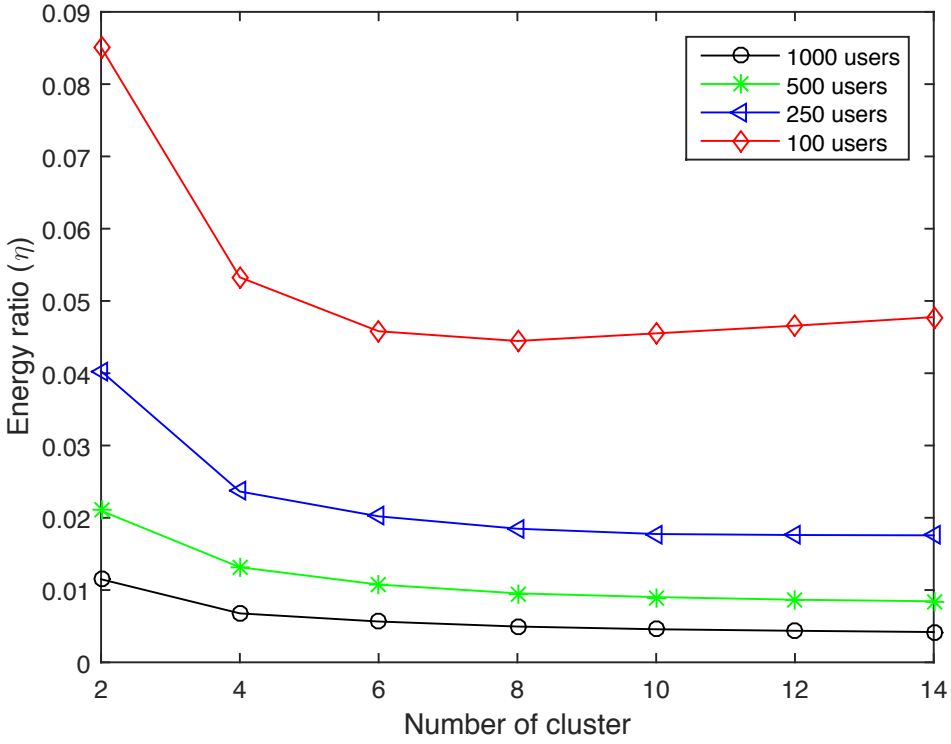

Figure 5.2 – The energy efficiency performance for different cluster number.

Firstly, for evaluating the energy consumption in the Equations (5.8) and (5.10), we present a classic model [107] which includes the power consumption of the transmitting and the receiving in the Equations (5.23) and (5.24),

$$p_{tx}(n_1, n_2) = (\alpha_{11} + \alpha_2 d(n_1, n_2)^D)r \tag{5.23}$$

$$p_{rx} = \alpha_{12} r \tag{5.24}$$

where $p_{tx}(n_1, n_2)$ is the transmitting power consumption from node n_1 to node n_2 and $d(n_1, n_2)$ is the distance between node n_1 to node n_2, D is the path loss index. p_{rx} is the receiving power consumption. Parameters in Equations (5.23) and (5.24) are respectively α_{11} = 45 nJ/bit, α_{12} = 135 nJ/bit, α_2 = 10 pJ/bit/m^2 (D = 2) or 0.001 pJ/bit/m^4 (D = 4) [107].

According to the model and the Equation (5.11), we evaluate the energy ratio of the proposed CSS based on K-means clustering algorithm with four different numbers of sensor nodes (1000, 500, 250 and 100) which the number of clusters changes from 2 to 14. As shown in Figure 5.2, the energy ratio is between 0 and 0.085 and decreases along with the increase in the number of clusters. Clearly, the energy consumption of

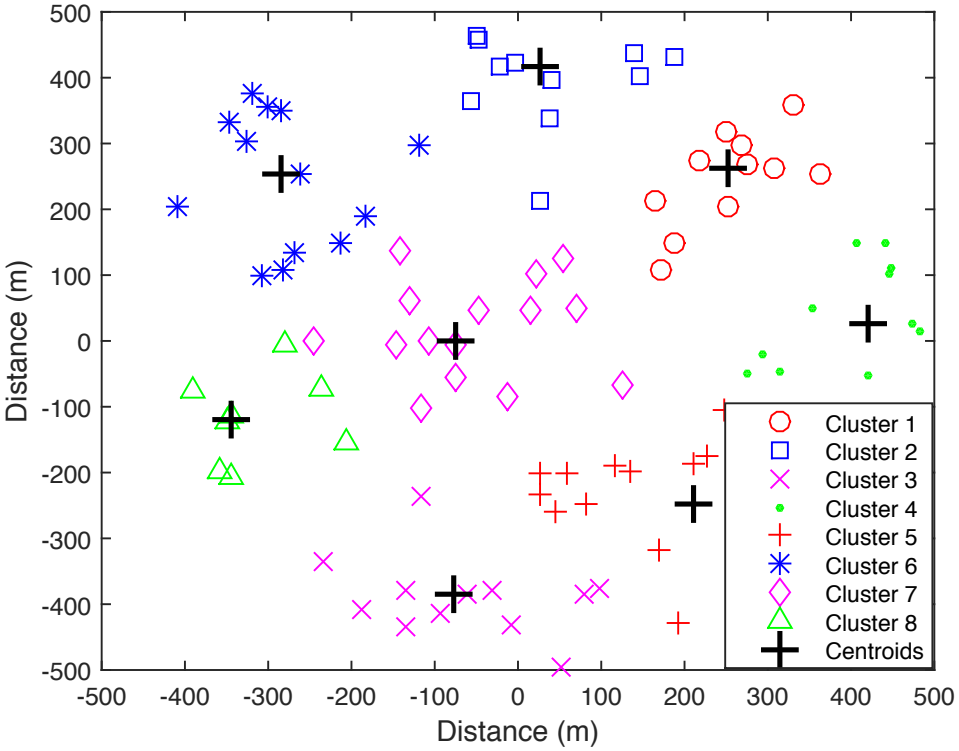

Figure 5.3 – 100 SUs are scattered into 8 clusters with K-means clustering algorithm.

the clustered CSS is under the energy consumption of the broadcast CSS. And when the number of clusters is 7 or 8, the CSS based on K-means clustering algorithm has the highest energy ratio relatively to the broadcast CSS scheme. For example, when the number of SUs is 250 and the number of cluster is 8, the energy ratio is about 0.02, that is the CSS based on K-means clustering algorithm reduces up to 92% the energy consumption compared with the broadcast CSS. Figure 5.3 shows the distribution of 100 sensor nodes after using K-means clustering algorithm.

Secondly, we assess again the detection reliability and energy efficiency of the proposed CSS scheme in each cluster. In the following, taking into account one cluster in CWSNs, we assume that there are ten SUs (one of them is faulty) which are distributed in different locations for conducting the local spectrum sensing. For clearly showing the improvement of the proposed double reliability evaluation algorithm, the comparison between proposed method and the other methods are shown in Figure 5.4, where the SNR at SU1-SU5 are -14 dB, SNR at SU6-SU10 are changed from -22 dB to -6 dB. It shows the probability of detection of the proposed method and the method in [115] and [95] with one faulty node. In this simulation, we make use of the double reliability evaluation algorithm at FC. According to Figure 5.4, the probability of detection of

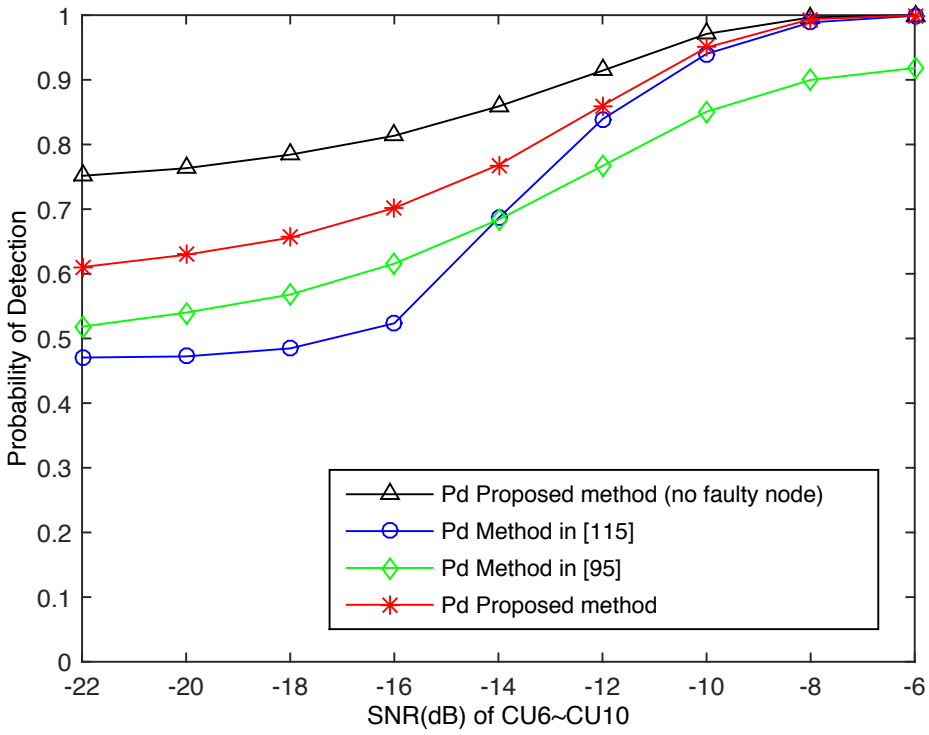

Figure 5.4 – Probability of detection comparison between proposed algorithm and other methods.

the proposed method is better when there is no faulty nodes. Under the condition of one faulty SU over ten SUs, the probability of detection increases with the increase of SUs' SNR. However, the performance of our method is superior to the method in [95] at least and better than the method in [115] when SNR is below -12dB. That is to say, the double reliability evaluation successfully removes the faulty node and reduces its interference.

In addition, there are often more than one faulty user in the cluster in realistic systems. Figure 5.5 shows that the detection performance brings down with the increasing number of faulty nodes, where the SNRs at SUs are between -22 dB and -10 dB. However, when the ratio of faulty nodes is 20%, the probability of detection is better than the methods in [115] and [95] where the ratio of faulty nodes of which are 10%. It shows that our method is more robust compared to the other methods when the faulty users number increases. Moreover, Figure 5.5 shows also that the curve of proposed method including 30% and 40% faulty nodes are below the diagonal. That is because a large number of faulty nodes in the cluster affect seriously the decision of the cluster head. It can be interpreted as faulty nodes behave as malicious nodes who mislead the

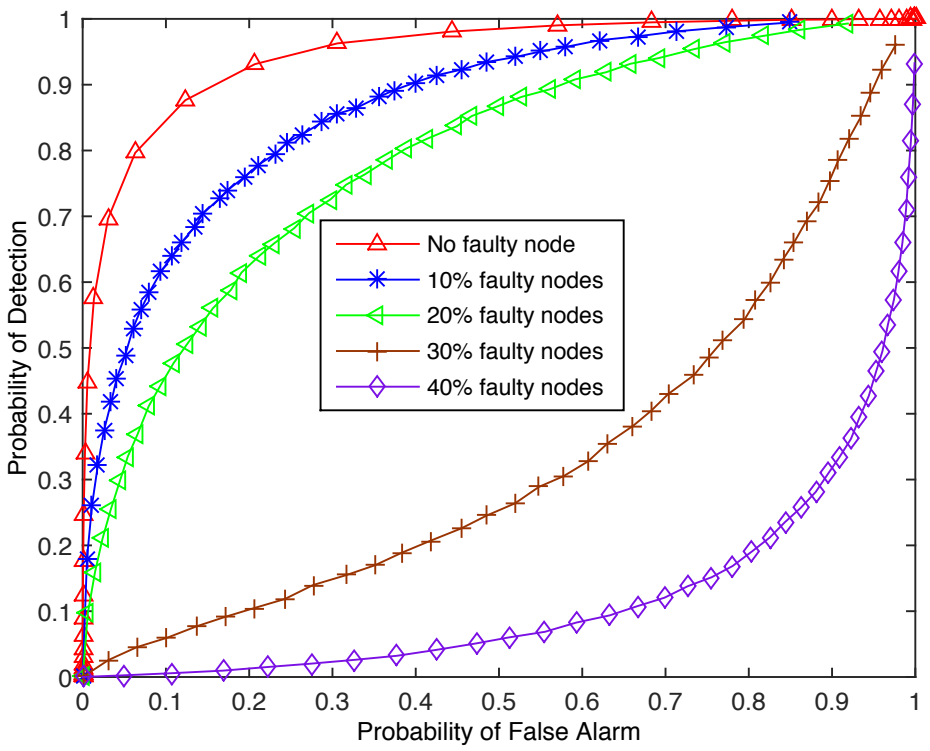

Figure 5.5 – Probability of detection comparison of proposed double reliability evaluation algorithm.

decision process.

Finally, after removing the faulty node in each cluster, we reduce the transmission energy consumption for each cluster where some faulty nodes have been identified. In order to demonstrate the energy consumption reduction, Figure 5.6 presents the energy consumption of each cluster in CWSNs. As shown, when we consider that 100 SUs are scattered into 8 clusters with K-means clustering algorithm inside a circle of radius 500m, for each cluster (C1-C8), the energy consumption after removing the faulty nodes is appreciably lower than before removing the faulty node, especially in cluster C4 and C7. That is because we remove the faulty node according to the proposed double reliability evaluation algorithm, thus reduce the power consumed in transmitting information from the faulty node to the cluster head. Obviously, for each cluster, the proposed method can save energy, then for the whole network, the energy consumption after removing the faulty node is also significantly lower. That is to say, the proposed method is more efficient in term of energy for large networks.

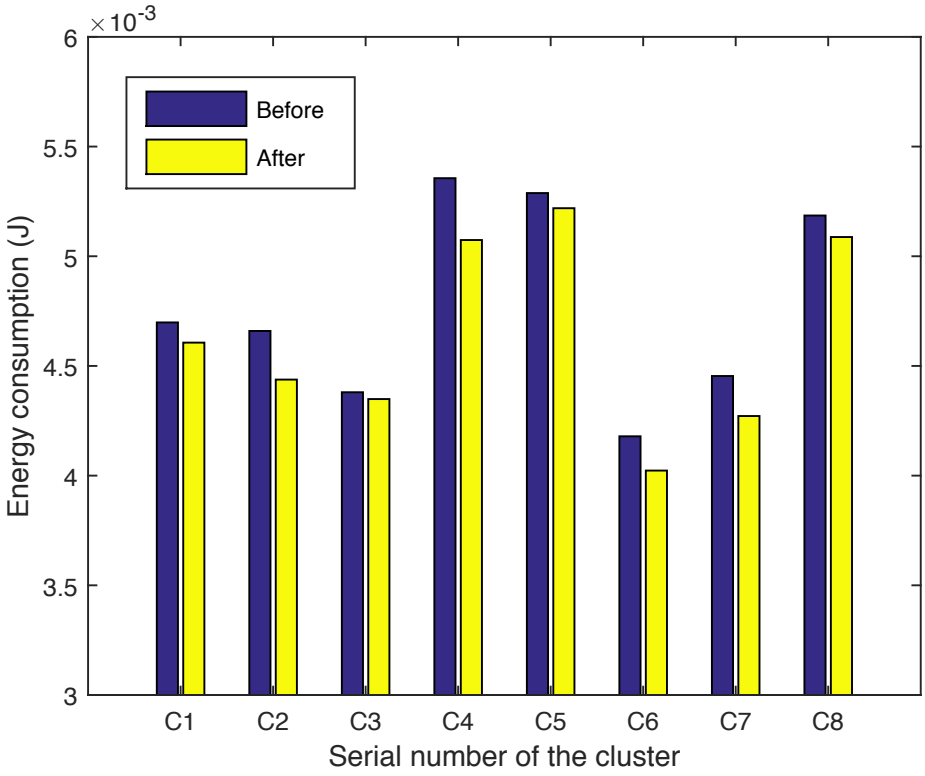

Figure 5.6 – Energy consumption in each cluster from C1 to C8.

5.4 Conclusion

In this chapter, we addressed the problem of the improvement of the CSS process in CWSNs. In such a framework, by considering that the energy is scarce resource which needs to be managed efficiently, we proposed a robust and energy efficient technique. Firstly, the method aims to divide the nodes into a few clusters which brings the advantage of making a CSS decision in each covered by the clusters. This clusters organization also allows to reduce the distance between the nodes involved in the CSS, which reduces the energy consumption devoted to the communications required by the process. Secondly in this work, we consider that some nodes in the clusters can be faulty. Indeed generally speaking, with some heterogeneous nodes in CWSNs, the chance to get deficient nodes is far from being negligible. Then in this work we proposed a combined double reliability evaluation algorithm with the D-S theory of evidence which allows to detect those unreliable nodes and allows to make a more robust decision. This last technique can also help to save some energy in the network. Finally, many other improvements could be made to optimize the CSS process in CWSNs. In this proposed work, some strong assumptions have been used regard-

ing the prior knowledge of the SUs positions or the SNR encountered in the channels. Future studies should be devoted to the development of less dependent techniques to such energy-consuming estimations, and to the optimization of energy consumption in the whole network.

6

Conclusion and future work

In this chapter, we make a conclusion of this dissertation and discuss the further works. In detail, a brief conclusion is drawn in the next section whereas some perspectives for future works are mentioned in Section 6.2.

6.1 Conclusion

In this thesis, we explore the spectrum sensing (SS) techniques in cognitive wireless sensor networks (CWSNs). Due to the scarcity of spectrum resource and the low spectrum utilization, cognitive radio (CR) technology as a very promising solution is proposed and applied in wireless sensor networks (WSNs). There are various methods of spectrum sensing for CR in the literature, but a very few of them seem to be really suitable in WSNs framework. As a matter of fact, the constrained resource of the sensor nodes, namely hardware limitations, power limitation, sensing duration and reliability, are rarely considered. Therefore, considering these limitations above, we propose to make spectrum sensing decisions from small sample size. Then, some efficient SS methods with small sample size are proposed to improve the energy efficiency in CWSNs.

At the beginning, this dissertation presents the background of the development of CR technology, the cognition mechanism of CR which includes spectrum sensing, spectrum mobility, spectrum decision and spectrum sharing, and the advantages of

using CR in WSNs such as efficient spectrum utilization, multiple channels utilization, energy efficiency and global operability. After that, an overview of the developed SS techniques is given in chapter 2, which mainly includes performance indicators of SS techniques, local spectrum sensing (LSS) and cooperative spectrum sensing (CSS). In local spectrum sensing, several methods are presented such as MFD, CFD, ED, WBS, EBS,GoF test based sensing and wideband sensing. In cooperative spectrum sensing, centralized CSS and distributed CSS are described. In detail, the different data fusion methods of fusion center (FC) in centralized CSS are introduced, which are hard-decision combining data fusion, soft-decision combining data fusion, Bayesian fusion rule, Neyman-Pearson criterion, fuzzy fusion rule and Dempster-Shafer (D-S) theory of evidence. However, the existing various methods of spectrum sensing for CR in the literature do not consider these limits of resource of sensor nodes. For example, energy detection is able to achieve a good detection performance only when the sample size is sufficiently large. Numerous covariance matrix or eigenvalue based detection methods have been proposed, but most of them have the requirements of the long sensing time (large sample size) and the high computational complexity. Motivated by these limitations, the proposed local spectrum sensing and cooperative spectrum sensing are presented in chapter 3 and chapter 4, respectively.

In chapter 3, we firstly exploit the student's t-distribution to cope with the small number of samples. It is demonstrated that the student's t-distribution test under small sample size can also provide a low error rates. Thus, according to this characteristic of student's t-distribution and taking into account several GoF tests, an efficient local spectrum sensing method is proposed on basis of both hypotheses of presence and absence of primary user (PU) signal, which is able to get a high reliability of detection. However, in order to focus on dealing with the small sample size, we do not consider the channel condition in the system model of the proposed method. Hence, considering the secondary user (SU) practically experiencing path loss, multipath and shadowing, we propose to adopt a cooperative spectrum sensing strategy based on multiple sensor nodes in order to improve the reliability of detection, which is based on an adjusted Tracy-Widom distribution that is suitable for small sample size in chapter 4.

However, small sample size really increases the uncertainty of the observation samples and reduces the reliability of final decision. Therefore, our efforts begin with the D-S theory of evidence that can deal with the uncertainty from the small observation samples and improve the reliability by fusing different data groups. According to the D-S theory of evidence, after coping with the small number of samples, some basic probability assignment (BPA) are estimated with the characteristic of the student's

t-distribution in chapter 3 or the adjusted Tracy-Widom distribution in chapter 4. Finally, relying on the fusion of different probability assignment estimations, we make a reliable final decision whether a PU signal is present or not. The simulation results referring to the performance comparisons are also given in chapter 3 and chapter 4, which also verifies the effectiveness of the proposed methods for small sample size scenarios.

In the end, considering the energy efficiency and the reliability of decision, a cooperative spectrum sensing scheme in CWSNs is proposed. In the proposed method, firstly, considering the energy consumption of sensor nodes, we propose a cluster-based CSS scheme where the energy consumption of the communications unit for the SU is reduced and the spectrum utilization of the spectrum hole for the whole network is improved. Secondly, taking the reliability problem into account, we propose a method that allows to consider simultaneously the reliability of each SU in the cluster and the mutually supportive degree among the whole set of SUs in the cluster, namely double reliability evaluation. Finally, after removing the nodes of low credibility, the energy efficiency and reliability of each cluster is improved. Simulation results show that the proposed CSS scheme clearly allows to save energy and provides a more robust decision under faulty nodes situation.

6.2 Future work

In this thesis, we concentrate on taking advantage of small sample size to solve the problem of the resource-constrained sensor nodes in WSNs by proposing some efficient spectrum sensing methods. Based on this work, some prospects are suggested for the future works.

- In this thesis, the noise power σ_w^2 is assumed to be known at each SU. However, knowledge of the noise power is not always realistic in practice. How to accurately estimate the noise power is a promising direction. In addition, how do the estimated noise power affect the proposed methods also should be studied.
- We consider one channel model in the proposed cooperative spectrum sensing method with small sample size. But in the real applications of CWSNs, the sensor nodes are probably deployed in any place such as in busy intersections, in a large building and in a forest. Therefore, more realistic channel model in specific environment (hotspot, indoor, urban and suburban area, etc.) should be considered in the future work.

- In the thesis, we propose some efficient spectrum sensing methods for small sample size, where some simulation results are given to verify the availability of the proposed methods. However, in most cases the validity of research works need to be further evaluated in a hardware testbed. Thus, in the future work the proposed method will be verified on a hardware platform.
- We take advantage of the basic D-S theory of evidence in order to make a final decision in the proposed methods. However, many enhanced D-S theory of evidence methods have been proposed in the literature. How do the enhanced D-S theory of evidence methods behave is a interesting study orientation. Besides, there are various fusion methods such as fuzzy fusion and Kalman filter, which is worthy of study.
- A trade off between energy efficiency and detection reliability is a very essential aspect to design the spectrum sensing algorithm. In the proposed robust and energy efficient cooperative spectrum sensing method, we give a rough balance between the energy efficiency of the whole networks and the detection reliability of each cluster. The optimal trade off between efficiency and reliability including the network and the node is a very important direction in the future.
- In this thesis, considering the constrained resource of the sensor node in CWSNs, we propose to deal with small sample size in order to design efficient algorithms, which reduce the detection reliability. In the future work, other methods that are energy efficient to the node should be investigated.

Appendixes

Appendix 1: Computation of $\hat{\sum}_{2c}$ the covariance matrix of $\hat{\mathbf{r}}^{\alpha}_{yy^*}$

In Equation (2.21), $\hat{\sum}_{2c}$ is the covariance matrix of $\hat{\mathbf{r}}^{\alpha}_{yy^*}$, which can be computed as [64]

$$\hat{\sum}_{2c} = \begin{bmatrix} \mathcal{R}_e\left\{\frac{\mathbf{Q}+\mathbf{Q}^*}{2}\right\} & \mathcal{I}_m\left\{\frac{\mathbf{Q}-\mathbf{Q}^*}{2}\right\} \\ \mathcal{I}_m\left\{\frac{\mathbf{Q}+\mathbf{Q}^*}{2}\right\} & \mathcal{R}_e\left\{\frac{\mathbf{Q}-\mathbf{Q}^*}{2}\right\} \end{bmatrix} \tag{A.1}$$

where the (i, j)-th entries of the two covariance matrices $\mathbf{Q}$ and $\mathbf{Q}^*$ are given by

$$\mathbf{Q}(i, j) = S_{f_{k_i} f_{k_j}}(2\alpha, \alpha) \tag{A.2}$$

and

$$\mathbf{Q}^*(i, j) = S^*_{f_{k_i} f_{k_j}}(0, -\alpha). \tag{A.3}$$

Here, $S_{f_{k_i} f_{k_j}}(2\alpha, \alpha)$ and $S^*_{f_{k_i} f_{k_j}}(0, -\alpha)$ denote the unconjugated and conjugated cyclic-spectrum of $f[n, k] = y[n]y^*[n + k]$, respectively. They can be estimated using fre-

quency smoothed cyclic periodograms as

$$\hat{S}_{f_{k_i} f_{k_j}}(2\alpha, \alpha) = \frac{1}{N_s L} \sum_{l=-(L-1)/2}^{(L-1)/2} \mathcal{W}(l) F_{k_i}(\alpha + \frac{2\pi l}{N_s}) F_{k_j}(\alpha - \frac{2\pi l}{N_s}) \tag{A.4}$$

$$\hat{S}^*_{f_{k_i} f_{k_j}}(0, -\alpha) = \frac{1}{N_s L} \sum_{l=-(L-1)/2}^{(L-1)/2} \mathcal{W}(l) F_{k_i}(\alpha + \frac{2\pi l}{N_s}) F^*_{k_j}(\alpha + \frac{2\pi l}{N_s}) \tag{A.5}$$

where $\mathcal{W}$ is a normalized spectral window of odd length L and

$$F_k(\omega) = \sum_{n=1}^{N_s} y[n] y^*[n+k] \text{exp}(-j\omega n). \tag{A.6}$$

B

Research and published papers

Journal papers

[1] MEN, Shaoyang, CHARGÉ, Pascal, et PILLEMENT, Sébastien. *A robust and energy efficient cooperative spectrum sensing scheme in cognitive wireless sensor networks*. International Journal Network Protocols and Algorithms, 2015, vol. 7, no 3, p. 140-156.

[2] MEN, Shaoyang, CHARGÉ, Pascal, et PILLEMENT, Sébastien. *Spectrum sensing with small sample size for wireless sensor network devices*. (IET Communications, Under review)

[3] MEN, Shaoyang, CHARGÉ, Pascal, et PILLEMENT, Sébastien. *Cooperative spectrum sensing with small sample size in cognitive wireless sensor networks*. (Springer Wireless Personal Communications, Under review)

Conference papers

[1] MEN, Shaoyang, CHARGÉ, Pascal, et PILLEMENT, Sébastien. *A robust cooperative spectrum sensing method against faulty nodes in CWSNs*. In : Communication Workshop (ICCW), 2015 IEEE International Conference on. London, U.K., June 2015, pp. 334-339.

[2] MEN, Shaoyang, CHARGÉ, Pascal, et PILLEMENT, Sébastien. *An Improved*

DS Theory Cooperative Spectrum Sensing Algorithm in Cognitive Wireless Sensor Networks. In : The third Sino-French Workshop on Information and Communication Technologies (SIFWICT 2015). Nantes, France, June 2015.

[3] MEN, Shaoyang, CHARGÉ, Pascal, et PILLEMENT, Sébastien. *A robust spectrum sensing based on bilateral hypotheses goodness-of-fit test in CWSNs*. to be submitted.

Bibliography

[1] ICT Regulation Toolkit. **ICT Regulation Toolkit**, 2010. 5, 13, 19, 20

[2] Paul Leaves, Klaus Moessner, Rahim Tafazolli, David Grandblaise, Didier Bourse, Ralf Tönjes, and Michele Breveglieri. **Dynamic spectrum allocation in composite reconfigurable wireless networks**. *Communications Magazine, IEEE*, **42**(5):72–81, 2004. 5, 19

[3] Qing Zhao and Brian M Sadler. **A survey of dynamic spectrum access**. *Signal Processing Magazine, IEEE*, **24**(3):79–89, 2007. 5, 20

[4] Ekram Hossain, Dusit Niyato, and Zhu Han. *Dynamic Spectrum Access and Management in Cognitive Radio Networks*. Cambridge University Press, New York, NY, USA, 1st edition, 2009. 5, 20

[5] Abdur Rahim, Sven Zeisberg, and Adolf Finger. **Coexistence study between UWB and WiMax at 3.5 GHz band**. In *Ultra-Wideband, 2007. ICUWB 2007. IEEE International Conference on*, pages 915–920. IEEE, 2007. 5, 20

[6] Joseph Mitola III and Gerald Q Maguire Jr. **Cognitive radio: making software radios more personal**. *Personal Communications, IEEE*, **6**(4):13–18, 1999. 5, 21

[7] ET FCC. **Docket No 02-135**. *Spectrum Policy Task Force Report*, 2002. 5, 21

[8] Ian F Akyildiz, Won-Yeol Lee, and Kaushik R Chowdhury. **CRAHNs: Cognitive radio ad hoc networks**. *AD hoc networks*, **7**(5):810–836, 2009. 5, 21

[9] Erik Axell, Geert Leus, Erik G Larsson, and H Vincent Poor. **Spectrum sensing for cognitive radio: State-of-the-art and recent advances**. *Signal Processing Magazine, IEEE*, **29**(3):101–116, 2012. 5, 21, 27, 28, 29

[10] Ian F Akyildiz, Brandon F Lo, and Ravikumar Balakrishnan. **Cooperative spectrum sensing in cognitive radio networks: A survey**. *Physical communication*, **4**(1):40–62, 2011. 5, 21, 27, 29, 79

[11] OZGUR B AKAN, OSMAN B KARLI, AND OZGUR ERGUL. **Cognitive radio sensor networks**. *Network, IEEE*, **23**(4):34–40, 2009. 6, 21, 79

[12] I.F. AKYILDIZ AND M.C. VURAN. *Wireless Sensor Networks*. Advanced Texts in Communications and Networking. Wiley, 2010. 7, 23

[13] LUCA RUGINI, PAOLO BANELLI, AND GEERT LEUS. **Small sample size performance of the energy detector**. *Communications Letters, IEEE*, **17**(9):1814–1817, 2013. 7, 23, 38, 65, 92

[14] YONGHONG ZENG AND YING-CHANG LIANG. **Maximum-minimum eigenvalue detection for cognitive radio**. In *Personal, Indoor and Mobile Radio Communications, 2007. PIMRC 2007. IEEE 18th International Symposium on*, pages 1–5. IEEE, 2007. 7, 23, 43

[15] T. J. LIM, R. ZHANG, Y. C. LIANG, AND Y. ZENG. **GLRT-Based Spectrum Sensing for Cognitive Radio**. In *IEEE GLOBECOM 2008 - 2008 IEEE Global Telecommunications Conference*, pages 1–5, Nov 2008. 7, 23, 43, 44

[16] YONGHONG ZENG AND YING-CHANG LIANG. **Spectrum-sensing algorithms for cognitive radio based on statistical covariances**. *Vehicular Technology, IEEE Transactions on*, **58**(4):1804–1815, 2009. 7, 23, 43, 44

[17] ABBAS TAHERPOUR, MASOUMEH NASIRI-KENARI, AND SAEED GAZOR. **Multiple antenna spectrum sensing in cognitive radios**. *Wireless Communications, IEEE Transactions on*, **9**(2):814–823, 2010. 7, 23, 43, 44, 80

[18] FENG LIN, ROBERT C QIU, ZHEN HU, SHUJIE HOU, JAMES P BROWNING, AND MICHAEL C WICKS. **Generalized FMD detection for spectrum sensing under low signal-to-noise ratio**. *Communications Letters, IEEE*, **16**(5):604–607, 2012. 7, 23, 43, 45, 80

[19] S.M. KAY. *Fundamentals of Statistical Signal Processing: Detection theory*. Prentice Hall Signal Processing Series. Prentice-Hall PTR, 1998. 13, 28, 29, 30, 32

[20] MANSI SUBHEDAR AND GAJANAN BIRAJDAR. **Spectrum sensing techniques in cognitive radio networks: a survey**. *International Journal of Next-Generation Networks*, **3**(2):37–51, 2011. 13, 27, 50

[21] TEVFIK YÜCEK AND HÜSEYIN ARSLAN. **A survey of spectrum sensing algorithms for cognitive radio applications**. *Communications Surveys & Tutorials, IEEE*, **11**(1):116–130, 2009. 13, 27, 41, 50

[22] ZHI QUAN, SHUGUANG CUI, ALI H SAYED, AND H VINCENT POOR. **Optimal multiband joint detection for spectrum sensing in cognitive radio networks**. *Signal Processing, IEEE Transactions on*, **57**(3):1128–1140, 2009. 13, 31, 50, 51

[23] JOOST CF DE WINTER. **Using the Student's t-test with extremely small sample sizes**. *Practical Assessment, Research & Evaluation*, **18**(10):1–12, 2013. 24

[24] MICHAEL A STEPHENS. **EDF statistics for goodness of fit and some comparisons**. *Journal of the American statistical Association*, **69**(347):730–737, 1974. 24, 47, 48, 49, 65

[25] SIMON HAYKIN. **Cognitive radio: brain-empowered wireless communications**. *Selected Areas in Communications, IEEE Journal on*, **23**(2):201–220, 2005. 27

[26] BEIBEI WANG AND KJ LIU. **Advances in cognitive radio networks: A survey**. *Selected Topics in Signal Processing, IEEE Journal of*, **5**(1):5–23, 2011. 29, 31

[27] CARLOS CORDEIRO, KIRAN CHALLAPALI, DAGNACHEW BIRRU, AND NOV SAI SHANKAR. **IEEE 802.22: the first worldwide wireless standard based on cognitive radios**. In *New Frontiers in Dynamic Spectrum Access Networks, First International Symposium on*, pages 328–337. IEEE, 2005. 30

[28] ANANT SAHAI, R TANDRA, AND M MISHRA. **Spectrum sensing: Fundamental limits**. *draft of the book chapter in Cognitive Radios: System Design Perspective*, 2009. 30

[29] DANIJELA CABRIC, ARTEM TKACHENKO, AND ROBERT W BRODERSEN. **Spectrum sensing measurements of pilot, energy, and collaborative detection**. In *Military Communications Conference, 2006. MILCOM 2006. IEEE*, pages 1–7. IEEE, 2006. 30, 33

[30] GYANENDRA PRASAD JOSHI, SEUNG YEOB NAM, AND SUNG WON KIM. **Cognitive radio wireless sensor networks: applications, challenges and research trends**. *Sensors*, **13**(9):11196–11228, 2013. 31

[31] DANIJELA CABRIC, SHRIDHAR MUBARAQ MISHRA, AND ROBERT W BRODERSEN. **Implementation issues in spectrum sensing for cognitive radios**. In *Signals, systems and computers, The Thirty Eighth Asilomar Conference on*, **1**, pages 772–776. IEEE, 2004. 31

[32] DEEPA BHARGAVI AND CHANDRA R MURTHY. **Performance comparison of energy, matched-filter and cyclostationarity-based spectrum sensing**. In *Signal Processing Advances in Wireless Communications (SPAWC), The Eleventh International Workshop on*, pages 1–5. IEEE, 2010. 31, 36

[33] SHIPRA KAPOOR, SVRK RAO, AND GHANSHYAM SINGH. **Opportunistic spectrum sensing by employing matched filter in cognitive radio network**. In *Communication Systems and Network Technologies (CSNT), 2011 International Conference on*, pages 580–583. IEEE, 2011. 31

[34] M. SALEHI AND J. PROAKIS. *Digital Communications*. McGraw-Hill Education, 2007. 31, 32

[35] MENGÜÇ ÖNER AND FRIEDRICH JONDRAL. **Cyclostationarity based air interface recognition for software radio systems**. In *Radio and Wireless Conference, 2004 IEEE*, pages 263–266. IEEE, 2004. 31

[36] PAULO URRIZA, ERIC REBEIZ, AND DANIJELA CABRIC. **Multiple antenna cyclostationary spectrum sensing based on the cyclic correlation significance test**. *Selected Areas in Communications, IEEE Journal on*, **31**(11):2185–2195, 2013. 31

[37] HARRY URKOWITZ. **Energy detection of unknown deterministic signals**. *Proceedings of the IEEE*, **55**(4):523–531, 1967. 31, 37, 74

[38] JINBO WU, TAO LUO, AND GUANGXIN YUE. **An energy detection algorithm based on double-threshold in cognitive radio systems**. In *Information Science and Engineering (ICISE), 2009 1st International Conference on*, pages 493–496. IEEE, 2009. 31

[39] CHANG LIU, MING LI, AND MING-LU JIN. **Blind Energy-Based Detection for Spatial Spectrum Sensing**. *Wireless Communications Letters, IEEE*, **4**(1):98–101, 2015. 31

[40] HAIYUN TANG. **Some physical layer issues of wide-band cognitive radio systems**. In *First IEEE International Symposium on New Frontiers in Dynamic Spectrum Access Networks, 2005. DySPAN 2005.*, pages 151–159, Nov 2005. 31, 41

[41] ANANT SAHAI, RAHUL TANDRA, SHRIDHAR MUBARAQ MISHRA, AND NIELS HOVEN. **Fundamental design tradeoffs in cognitive radio systems**. In *Proceedings of the first international workshop on Technology and policy for accessing spectrum*, page 2. ACM, 2006. 31, 41

[42] M. IQBAL AND A. GHAFOOR. **Analysis of Multiband Joint Detection Framework for Waveform-Based Sensing in Cognitive Radios**. In *Vehicular Technology Conference (VTC Fall), 2012 IEEE*, pages 1–5, Sept 2012. 31, 41

[43] YONGHONG ZENG, CHOO LENG KOH, AND YING-CHANG LIANG. **Maximum eigenvalue detection: Theory and application**. In *Communications, 2008. ICC'08. IEEE International Conference on*, pages 4160–4164. IEEE, 2008. 31, 41

[44] FEDERICO PENNA, ROBERTO GARELLO, AND MAURIZIO A SPIRITO. **Cooperative spectrum sensing based on the limiting eigenvalue ratio distribution in Wishart matrices**. *Communications Letters, IEEE*, **13**(7):507–509, 2009. 31, 41

[45] YONGHONG ZENG AND YING-CHANG LIANG. **Eigenvalue-based spectrum sensing algorithms for cognitive radio**. *Communications, IEEE Transactions on*, **57**(6):1784–1793, 2009. 31, 41, 80, 93

[46] XI YANG, KEJUN LEI, SHENGLIANG PENG, AND XIUYING CAO. **Blind detection for primary user based on the sample covariance matrix in cognitive radio**. *Communications Letters, IEEE*, **15**(1):40–42, 2011. 31, 41

[47] AYSE KORTUN, THARMALINGAM RATNARAJAH, MATHINI SELLATHURAI, CAIJUN ZHONG, AND CONSTANTINOS B PAPADIAS. **On the performance of eigenvalue-based cooperative spectrum sensing for cognitive radio**. *Selected Topics in Signal Processing, IEEE Journal of*, **5**(1):49–55, 2011. 31, 41

[48] NARUSHAN PILLAY AND HJ XU. **Blind eigenvalue-based spectrum sensing for cognitive radio networks**. *Communications, IET*, **6**(11):1388–1396, 2012. 31, 41

[49] ANDREAS BOLLIG AND RUDOLF MATHAR. **MMME and DME: Two new eigenvalue-based detectors for spectrum sensing in cognitive radio**. In *Global Conference on Signal and Information Processing (GlobalSIP), 2013 IEEE*, pages 1210–1213. IEEE, 2013. 31, 41

[50] LEI HUANG, JUN FANG, KEFEI LIU, HING CHEUNG SO, AND HONGBIN LI. **An Eigenvalue-Moment-Ratio Approach to Blind Spectrum Sensing for Cognitive Radio Under Sample-Starving Environment**. *Vehicular Technology, IEEE Transactions on*, **64**(8):3465–3480, 2015. 31, 41, 43, 45, 46, 80

[51] Y Norouzi, F Gini, MM Nayebi, and M Greco. **Non-coherent radar CFAR detection based on goodness-of-fit tests**. *Radar, Sonar & Navigation, IET*, **1**(2):98–105, 2007. 31, 46, 65

[52] Haiquan Wang and Wei Zhang. **Anderson-darling sensing of existence of unknown signals in a fading channel**. In *Proceedings of the 5th International Conference on Wireless communications, networking and mobile computing*, pages 1519–1522. IEEE Press, 2009. 31, 46

[53] Lei Shen, Haiquan Wang, Wei Zhang, and Zhijin Zhao. **Blind spectrum sensing for cognitive radio channels with noise uncertainty**. *Wireless Communications, IEEE Transactions on*, **10**(6):1721–1724, 2011. 31, 46, 66, 67, 68, 74, 75, 76

[54] Nhan Nguyen-Thanh and Insoo Koo. **Empirical distribution-based event detection in wireless sensor networks: an approach based on evidence theory**. *Sensors Journal, IEEE*, **12**(6):2222–2228, 2012. 31, 46

[55] Kamran Arshad and Klaus Moessner. **Robust spectrum sensing based on statistical tests**. *Communications, IET*, **7**(9):808–817, 2013. 31, 67

[56] Nikhil Kundargi, Yingxi Liu, and Ahmed Tewfik. **A Framework for Inference Using Goodness of Fit Tests Based on Ensemble of Phi-Divergences**. *Signal Processing, IEEE Transactions on*, **61**(4):945–955, 2013. 31

[57] Ming Jin, Qinghua Guo, Jiangtao Xi, and Yanguang Yu. **Spectrum sensing based on goodness of fit test with unilateral alternative hypothesis**. *Electronics Letters*, **50**(22):1645–1646, 2014. 31, 49

[58] DK Patel and YN Trivedi. **Goodness-of-fit-based non-parametric spectrum sensing under Middleton noise for cognitive radio**. *Electronics Letters*, **51**(5):419–421, 2015. 31, 74, 76

[59] Zhi Tian and Georgios B Giannakis. **Compressed sensing for wideband cognitive radios**. In *Acoustics, Speech and Signal Processing, 2007. ICASSP 2007. IEEE International Conference on*, **4**, pages IV–1357. IEEE, 2007. 31, 51

[60] Joel A Tropp, Jason N Laska, Marco F Duarte, Justin K Romberg, and Richard G Baraniuk. **Beyond Nyquist: Efficient sampling of sparse bandlimited signals**. *Information Theory, IEEE Transactions on*, **56**(1):520–544, 2010. 31, 51

[61] HONGJIAN SUN, WEI-YU CHIU, JING JIANG, ARUMUGAM NALLANATHAN, AND H VINCENT POOR. **Wideband Spectrum Sensing With Sub-Nyquist Sampling in Cognitive Radios**. *Signal Processing, IEEE Transactions on*, **60**(11):6068–6073, 2012. 31, 52

[62] ANANT SAHAI, NIELS HOVEN, AND RAHUL TANDRA. **Some Fundamental Limits on Cognitive Radio**. In *in Forty-second Allerton Conference on Communication, Control, and Computing*, 2004. 33

[63] WILLIAM A GARDNER. **Exploitation of spectral redundancy in cyclostationary signals**. *Signal Processing Magazine, IEEE*, **8**(2):14–36, 1991. 34

[64] AMOD V DANDAWATÉ AND GEORGIOS B GIANNAKIS. **Statistical tests for presence of cyclostationarity**. *Signal Processing, IEEE Transactions on*, **42**(9):2355–2369, 1994. 34, 35, 36, 117

[65] SCOTT ENSERINK AND DOUGLAS COCHRAN. **A cyclostationary feature detector**. In *Signals, Systems and Computers, 1994. 1994 Conference Record of the Twenty-Eighth Asilomar Conference on*, **2**, pages 806–810. IEEE, 1994. 34

[66] MENGÜÇ ÖNER AND FRIEDRICH JONDRAL. **Air interface identification for software radio systems**. *AEU-International Journal of Electronics and Communications*, **61**(2):104–117, 2007. 34

[67] JARMO LUNDÉN, VISA KOIVUNEN, ANU HUTTUNEN, AND H VINCENT POOR. **Spectrum sensing in cognitive radios based on multiple cyclic frequencies**. In *Cognitive Radio Oriented Wireless Networks and Communications, 2007. CrownCom 2007. 2nd International Conference on*, pages 37–43. IEEE, 2007. 34

[68] VESA TURUNEN, MARKO KOSUNEN, ANU HUTTUNEN, SAMI KALLIOINEN, PETRI IKONEN, AARNO PÄRSSINEN, AND JUSSI RYYNÄNEN. **Implementation of cyclostationary feature detector for cognitive radios**. In *Cognitive Radio Oriented Wireless Networks and Communications, 2009. CROWNCOM'09. 4th International Conference on*, pages 1–4. IEEE, 2009. 34, 36

[69] FADEL F DIGHAM, MOHAMED-SLIM ALOUINI, AND MARVIN K SIMON. **On the energy detection of unknown signals over fading channels**. In *Communications, 2003. ICC'03. IEEE International Conference on*, **5**, pages 3575–3579. IEEE, 2003. 37

[70] ROBERT F MILLS AND GLENN E PRESCOTT. **A comparison of various radiometer detection models**. *Aerospace and Electronic Systems, IEEE Transactions on*, **32**(1):467–473, 1996. 38

[71] SELAMI CIFTCI AND MURAT TORLAK. **A comparison of energy detectability models for spectrum sensing**. In *Global Telecommunications Conference, 2008. IEEE GLOBECOM 2008. IEEE*, pages 1–5. IEEE, 2008. 38

[72] ANANT SAHAI AND DANIJELA CABRIC. **Spectrum sensing: fundamental limits and practical challenges**. In *Proc. IEEE International Symposium on New Frontiers in Dynamic Spectrum Access Networks (DySPAN)*, 2005. 41

[73] RAHUL TANDRA AND ANANT SAHAI. **Fundamental limits on detection in low SNR under noise uncertainty**. In *Wireless Networks, Communications and Mobile Computing, 2005 International Conference on*, **1**, pages 464–469. IEEE, 2005. 41

[74] SHENG WANG AND NAZANIN RAHNAVARD. **Eigenvalue-based cooperative spectrum sensing with finite samples/sensors**. In *Information Sciences and Systems (CISS), 2012 46th Annual Conference on*, pages 1–5. IEEE, 2012. 46

[75] FENG LIN, ROBERT C QIU, AND JAMES PAUL BROWNING. **Spectrum sensing with small-sized data sets in cognitive radio: Algorithms and analysis**. *Vehicular Technology, IEEE Transactions on*, **64**(1):77–87, 2015. 46

[76] NORNADIAH MOHD RAZALI AND YAP BEE WAH. **Power comparisons of shapiro-wilk, kolmogorov-smirnov, lilliefors and anderson-darling tests**. *Journal of Statistical Modeling and Analytics*, **2**(1):21–33, 2011. 47

[77] R. D'AGOSTINO AND M. STEPHENS. *Goodness-of-fit-techniques*, **68**. CRC press, 1986. 47

[78] D TEGUIG, V LE NIR, AND B SCHEERS. **Spectrum sensing method based on goodness of fit test using chi-square distribution**. *Electronics Letters*, **50**(9):713–715, 2014. 48

[79] D TEGUIG, V LE NIR, AND B SCHEERS. **Spectrum sensing method based on likelihood ratio goodness-of-fit test**. *Electronics Letters*, **51**(3):253–255, 2015. 48

[80] HAIQUAN WANG, EN-HUI YANG, ZHIJIN ZHAO, AND WEI ZHANG. **Spectrum sensing in cognitive radio using goodness of fit testing**. *Wireless Communications, IEEE Transactions on*, **8**(11):5427–5430, 2009. 48, 65, 66, 67

[81] GUOWEI ZHANG, XIAODONG WANG, YING-CHANG LIANG, AND JU LIU. **Fast and robust spectrum sensing via Kolmogorov-Smirnov test**. *Communications, IEEE Transactions on*, **58**(12):3410–3416, 2010. 49, 65

[82] DAVID L DONOHO. **Compressed sensing**. *Information Theory, IEEE Transactions on*, **52**(4):1289–1306, 2006. 51

[83] FANZI ZENG, CHEN LI, AND ZHI TIAN. **Distributed compressive spectrum sensing in cooperative multihop cognitive networks**. *Selected Topics in Signal Processing, IEEE Journal of*, **5**(1):37–48, 2011. 51

[84] KHALID HOSSAIN AND BENOÎT CHAMPAGNE. **Wideband spectrum sensing for cognitive radios with correlated subband occupancy**. *Signal Processing Letters, IEEE*, **18**(1):35–38, 2011. 52

[85] ZHI QUAN, SHUGUANG CUI, H VINCENT POOR, AND ALI H SAYED. **Collaborative wideband sensing for cognitive radios**. *Signal Processing Magazine, IEEE*, **25**(6):60–73, 2008. 55

[86] WEI ZHANG, RANJAN K MALLIK, AND KHALED LETAIEF. **Optimization of cooperative spectrum sensing with energy detection in cognitive radio networks**. *Wireless Communications, IEEE Transactions on*, **8**(12):5761–5766, 2009. 55

[87] JUN MA, GUODONG ZHAO, AND YE LI. **Soft combination and detection for cooperative spectrum sensing in cognitive radio networks**. *Wireless Communications, IEEE Transactions on*, **7**(11):4502–4507, 2008. 56

[88] PENG QIHANG, ZENG KUN, WANG JUN, AND LI SHAOQIAN. **A distributed spectrum sensing scheme based on credibility and evidence theory in cognitive radio context**. In *Personal, indoor and mobile radio communications, 2006 IEEE 17th international symposium on*, pages 1–5. IEEE, 2006. 57, 63, 92, 93, 94

[89] SAMAN ATAPATTU, CHINTHA TELLAMBURA, AND HAI JIANG. **Energy detection based cooperative spectrum sensing in cognitive radio networks**. *Wireless Communications, IEEE Transactions on*, **10**(4):1232–1241, 2011. 57

[90] BAHADOR KHALEGHI, ALAA KHAMIS, FAKHREDDINE O KARRAY, AND SAIEDEH N RAZAVI. **Multisensor data fusion: A review of the state-of-the-art**. *Information Fusion*, **14**(1):28–44, 2013. 57

[91] Z CHAIR AND PRAMOD K VARSHNEY. **Optimal data fusion in multiple sensor detection systems**. *Aerospace and Electronic Systems, IEEE Transactions on*, (1):98–101, 1986. 59

[92] LOTFI A ZADEH. **Information and control**. *Fuzzy sets*, **8**(3):338–353, 1965. 60

[93] GLENN SHAFER ET AL. *A mathematical theory of evidence*, **1**. Princeton university press Princeton, 1976. 61, 85

[94] NHAN NGUYEN-THANH AND INSOO KOO. **Evidence-theory-based cooperative spectrum sensing with efficient quantization method in cognitive radio**. *Vehicular Technology, IEEE Transactions on*, **60**(1):185–195, 2011. 63, 81

[95] YONG HAN, QIANG CHEN, AND JIAN-XIN WANG. **An enhanced DS theory cooperative spectrum sensing algorithm against SSDF attack**. In *Vehicular Technology Conference (VTC Spring), 2012 IEEE 75th*, pages 1–5. IEEE, 2012. 63, 108, 109

[96] JINLONG WANG, SHUO FENG, QIHUI WU, XUEQIANG ZHENG, YUHUA XU, AND GUORU DING. **A robust cooperative spectrum sensing scheme based on Dempster-Shafer theory and trustworthiness degree calculation in cognitive radio networks**. *EURASIP Journal on Advances in Signal Processing*, **2014**(1):1–12, 2014. 63

[97] C. FORBES, M. EVANS, N. HASTINGS, AND B. PEACOCK. *Statistical Distributions*. Wiley series in probability and statistics. Wiley, 2011. 69

[98] QI CHEN, AMANDA WHITBROOK, UWE AICKELIN, AND CHRIS ROADKNIGHT. **Data classification using the Dempster–Shafer method**. *Journal of Experimental & Theoretical Artificial Intelligence*, **26**(4):493–517, 2014. 73

[99] YONG SOO CHO, JAEKWON KIM, WON YOUNG YANG, AND CHUNG G KANG. *MIMO-OFDM wireless communications with MATLAB*. John Wiley & Sons, 2010. 82

[100] CHENGSHAN XIAO, YAHONG ROSA ZHENG, AND NORMAN C BEAULIEU. **Novel sum-of-sinusoids simulation models for Rayleigh and Rician fading channels**. *IEEE Transactions on Wireless Communications,*, **5**(12):3667–3679, 2006. 82

[101] A.M. TULINO AND S. VERDÚ. *Random Matrix Theory and Wireless Communications*. Foundations and trends in communications and information theory. Lightning Source, 2004. 84, 85

[102] IAIN M JOHNSTONE. **On the distribution of the largest eigenvalue in principal components analysis**. *Annals of statistics*, pages 295–327, 2001. 84, 85, 86

[103] CRAIG A TRACY AND HAROLD WIDOM. **On orthogonal and symplectic matrix ensembles**. *Communications in Mathematical Physics*, **177**(3):727–754, 1996. 85, 88

[104] ZONGMING MA ET AL. **Accuracy of the Tracy–Widom limits for the extreme eigenvalues in white Wishart matrices**. *Bernoulli*, **18**(1):322–359, 2012. 86

[105] MOMAR DIENG. **Distribution functions for edge eigenvalues in orthogonal and symplectic ensembles: Painlevé representations**. *International Mathematics Research Notices*, **2005**(37):2263–2287, 2005. 88

[106] I GARRISON, RK MARTIN, WA SETHARES, B HART, W CHUNG, J BALAKRISHNAN, RA CASAS, TJ ENDRES, P SCHNITER, MG LARIMORE, ET AL. **DTV channel characterization**. In *Conference on Information Sciences and Systems (CISS)*, 2001. 90

[107] MANISH BHARDWAJ AND ANANTHA P CHANDRAKASAN. **Bounding the lifetime of sensor networks via optimal role assignments**. In *IEEE INFOCOM*, **3**, pages 1587–1596. INSTITUTE OF ELECTRICAL ENGINEERS INC (IEEE), 2002. 97, 107

[108] R.T. S. *Wireless Communications: Principles And Practice, 2/E*. Pearson Education, 2010. 97

[109] RUILIANG CHEN, JUNG-MIN PARK, Y THOMAS HOU, AND JEFFREY H REED. **Toward secure distributed spectrum sensing in cognitive radio networks**. *Communications Magazine, IEEE*, **46**(4):50–55, 2008. 97

[110] RUI XU, DONALD WUNSCH, ET AL. **Survey of clustering algorithms**. *Neural Networks, IEEE Transactions on*, **16**(3):645–678, 2005. 100

[111] AMEER AHMED ABBASI AND MOHAMED YOUNIS. **A survey on clustering algorithms for wireless sensor networks**. *Computer communications*, **30**(14):2826–2841, 2007. 100

[112] JAMES MACQUEEN ET AL. **Some methods for classification and analysis of multivariate observations**. In *Proceedings of the fifth Berkeley symposium on mathematical statistics and probability*, **1**, pages 281–297. Oakland, CA, USA., 1967. 101

[113] CHIA-HAN LEE AND WAYNE WOLF. **Energy efficient techniques for cooperative spectrum sensing in cognitive radios**. In *Consumer Communications and Networking Conference, 2008. CCNC 2008. 5th IEEE*, pages 968–972. IEEE, 2008. 103

[114] WENFANG XIA, SHU WANG, WEI LIU, AND WENQING CHEN. **Cluster-based energy efficient cooperative spectrum sensing in cognitive radios**.

In *Wireless Communications, Networking and Mobile Computing, 2009. WiCom'09. 5th International Conference on*, pages 1–4. IEEE, 2009. 103

[115] NHAN NGUYEN-THANH AND INSOO KOO. **An enhanced cooperative spectrum sensing scheme based on evidence theory and reliability source evaluation in cognitive radio context**. *Communications Letters, IEEE*, **13**(7):492–494, 2009. 104, 108, 109

[116] STEPHEN J SHELLHAMMER, RAHUL TANDRA, JAMES TOMCIK, ET AL. **Performance of power detector sensors of DTV signals in IEEE 802.22 WRANs**. In *Proceedings of the first international workshop on Technology and policy for accessing spectrum*, page 4. ACM, 2006. 106

UNIVERSITE BRETAGNE LOIRE

UNIVERSITÉ DE NANTES

Thèse de Doctorat

Shaoyang MEN

Techniques de détection du spectre dans les réseaux cognitifs de capteurs sans fil

Spectrum sensing techniques in cognitive wireless sensor networks

Résumé

Dans cette thèse, nous étudions l'optimisation des techniques de détection du spectre dans le contexte des réseaux cognitifs de capteurs sans fil. L'objectif de ces techniques est de déterminer l'occupation ou la disponibilité du canal. Tout d'abord, une vue d'ensemble des techniques de détection du spectre développées dans la littérature est fournie. Ensuite, les défis posés par le cadre applicatif des réseaux de capteurs sans fil sont décrits ; il s'agit de considérer dans le processus de décision les ressources et les capacités limitées des nœuds du réseau. Ainsi, plusieurs méthodes de détection du spectre sont proposées dans cette thèse. Certaines s'appliquent uniquement localement au niveau d'un nœud, tandis que d'autres mettent en œuvre une stratégie coopérative entre les nœuds pour une meilleure détection du spectre. En premier lieu, afin de diminuer la durée d'observation du canal et de réduire la consommation d'énergie, le problème adressé est celui de la détection du spectre à partir d'un très petit nombre d'échantillons. Deux techniques reposant sur la statistique des échantillons sont donc proposées afin d'améliorer la décision concernant la disponibilité ou non du canal : une détection locale du spectre basée sur un test Goodness-of-Fit et, une détection coopérative du spectre basée sur la théorie des croyances de Dempster-Shafer. Puis, le problème de l'optimisation de l'efficacité énergétique à l'échelle du réseau est abordé. Une nouvelle technique basée sur un algorithme de classification est alors proposé. Cette dernière permet d'améliorer la fiabilité de la détection, notamment par sa capacité à rejeter du processus de décision les nœuds qualifiés de défectueux ou moins fiables.

Mots clés

Détection du spectre, Réseaux cognitifs de capteurs sans fil, Echantillons de taille faible, Théorie des croyances de Dempster-Shafer.

Abstract

In this thesis we investigate the required efficiency and reliability trade-off of spectrum sensing techniques in cognitive wireless sensor networks (CWSNs). An overview of the developed spectrum sensing techniques in the literature is provided. Then, considering the challenges posed by the framework of resource-constrained nodes in CWSNs, we propose several improved local and cooperative methods for spectrum sensing. Firstly, in order to minimize the channel observation duration and to get reduced power consumption, the problem of running the spectrum sensing process from a small sample size is addressed. We thus propose two techniques in order to increase the strength of the decision on the presence or not of a signal: local spectrum sensing based on the goodness-of-fit (GoF) principle and cooperative spectrum sensing based on the Dempster-Shafer (D-S) theory of evidence. Moreover, considering the energy efficiency of the whole network and the reliability of the decision, a robust and energy efficient cooperative spectrum sensing scheme is proposed. This latter is based on a clustering algorithm and utilizes a double reliability evaluation. Compared with the methods in the literature, the proposed method present an improved performance of detection, and is designed to support harsh channel conditions and faulty nodes.

Key Words

Spectrum sensing, Cognitive wireless sensor networks, small sample size, Dempster-Shafer theory of evidence.